TÉCNICO LISBOA

Integration of a concentrating solar thermal system in an expanded cork agglomerate production line

António Ascenção Castro

Thesis to obtain the Master of Science Degree in

Energy Engineering and Management

Supervisors: Prof. Luís Filipe Moreira Mendes

Dr. João Pereira Cardoso

Examination Committee

Chairperson: Prof. Edgar Caetano Fernandes

Supervisor: Prof. Luís Filipe Moreira Mendes

Member of the Committee: Dr. João Augusto Farinha Mendes

November 2016

Acknowledgments

First of all, thanks to my parents, that even at thousands of kilometers away, always gave me their continuous support and were really important in this step of my life. Also, thank you to my sisters for making my life better and cheerful.

Big thanks to my supervisors, always available and helpful during the many stages of the work.

Special thanks to my girlfriend for her support and patience during these last months.

Finally, thanks to everyone involved in the development of the work.

Abstract

The expanded cork agglomerate, known by its remarkable insulation properties, is one of the many products offered by the traditional cork industry in Portugal. Its manufacture process is carried out in autoclaves that require the use of a high temperature steam flow to expand the cork resins. Nowadays, most industries produce this thermal energy with steam generation units powered by fossil fuels or biomass.

On the other hand, solar heat for industrial processes is a growing market that seeks to increase renewable energy use and sustainability in the industrial sector, therefore the present work aimed to assess the use of concentrating solar collectors in the thermal energy production system of an operating facility: Sofalca, Lda, which uses an on-site produced residue called cork powder to power its boiler.

In order to satisfy thermal demands, a parabolic trough solar system was studied with the purpose of preheating the feedwater of the boiler via an external heat exchanger. The solar field model was dimensioned to provide the water with sufficient heat to reach a maximum temperature of 170ºC at 8 bar of pressure.

The criterion of the analysis was the maximization of solar energy supply at the most economically favorable conditions, which resulted in a system configuration capable of achieving a solar fraction of 41% at a levelized cost of energy of 8.3 c€/kWh. However, calculations also indicated that the economic feasibility of the studied scenario is dependent on the market price of sale of the saved cork powder.

Key words: Parabolic Trough, Expanded Cork Agglomerate, Solar heat, TNRSYS, Concentrating Solar Power.

Resumo

O aglomerado expandido de cortiça, conhecido pelas suas notáveis propriedades de isolamento, é um dos vários produtos que a indústria corticeira portuguesa oferece. É fabricado em autoclaves que requerem um fluxo de vapor a altas temperaturas para a expansão da resina da cortiça. Hoje em dia, as indústrias obtêm esta energia térmica com caldeiras de vapor, recorrendo a combustíveis fósseis ou biomassa.

Por outro lado, o calor solar para processos industriais é um mercado crescente que visa aumentar o uso da energia renovável e sustentabilidade no setor, por conseguinte o presente trabalho teve como objetivo analisar o uso de coletores de concentração solar no sistema de produção de energia térmica de uma instalação operacional: Sofalca, Lda, que utiliza pó de cortiça para abastecer a sua caldeira.

Para satisfazer as necessidades térmicas estudou-se um sistema solar de calha parabólica com o objetivo de pré-aquecer a água de alimentação da caldeira através de um permutador de calor externo. O modelo de campo solar foi dimensionado para fornecer a água com calor suficiente para atingir uma temperatura máxima de 170°C a uma pressão de 8 bar.

O critério da análise foi a maximização de fornecimento de energia solar em condições economicamente favoráveis, o que resultou numa configuração capaz de atingir uma fração solar de 41% com um custo unitário médio atualizado de energia de 8,3c€/kWh. No entanto, os cálculos indicaram que a viabilidade económica do cenário estudado depende do preço de venda do pó de cortiça que não seria utilizado no sistema.

Palavras-chave: Calha parabólica**,** Aglomerado Expandido de Cortiça, Energia solar, TRNSYS, Sistemas solares de concentração.

Table of contents

List of tables

List of figures

Nomenclature

a	Discount rate (%)
a_1	Heat loss coefficient
a_2	Temperature dependence of the heat loss coefficient
$A_{aperture}$	Aperture area of the parabolic collector (m^2)
c	Annual cash flow (€)
C	Heat capacity (W/K)
$ConcRat$	Concentration ratio of the collector
d_{om}	O&M expenses (%)
E_{annual}	Useful energy produced by year
$F_R(\tau\alpha)_n$	Intercept efficiency (Optical)
$F_R U_L$	Efficiency slope (W/m^2K) (Loss coefficient)
G	Direct normal irradiance (W/m^2)
h	Convective heat transfer coefficient (W/m^2K)
h_x	Specific enthalpy (kJ/kgK)
HV	Heating value (MJ/kg)
i	Discount rate factor (%)
I_t	Total investment costs (€)
I_{beam}	Beam solar radiation incident on the collector (kJ/hm^2)
IAM	Incidence angle modifier
$m_{corkpowder}$	Annual mass savings of cork powder (kg)
$\dot{m}$	Fluid mass flow (kg/h)
n	Lifetime of the project (years)
I_t	Total investment costs (€)
η_i	Overall efficiency of the collector
η_o	Optical efficiency of the collector
η_{boiler}	Biomass boiler efficiency
NTU	Number of transfer units
$N_{parallel}$	Number of collector strings in parallel
PP_d	Discounted payback period (years)
Q_u	Useful energy gains in the collector (kJ)
$\dot{Q}_u$	Useful energy rate in the collector (kJ/h)
$\dot{Q}$	Heat rate (kW)
R_1	Flow rate modifier
R_2	Series collector modifier
T_x	Fluid temperature (ºC)
T_m	Mean temperature (ºC)
T_{amb}	Ambient temperature (ºC)
T_i	Inlet temperature (ºC)
T_m	Mean temperature (ºC)
T_1	Interest rate (%)
T_2	Risk associated rate (%)
T_3	Inflation rate (%)
UA	Overall heat transfer coefficient (kJ/hK)

Abbreviations

CSP	Concentrating solar power
CST	Concentrating solar thermal
ECA	Expanded Cork Agglomerate
EW	East-West
HTF	Heat transfer fluid
IAM	Incidence angle modifier
ICB	Insulation cork board
IEA	International Energy Agency
$LCOE$	Levelized cost of energy
$LCOH$	Levelized cost of heat
NS	North-South
$O\&M$	Operation and Maintenance
PTC	Parabolic trough collector
SCA	Solar collector assembly
SHC	Solar heating and cooling programme
$SHIP$	Solar heat for industrial processes
$STAGE-STE$	Scientific and Technological Alliance for Guaranteeing the European Excellence in Concentrating Solar Thermal Energy
TES	Thermal energy storage

CHAPTER 1. INTRODUCTION

The cork industry is a traditional and important activity in Portugal, offering a wide variety of products derived from the bark of the cork oak; and among them, the Expanded Cork Agglomerate (ECA). ECA is used in thermal insulation, acoustical absorption and vibration damping applications, as well as a raw material for furniture, decoration and other products, with the advantage of a strong ecological nature.

The production of the mentioned agglomerate involves a significant heat demand, considering the high temperature steam requirement in part of the manufacture process. In general, the procedure is based on the expansion of natural resins using water vapor at temperatures above 300ºC. To generate it, specialized industries are equipped with steam boilers that operate mainly with biomass.

When thinking on alternatives or complementary technologies for this heat generation scenario, many commercially mature options are found, namely conventional fossil fueled or biomass boilers. Nevertheless, current energy trends walk towards sustainability and nature preservation paths, acknowledging that the future world panorama is certainly focused on the use of renewable solutions for heat and electricity generation. In this context, concentrating solar energy stands as one of the most promising areas, embracing both industrial and utility scales.

Considering the heat requirements, global energy trends and the currently used technology of generation, the present project aims to study the integration of concentrating solar thermal (CST) systems in the ECA manufacture process, analyzing if the collected energy is capable of satisfying the thermal demands, and characterizing its technical and economic performance under certain conditions of operation. Among the technology alternatives, a linear focus CST system, specifically the parabolic trough, is the one selected, since it is the most commercially mature and presents attributes that are suitable for the application.

The project aims to evaluate real data provided by the industry in order to model and simulate the integration of the mentioned processes, thus looking for adequate and technically and economically attractive solutions. Annual performance results, complemented with daily behavior information helps in the selection of the most favorable integration scenario.

1.1 Problem Description and Framework

Many industrial facilities around the world require heat to drive its many production processes and support its continuous operation, relying most of the time on conventional sources to provide it. The industrial energy demand is usually in the low and medium temperature range (up to 400ºC approximately), as stated by the SHC (2015) report which refers that “in several specific industry sectors, such as food, wine and beverages, transport equipment, machinery, textiles, pulp and paper, the share of heat demand at low and medium temperatures is around 60%” when considering the total heat demand. The same report indicates that in the EU27 countries, around 28% of the overall energy demand comes from industries. In the specific case of the cork processing industries, they require heat for most of its products, though in different quantities and forms. Referring the ECA production process,

one of the most relevant phases consists of the cork agglomeration procedure, which is a thermochemical treatment performed with steam injection in autoclaves at an average temperature of around 340ºC (Gil, 1996), making it possible to be considered as a medium temperature process.

Nowadays, industrial applications seek, when possible, the required heat supply on sustainable technologies that are economically viable and environmentally friendly. Solar energy coupled to industrial applications is seen as a good option and has been subject of study and a relevant point in the *International Energy Agency* (IEA) agenda. In this area, a task called *Solar Heat Integration in Industrial Processes* emerges, which indicates that solar thermal systems have a significant potential in the sector, even though it is still at an early stage of progress (SHC, 2015). Said Task, identified as Task 49/Task IV, is linked to Solar Heat for Industrial Processes (SHIP) and results from the collaboration between the *Solar Heating and Cooling Programme* (SHC) and the *SolarPACES* network (both created by the IEA), with the purpose of joining efforts to provide knowledge and technology to promote the integration of solar energy into industrial applications. The association is characterized by a set of research, development and demonstration projects.

This joint task conducts studies on the potential of the technology by dividing the work into three subtasks: process heat collectors, process integration and intensification, and design guidelines (SHC, 2015). All these areas will improve with the performance of studies and successful integration of solar thermal systems in production processes. Task 49 has also set as an objective; “to lower the barriers for market deployment and to disseminate the knowledge to the main target groups” (SHC, 2015). According to Brunner (2015) the scope of the Task includes all industrial applications that are thermal driven and running at temperatures up to 400ºC. Note that temperatures above 150ºC require the use of solar concentrator technologies, such as collectors like Compound Parabolic Concentrators, or Imaging Collector systems, like the Parabolic Trough arrays (IEA-ETSAP & IRENA, 2015).

Considering the previously described, one can say that the present work is framed into a larger study field and worldwide strategy, taking the mentioned task as a reference and impulse, and emphasizing the relevance and potential future of the topic. At present, the Task is already completed and results delivered, nevertheless, the concern on SHIP is still relevant and will surely grow, noting that the subject has been a focus of the IEA-SHC since 2003 (with completed Task 33). Interesting results from Task 49 deliverables include solar process heat potential studies carried out in Portugal and Spain, where suitable sectors and industries were identified (at a maximum temperature of 160ºC), as found in report C5 ((Platzer, 2015). Other studies were performed, in which a technical potential of 4.4% is defined for Portugal (as a function of the available area and 60% of solar fraction), highlighting the fact that a cork processing facility was included in the study (Schweiger, et al., 2001). Among the available task documents there are integration and performance assessment guidelines, which play an important role in the present project since they set the foundations for the technical and economic phases of the evaluation.

Apart from IEA Tasks, the European Union energy dedicated organizations have also studied the potential of solar heat in industrial processes. The 5th Framework research, technological development and demonstration programme approached this subject back in the 1998-2002 period with

the *POSHIP* project, which conducted studies in Portugal's potential and Portuguese application (Schweiger, et al., 2001). Currently, the 7th Framework programme through the STAGE-STE alliance, formed a group of mainly coordination and research and development activities (Work Packages) to address CST systems. SHIP applications with Parabolic Trough collectors are considered within the Work Package 11, called *Linear focusing solar concentrating technologies*. This package is divided in Tasks, highlighting the 11.1, focused on *Small scale and low cost installations for power and industrial process heat applications* (STAGE-STE, n.d.). The present case study is performed within its scope.

Regarding the integration of the production line of ECA with a solar energy system, the referred information suggests that a suitable solution is the use of a CSP system to provide the medium temperature fluid, such as the Parabolic Trough, which is already utilized for SHIP integration applications, as found on the SHIP Database (AEE INTEC, 2015). The same site refers that a cork processing facility is also already coupled with solar systems, though for a different product and process than the one involved in this study.

One of the approaches of the proposed work is based on the integration analysis, where "the aim is to identify the most technically and economically suitable integration point and the most suitable integration concept" (Muster B. , 2015), knowing that the layout of the plant and its heat supply is a key aspect. Regarding this, the study is set to be performed with data from an operating facility, specifically from *Sofalca – Sociedade Central de Produtos de Cortiça, Lda*, specialized in expanded agglomerates production. They currently use cork powder (biomass) as a feedstock for the steam generation unit thus the combination of systems seeks to replace or hybridize the existing one, analyzing the economic and industrial value of the cork powder, and its potential savings during the year.

The development of the subject will define the technical and economic feasibility of this integration and hopefully offer results that could be relevant for the objectives set by Task 49/Task IV collaboration and the Task 11.1 of the STAGE-STE project.

1.2 Objectives

General objective

Evaluation of the technical and economic feasibility of a parabolic trough solar concentrating system coupled to the heat supply of the Expanded Cork Agglomerate production line.

Specific objectives

- Bibliographic revision and research on the aspects related to the subject of study.
- Assessment and identification of the thermal energy needs of the industrial process.
- Definition of the integration concept and integration point.
- Design and modelling of the solar field.
- Design and modelling of the integrated solar/industrial system.
- Development of the optimization and performance evaluation of the integrated model.

1.3 Methodology

The present work relies on the use of qualitative and quantitative analysis methods from many areas of engineering. However, the use of computational tools for the solar integration design is crucial for the work.

In this matter, transient system simulation tool TRNSYS is chosen to model and simulate the thermal and energetic behavior of the system. Using its embedded physical phenomena equation components, the equipment that comprises these types of thermal power systems are modeled and simulated. The selection of this particular software is based on its mature use in the solar thermal area and its flexibility in terms of possibilities. For specific problems that appear throughout the development of the model, other tools are utilized.

1.4 Structure of the dissertation

The present document is organized into six chapters, as described below:

Chapter 1. Introduction: i.e. the current chapter, in which a description of the purpose of the work is presented. The subject of study is exposed along with its main and specific objectives. The methodology of the study is also approached.

Chapter 2. Conceptual Framework: involves the theoretical basis and references required to understand the aspects that are comprised in the development of the subject. Information regarding the employed methodology is also included.

Chapter 3. Solar Heat Integration Assessment: summarizes the analysis of the specific industrial process, highlighting its current heat supply characteristics. An assessment on the energy demand parameters and profile is presented, as well as the potential solar integration approaches.

Chapter 4. System Design: comprises the steps performed to build a potentially suitable solar heat integrated system. Considerations taken for the software modelling of the system are described, including information about the involved equipment. A *pre-defined* SHIP system is obtained by the end of this chapter.

Chapter 5. Optimization and Performance Assessment: simulations of the *pre-defined* system are performed for various settings, yielding a set of results that are presented and analyzed in this chapter. Technical and economic performance indicators are obtained, which help in the selection of the most suitable solar system configurations for the proposed industrial process.

Chapter 6. Conclusions and Recommendations: presents the final and main remarks of the study, also approaching recommended steps for future studies.

CHAPTER 2. CONCEPTUAL FRAMEWORK

Providing detailed information about the specific industrial process and the concentrating solar technologies is crucial to properly understand the proposed project and its objectives, considering also the theoretical basis behind the integration procedure between both sectors. Hence, the present chapter provides this material, along with information regarding the software simulation and the theoretical data related to the economic performance indicators.

2.1 Industrial Process: Expanded Cork Agglomerate Production Line

This section approaches the ECA production line and some of its technical aspects, while also describing the material used to provide heat to the process (cork powder). Before introducing the output product, a brief characterization of the cork as a raw material is presented.

2.1.1 Cork as a raw material

Cork is a natural product obtained from the outer bark of the cork oak tree (Quercus suber), as seen in Fig. 1. Originated in the Mediterranean area, most of its exploitation is found in Portugal and Spain (Pereira, 2007); in which the first one is the major cork producer in the world, being responsible for more than half of all the volume in cork processing (Gil, 2013). Cork products feed an important industrial sector, being exported all over the world since its properties are appreciated for many applications. Among the properties, cork is light weighted, compressible and impermeable to liquids and gases, has a low thermal conductivity, high damping capacity, low density and good electrical insulation, and presents chemical and biological inertness characteristics (Pereira, 2007).

In general, cork based products currently obtained are utilized in a great range of applications, as summarized next (Barros, 2013): stoppers for alcoholic beverages, coating for civil works, thermal, acoustic and vibratory insulation, decoration and furniture applications, clothing sector, automotive industry, chemical and pharmaceutical industry, and aeronautic and military industry.

Fig. 1. Cork oak tree *(Grilo, 2014)*.

2.1.2 The cork processing industry

According to Gil (1996), the cork processing industry comprises several related areas, where the input material, the technology and the outputs represent the differences. The same author divides the cork sector into four other subsectors: preparation activities, transformation by cutting or carving, granulation, and production of agglomerates.

The sector can also be classified according to its output materials, where two main streamlines are characterized by Pereira (2007): production of stoppers and discs of natural cork, and production of agglomerates of cork particles. On the other hand, Gil (1996) expands this classification by specifying the products according to the transformation process, as summarized in Fig. 2. Note that the different processes or subsectors could be found in unrelated facilities, globally integrated or joint in a single location.

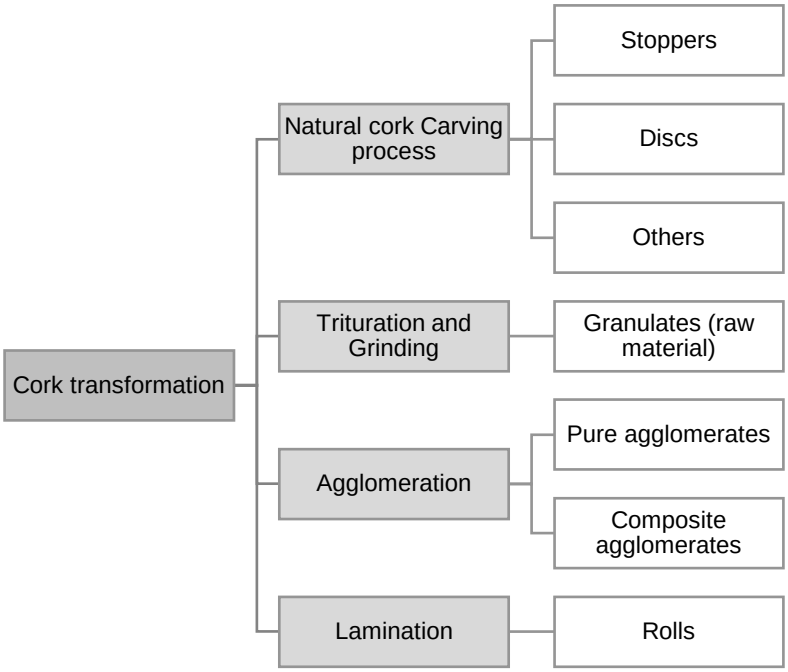

Fig. 2. Cork transformation processes and its main products. Built with information from Gil (1996).

Concerning the energy component in this type of facilities, its demand is usually met using various sources, such as cork powder, firewood, vegetable waste, liquid fuels and electric energy (Gil, 1996). Cork powder is mostly used to generate steam in boilers in ECA facilities, while the liquid fuels play an important role in heating, drying and transport processes of every sector, as well as the electricity, which is common to all of them. Energy demand is addressed again in the ECA manufacture description.

When it comes to the resulting residues of the cork processing, it is convenient to identify and classify each one according to its source, given the variety of procedures present in the transformation of the material. In the first place, the stopper and disc production originates trims of cooked material pieces that are not used, nevertheless, they can be milled in the granulation subsector along with refuse products (Pereira, 2007). From the ECA manufacture, waste constituted by condensed compounds

extracted from the particles in the autoclave are found in the outlets of the system, in this case, no known application is currently established (Gil, 1996), though studies suggest the possibility of treatment by anaerobic digestion, for the recovery of its energetic potential through methane production (Gil, 2013), in the same field, gasification could also be a possibility. A considerably relevant residue is *cork powder*, which is obtained throughout the many industrial cork processes, however its different sources make it a residue that can present diverse properties. Considering its energetic value, it will be further described ahead.

2.1.2.1 Cork Agglomerates production

This subsector provides an outlet for the residual by-products, residual raw materials and virgin cork (that does not enter any other processing line), that is, in a first process, passed through the trituration and grinding sections. In general, cork agglomerates result from the processing of granules under the action of pressure, temperature and in some cases, a binding agent. The derived materials can be classified into three groups (Pereira, 2007):

- Agglomeration of cork with adhesives: process where the accumulation of the granules occurs using an external resin (adhesive) under moderate pressure and heating. Popular agglomerated stoppers are produced with this method.
- Cork agglomerate composites with rubber: “made by mixing and binding cork granules with natural or synthetic rubber” (Pereira, 2007), obtaining products suitable for demanding applications, such as: sealing systems in the automotive industry, industrial machinery insulation, among others.
- Expanded cork agglomerate: consists of a material that is purely composed of cork, in which their granules are thermally bonded thanks to the natural resins integrated into cork’s chemical composition. A heat source is needed for the thermochemical degradation of the inner structures, resulting on a dark brown color induced by the temperature (Gil, 1996).

Expanded cork agglomerate production

Also known as Insulation Cork Board (ICB) or simply Black Cork Agglomerate, the ECA is, as previously stated, a material that comes from the aggregation of the raw cork granules, which is a consequence of the volumetric expansion and natural resin exudation that takes place under the action of the temperature of a thermal fluid (SOFALCA, 2015).

Concerning the input materials for this type of agglomerate, Pereira (2007) indicates that the cork that is not boiled or used whatsoever goes directly for the production of granulates, that will be processed as ECA afterwards. These raw materials are mainly constituted by: planks of insufficient quality or dimension, stained, burned or dead cork trees and virgin cork (from pruned trees or first removal). In the same topic, Gil (1996) adds that the roughest granulates are the ones used, with a particle size within the range of 5-20 mm, obtained mainly from virgin cork. The same author highlights the fact that the worst qualtiy cork is used for the ECA, being this one of the interesting factors associated with the product.

The manufacture process begins with the extraction of the virgin cork from the branches or prunings, followed by the trituration and grinding previously addressed. As described by Gil (1996), the particle size attained depends on the type of agglomerate to produce. The preparation process continues with a cleaning section that removes impurities like cork powder and wood log pieces, mainly with densimetric separators. The final step in the preparation covers the drying, with a flow of hot air (at around 110ºC) or heating of the storage silos until reaching the ideal humidity (Gil, 1996).

The next phase is the agglomeration, which is performed through thermochemical treatment in autoclaves. This process consists of a block production where the granules are heated with superheated steam in an autoclave that is the mold itself (Pereira, 2007), therefore it provides the rectangular shape (or any other required shape) that is seen in Fig. 3.

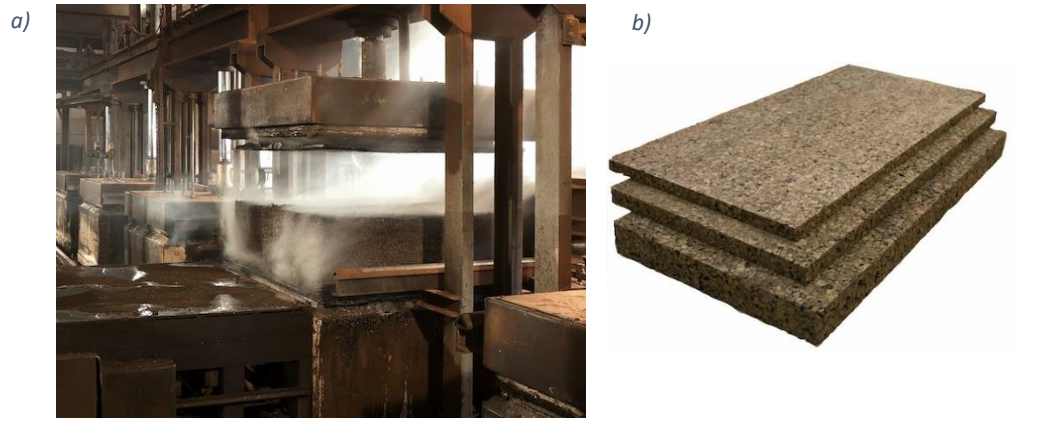

Fig. 3. ECA production in an autoclave (a) and ECA after cutting (b). (ModernEnviro, 2014).

The detailed agglomeration procedure inside the autoclave is now described: the dry granulate is introduced into the autoclave until reaching a predefined level, which is selected according to the desired volumetric mass of the product (Gil, 1996). Afterwards, a light compression of the matter is done to compact the mix and define its final density; at this point a flow of “steam is injected through the openings in the bottom face and bottom edge of the lateral faces of the autoclave” (Pereira, 2007). This superheated steam *bakes* the materials at temperatures of around 300-350ºC and under a 40 kPa gauge pressure, for approximately 20 minutes. For the same process, Gil (1996) specifies that the range of temperatures is around 300-370ºC with an average of 340ºC, and in terms of pressure, the value is the same but could vary between 30 and 60 kPa (gauge).

The high temperature steam flow is responsible for the thermochemical degradation of the cork cell wall, with its previous increase in volume; this degradation originates byproducts that act as natural adhesives between the granules, thus forming the expanded agglomerate (Silva, et al., 2005). Silva et al. (2005) expose that “it has been reported that suberin acts as the main binding agent in insulation corkboard”. The same authors indicate that: “the expansion results in an increase in cell volume of about 100%, and the thermochemically degraded cell wall material is responsible for the final dark appearance and the weight loss (approximately 30% of the initial weight).” The dark color can be appreciated in the ECA block of Fig. 3.

Regarding the residence time of the steam-baking, the value is imposed by the humidity percentage, the vapor temperature and the volume/mass fractions, with periods going from 17 to 30 minutes (Gil, 1996). After this, the steam is discharged throughout the exit tubes placed in the superior face of the autoclave, passing later through a cooling chamber, where cold water flows and lowers the temperature of the steam down to 120ºC, condensing a considerable number of substances. The cooling water is now warm and its energy can be used (Gil, 1996), however this process is not found at Sofalca.

Once the blocks exit the autoclave (prior compression is possible if the desired product density requires it), they are moved to a cooling machine that sprays recycled boiling water (around 100ºC) for cooling and dimensional stabilization purposes. After complete cooling, the blocks are cut to the size and thickness desired. The materials left behind are re-granulated and recycled for the same purpose (Silva, et al., 2005).

When it comes to the steam requirements of the process, relevant for the proposed solar integration, it has been reported that water vapor is mainly produced by biomass fired boilers, usually with the cork powder that is obtained from almost every processing phase of the cork. Technically speaking, the steam flow required for each autoclave is estimated around 700 kg/h in a 400ºC operation. For 6 autoclaves, pressure in the boiler should be around 785 kPa (Gil, 1996). The same author also refers that: for an ECA production of 40.000m^3/year, the steam consumption is around 7.000 kg//h, which is equivalent to a consumption of 1,5m^3 of water per cubic meter of agglomerate (if cooling water is included and no reuse is performed). Then, energy demand could be established as: 26,7 MJ of energy from biomass and 4,9 MJ of electricity for one kilogram of agglomerate.

The last paragraph gives a first impression of the energy and resource demand of this class of process. For the solar integration in a specific ECA production line, real data from the heat generation process is required.

Expanded cork agglomerate properties

Given its many characteristics, ECA can be used as thermal insulation, acoustic insulation or vibration absorption. As mentioned above, the densities of the product can be established in the agglomeration process, by changing the filling level in the autoclave, the compression, the pressure or the residence time. Properties of each type of product are presented in Table 1.

Table 1. Properties of ECA according to its final application (Silva, et al., 2005).

Type of insulation	Density, kg m^{-3}	Thermal conductivity at 20°C ($\times 10^{-5}$ kJ m^{-1} s^{-1} K^{-1})	Permeability to water vapour ($\times 10^{-12}$ kg Pa^{-1} s^{-1} m^{-1})
Acoustical	80–100	3·7	8·3–21
Thermal	100–150	4·0–4·2	4·2–12
Anti-vibration	175–320	4·8–5·7	2·1–8·3

In terms of working temperature, a range of 97-383K is reported (Silva, et al., 2005), thus confirming its great thermal behavior capabilities.

Cork powder

Cork powder (Fig. 4) is a residual material from the many industrial cork processes, constituted mainly by gross impurities, dust and particles of insufficient dimension (lower than 0,25 mm) (Pintor, et al., 2012), and heavy granules. The biggest share comes from suction of residues in several operations: trituration, separation, etc. Note that the "industrial transformation of cork generates up to 25% (weight) of cork dust as byproduct" (Silva, et al., 2005).

The main use of this cork dust is as fuel for steam generation in boilers, feeding processes with a residue that comes from the many production lines. A small share is also used in the low quality stopper production, the linoleum manufacture, the explosives production, soil control and others; i.e., in applications of low added value (Gil, 1997) . For the ECA production, an average amount of 180 kg of cork powder is required to supply steam for the manufacture of one cubic meter of agglomerate (Gil, 1996).

In terms of energy, it is relevant to mention that some factories are self-sufficient with cork powder as the feedstock of the steam generator (Gil, 1996) considering that its heating value is close to half of fuel oil (High Heating Value between 15-28 MJ/kg). However, since it is originated in various sources, the heating value is variable, obtaining the highest one (around 29,3 MJ/kg) from the ECA final phases of cutting. A mixture of powder from several sources is also used and called *burning powder* (Pintor, et al., 2012).

Fig. 4. Cork powder sample (Nunes, Matias, & Catalão, 2013).

Referring other possible applications is important regarding the proposed topic, since the replacement (partial) of the cork powder boiler by a solar system is one of the possibilities addressed by the study, and the economical or industrial value is of interest. In this field, Gil (1997) mentions that some other studies consider the application of this material in the following areas: manufacture of different agglomerates, briquette production, source of chemicals, and agricultural substrates. Other works suggest that it could be useful to produce wax for regular utilization, if treated with sodium hydroxide (Gil, 1996). Given its functionality in burning applications, the co-generation purpose could be

an attractive solution for cork powder outside the production area, however its low density makes the transportation and handling difficult.

Table 2 presented below shows various applications, according to specific studies or researches developed on the area:

Table 2. Research on cork powder applications.

Authors (Reference)	Title	Application
(Godinho, et al., 2001)	*Properties and processing of Cork Powder filled cellulose derivatives composites*	Use of cork powder as a filler to reinforce hydroxypropyl cellulose matrixes, yielding higher mechanical properties to the composite.
(Pintor, et al., 2012)	*Use of cork powder and granules for the adsorption of pollutants: A review*	Cork powder used to prepare activated carbon, which can be utilized in the adsorption of pollutants in water treatment processes.
(Silva, et al., 2005)	*Cork: Properties, Capabilities and Applications*	Use of the residues in heavy metal biosorption, given good performance and low cost.
(Nunes, Matias, & Catalão, 2013)	*Energy recovery from cork industrial waste: production and characterization of cork pellets*	Densification of cork residues to produce pellets for incineration applications (addressing the low density fuel issue).

Now, concerning the market price of the material, it is difficult to establish a single sales value, since most of the mentioned applications are scientific approaches or still subjects of study. The energetic purpose previously mentioned seems like the most applied end-use, but its low density significantly reduces its market development due to the costs of transportation. On the other hand, online sales services offer cork powder as a suitable product for gardening and artistic applications, as well as for buoyancy control in hook baits for fishing (CorkSpirit, 2016); with an approximate value of 90 €/kg, nevertheless, the size of the market seems reduced. The pelletization, as seen in Table 2, is a studied alternative, and another work (developed by Barros, 2013) suggests its combinaton with wood sawdust, in which a 30% of cork powder is used. The reported average price of sale in the market is 0,23 €/kg, although a 0.08-0.09 €/kg production cost must be taken into account, apart from pelletization equipment investment.

2.2 Concentrating Solar Power

A general overview on the Concentrating Solar Power (CSP) technologies is presented, giving special attention to the Parabolic Trough system, since it is the one selected. General information from its operation and components is included, addressing briefly the economic component.

2.2.1 General overview

To benefit from the beam (or direct) radiation that reaches the surface of the Earth, CSP systems employ an array of mirrors that concentrate the rays of the sun into a special receiver; then, through a transfer fluid, these concentrated rays can be directly or indirectly used to produce useful energy, such as heat, electricity and fuels. (Lovegrove & Stein, 2012). As can be seen in Fig. 5, the working principle is the following: a heat transfer fluid (HTF) is heated at high temperatures with the concentrated rays while it passes through a focal line or point, it will later exchange its energy with another fluid or work directly in the process (depending on the HTF and process objective). If the aim is to produce electricity, from this point, the process is similar to the one employed in conventional thermal power plants, where a flow of steam or gas drives a turbine to produce electrical power.

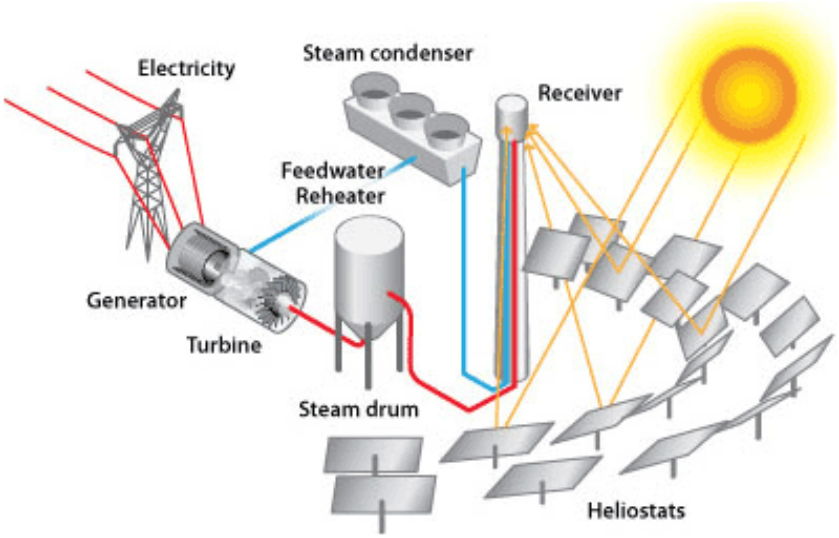

Fig. 5. Schematized operation of a Power Tower CSP technology type (U.S. Department of Energy, 2013).

Evidently, the operation of this power facilities is restricted to the periods of radiation and its variability during the day, nevertheless, the inclusion of a thermal energy storage system (with a possible oversize of the solar field) allows continuous and stable generation, even during periods of absence of solar energy (Castro, 2012), making this technology a manageable alternative, feature that is not present on many other renewable energy systems (especially solar PV and wind). Also, hybridization can be an option for the commercial facilities focused on thermal energy production, using fossil fuels or biomass backups when the solar field does not supply enough energy. Hybridization is also can also be relevant for the start-up of the power plant and its nighttime operation.

Concentrating Solar Thermal systems are composed of several subsystems in charge of specific functions: radiation concentration system, reception system, power conversion system, and in some cases thermal energy storage systems. Its characteristics depend on the type of technology and application, as will be seen ahead (Silva M. , 2002). The first system is constituted by the array of mirrors and trackers, which are responsible for the reception and convergence of the radiation into the reception

system; where the enthalpic increase of the HTF occurs. The energy obtained is then used as required: electricity generation or process heat.

As previously referred, CST systems are divided in two major groups, according to the concentration technique: linear focus and point focus. Focal line systems include the Parabolic Trough and the Lineal Fresnel Reflectors, while the focal spot variant is represented by the Solar Tower and the Parabolic Dishes. Guiding the mirrors to a single point, as in focal spot concentration, induces considerably high temperatures in the receiver, due to high rates of concentration. On the other hand, in the focal line variant, lower temperatures are reached, considering the lower rate of convergence of the radiation and the more limited degree of freedom of the solar tracking system. A brief description of each available technolgy is presented next:

2.2.1.1 Solar tower

Also known as the central receiver tower, this CSP technology consists on hundreds or thousands of organized mirrors called heliostats that, with a 2-axis tracking system, reflect the direct solar radiation towards a focal point located in the top of a tower (Castro, 2012), as represented in Fig 5. Said tower supports the receiver where the HTF runs, getting considerably high temperatures (800-1000ºC, though current applications work around 400-600ºC range) due to the high rates of concentration (up to 1000 times), operating under reduced losses (Lovegrove & Stein, 2012), and presenting good conditions for thermal energy storage.

Along with the Parabolic Trough technology, the Solar Tower presents a high degree of maturity, with several commercial electrical plants operating in many countries. Fig. 6 shows *Ivanpah Solar Electric Generating System (ISEGS)*, a 392 MW (Gross capacity) facility located in Mojave Desert (USA).

Fig. 6. Ivanpah Solar Power Tower facility (BrightSource Energy, n.d.)

2.2.1.2 Parabolic Dish system

As seen in Fig. 7, they are focal spot systems composed basically by two elements: a paraboloidal mirror that works as the concentrator, and a point receiver, where it is possible to heat a

HTF or produce electricity directly (Joga, 2012). Schiel & Keck (2012) add that five elements can be considered: a parabolic concentrator, a tracking system (2-axis), a solar heat exchanger (receiver), a control unit and an optional Stirling engine. Therefore, it is evident that the technology can provide either process heat or electricity, this last is generated directly in each module in an engine working under the Stirling cycle or by coupling the system to a small gas turbine.

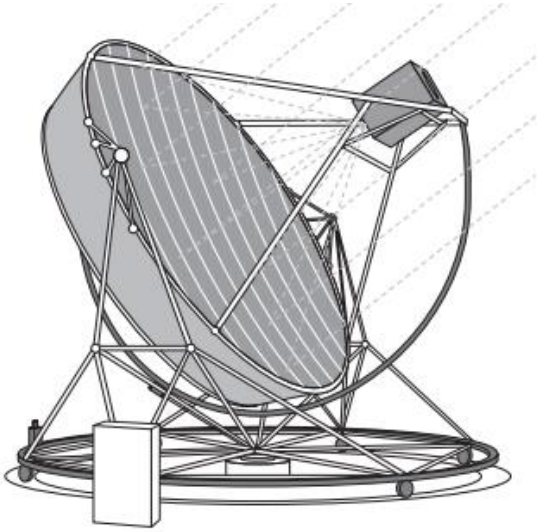

Fig. 7. Schematic representation of the Parabolic Dish solar system (Schiel & Keck, 2012).

Dish Stirling arrangements are suitable to support small and large grid connected systems, as well as stand-alone applications, since they are modular installations (10-25kW), easy to couple in irregular topographies (Schiel & Keck, 2012). Note that they have the highest concentration ratios (1500-4000) among all the available technologies.

2.2.1.3 Parabolic Trough

Its energy transformation process follows the basic principle previously described, though with the particularity of linear focus concentration; in this matter, Castro (2012) adds that the solar energy is collected in great parabolic curved mirrors (Fig. 8), capable of tracking the sun in one axis; directing it to an absorber tube, where temperatures can reach the 400ºC scale. Additionally, Lovegrove and Stein (2012) state that the assembly of the mirrors and the receiver is mounted on the same frame.

Inside the tubes, the HTF receives the concentrated energy as it flows through it; until reaching a certain temperature. At this point, it fulfills the conditions to supply heat for a thermodynamic cycle or any industrial process, whether directly or indirectly, depending on the HTF and the process fluid (if that is the case).

Parabolic trough CST technology presents the most mature development between the four technologies, with several commercial plants in operation and many systems providing process heat around the world, therefore, it represents a good alternative for integration in industrial applications.

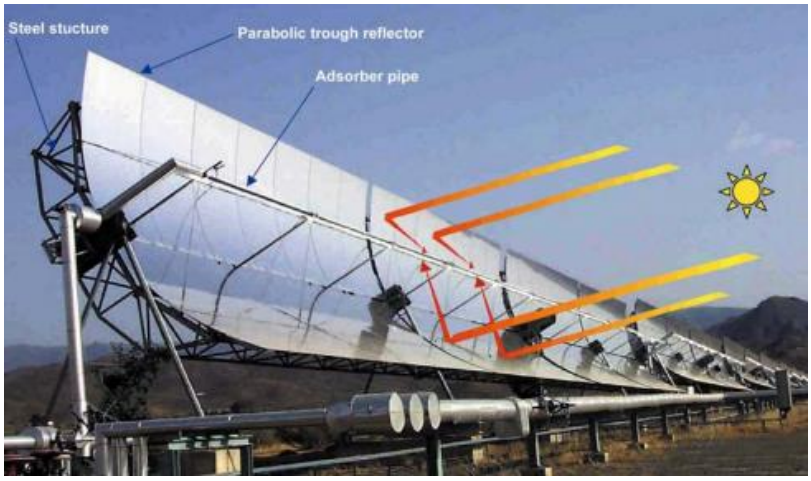

Fig. 8. Assembly of mirrors and receiver of a Parabolic Trough system (Kearney, 2007).

2.2.1.4 Linear Fresnel Reflectors

Solar thermal systems with this technology operate under the same principle used in Parabolic Trough facilities, this is, concentrating energy in a focal line. In this case, rows of almost flat rectangular mirrors, that follow the position of the sun, reflect the radiation in a stationary (fixed) tube that is placed a few meters above. Likewise, the mirror array moves independently on one axis (Lovegrove & Stein, 2012). Thus, it is differentiated by the mode of assembling the receiver and the collectors, as can be seen in Fig. 9.

Joga (2012) states that if this system is compared with the Parabolic Trough, the solar field area required is considerably smaller, bringing the investment costs to lower values. The same author indicates that the heat transfer fluid for this systems is currently restricted to water for a Direct Steam Generation, thus eliminating the necessity of heat exchangers, nevertheless, the steam temperature in the output is lower than the one obtained in the other technologies (300-400ºC range), limiting the thermal storage capacity potential. From the point of view of commercial operation experience, it is less developed than the parabolic trough, but as seen from its characteristics, Fresnel technology has a considerable potential for several applications.

Fig. 9. Linear Fresnel Reflector from the Solar Down facility (Rajasthan, India) (AREVA Inc., 2012).

2.2.2 Parabolic Trough Concentrating Solar System

A brief description on the Parabolic Trough technology was already presented, nevertheless, detailed information should be introduced since the integration process is focused on this variant.

To begin with, a simple explanation on the technology is given by Zarza (2012), who states that "the larger collector aperture area concentrates reflected direct solar radiation onto the smaller outer surface of the receiver tube, heating the fluid that circulates through it. The solar radiation is thus transformed into thermal energy in the form of sensible or latent heat of the fluid", this thermal energy is then used to feed an industrial process or a power cycle to produce electricity, as in its first commercial CSP application back in 1984 (ESTELA, 2010).

The called PTC (from the term Parabolic Trough collectors) facilities consist of modular arrays of single-axis-tracking collectors disposed in many parallel rows, which compose solar fields of hundreds or thousands of assemblies usually aligned in a North-South axis disposition (NREL, 2010). The commercially available systems include large and small collector schemes; the large ones are evidently of higher dimensions and considerable aperture areas and aimed at the electricity generation. One example is the Eurotrough collector design, that appeared as the result of a 1998 European consortium focused on PTC development for CSP.

Fig. 10. Solana Generating Station. Power block and TES in the center (ABENGOA SOLAR, 2013).

Concentrating Solar Power plants based on the large collector Parabolic Trough technology have been around for decades, reaching remarkable capacities and features. Tens of facilities are currently in operation and under development, given the good results obtained after years of generation. Nowadays, the average power capacity among plants is around 50 MWe, though technical advance in the area, generation flexibility features and environment-friendly politics made larger projects possible. Noticeable examples are the *Solana Generating Station* (Fig. 10)*, Genesis Solar Energy Project* and the *Mojave Solar Project*, all located in the United States and with a nominal installed capacity of 250 MWe. Another remarkable project is the *Pedro de Valdivia* project, a 360 MWe plant currently under development in Chile (NREL, 2016).

On the other hand, small collectors were developed for process heat applications, considering the lower heat demand if compared with CSP power plants. A wide range of industrial applications could

be covered by this alternative: agricultural sector, food industry, biofuel production, desalination, among others. Concerning the collector design, several were developed according to the temperature required, so the materials and dimensions are suited for the specifications (Zarza, 2012).

Solar systems design companies like *SOLITEM GmbH* develop small collectors (as shown in Fig. 11) for process heat applications in the industrial and commercial field. Its currently designed PTCs operate between temperatures of 100 and 250ºC, with aperture widths going up to 5 meters. It is relevant to state that in the SHIP Database, most PTC solar process heat systems employ small schemes, presenting a wide range of operating temperatures, reaching 250ºC of maximum value in the solar loop. (AEE INTEC, 2015).

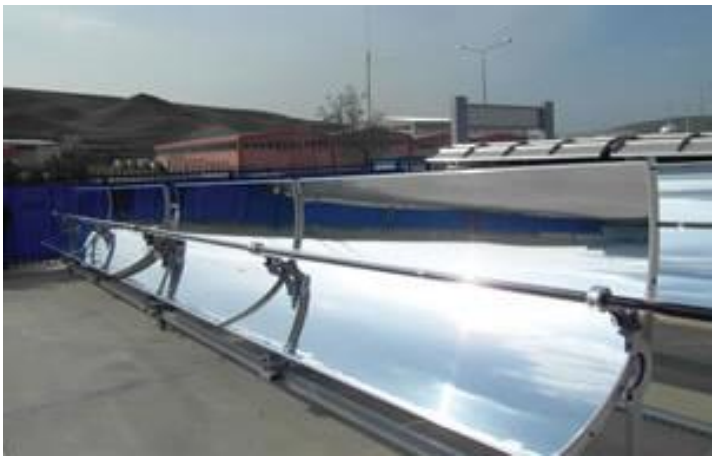

Fig. 11. Solitem PTC 1100 (Solitem, 2013).

2.2.2.1 Technical features of the Parabolic trough collectors

Each collector assembly is composed of a set of subsystems: concentrator structure, mirrors or reflectors, linear receiver and the collector balance of the system. Brief considerations on the subject are presented below:

- **Concentrator structure**: in other words, the skeleton of the collector, which supports the rest of the equipment in an optical alignment, namely the mirrors and the receiver. It is designed to resist the external conditions (e.g., wind), while allowing its own rotation so the reflector and receiver are able to track the sun (NREL, 2010).
- **Reflectors:** parabolic shaped mirrors constituted by a glass with a reflective support, responsible for the reflection of the radiation into the focal line. They can be manufactured with fine or thick glass (Bianchini, 2013) of high transmittance, and usually with a silver layer on its backside, achieving solar specular reflectivity of around 93.5% (NREL, 2010). Alternative concepts are under research and development tasks aiming to reduce costs and improve reliability and performance.
- **Linear receiver:** represents the heat collection element and it is located at the focal line of the parabolic mirror, where the HTF is heated as it flows through it. The receiver is composed of two concentric pipes (as seen in Fig. 12), the inner one is made of stainless steel and it contains the HTF, while the surrounding one is a low-iron borosilicate glass with an anti-reflective coating, with the purpose of maximizing the solar transmittance. The steel pipe is also covered with a solar

selective absorber surface, which provides high solar absorptance and low emittance of the infra-red radiation (Zarza, 2012). In some cases, between the pipes there is a vacuum-tight enclosure that significantly reduces the heat losses (NREL, 2010).

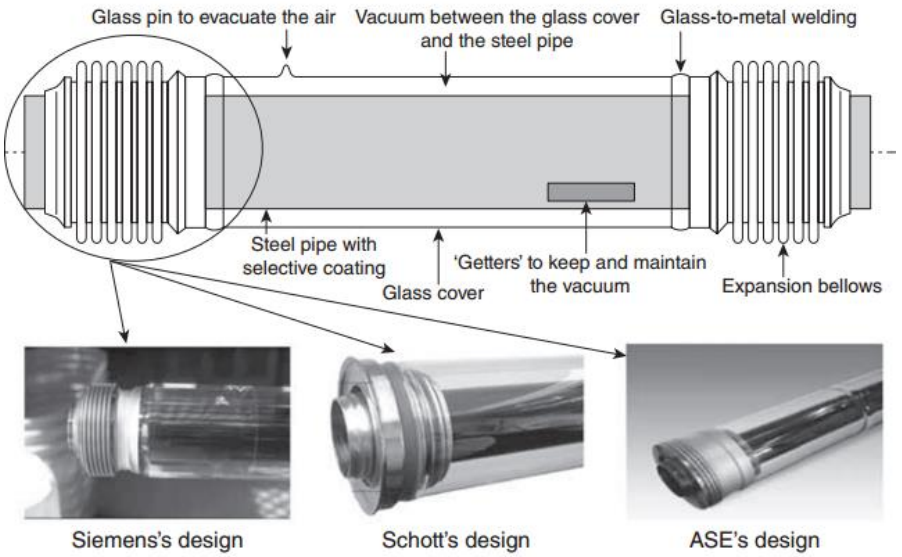

Fig. 12. Common receiver of a PTC (Zarza, 2012).

- **Collector balance of the system**: includes some other key components in the solar field: pylons and foundations that provide support for the structure, drives that position the collector to track the sun, controls responsible for tracking and operation parameters monitoring, and collector interconnect, that links the mirror assemblies allowing them to move independently (NREL, 2010).

Energy conversion efficiency

The energy conversion process starts with the incoming solar energy and ends with useful thermal energy delivered in the output. Evidently not all the energy that reaches the collector is transformed into heat, since energy losses occur during the process. These losses come from three different sources, as stated by Zarza (2012):

- Optical losses: due to mirror reflectivity, intercept factor, glass transmissivity, and absorptivity of the steel pipe. Represented by the optical efficiency ($\eta_{opt,0^\circ}$).
- Geometrical losses: influenced by the incidence angle (If existing). Represented by the IAM ($K(\varphi)$).
- Thermal losses: occurring in the receiver pipe, usually quite reduced. They follow the heat transfer laws. Represented by thermal efficiency (η_{th}).

Concerning the latter, Fig. 13 represents an overall energy balance of a collector loop, showing the sources of losses mentioned (The order of the above list respects the actual order of the losses).

Other aspects could be considered to estimate the efficiency of conversion of a PTC, such as the soling factor, which indicates the ratio of difference between real operation and a fully clean collector operation. However, optical losses are usually the most significant among the rest. Overall efficiencies for commercial plants are normally high for high temperature operation, specifically around 70%, while

for industrial or low temperature applications, efficiencies are found between 50 and 65 % (for a 250ºC operation) (Zarza, 2012). One can say that the efficiency depends on the conditions of operation and the design parameters of the collector, though most current systems present close efficiency values.

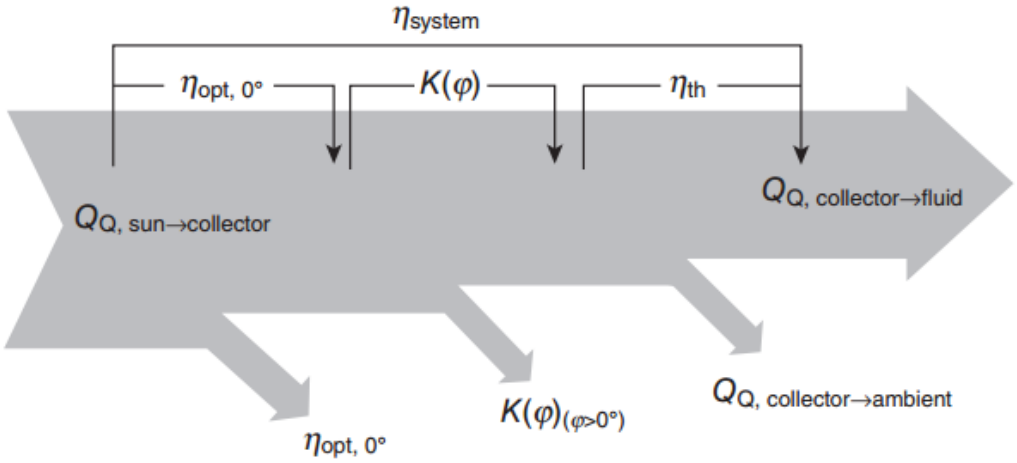

Fig. 13. Overall energy balance of a PTC represented in terms of the efficiencies (Zarza, 2012).

Heat transfer fluids

Being in charge of receiving and transporting the energy for the process, the HTF selection is crucial in any Parabolic Trough facility, having a strong influence on its efficiency and design. Heat transfer fluids need to have a high thermal capacity without losing its physical and chemical characteristics, i.e. not degrading at the temperature it is required to work under (Bianchini, 2013). Benoit, Spreafico, Gauthier, & Flamant (2016) add that they require high thermal stability, high thermal conductivity and a broad operating temperature range.

Single-phase liquids provide the best heat transfer coefficients and stable operation, so commonly, PTCs use thermal oils for temperatures above the 200ºC mark, while for lower values, a mixture of water/ethylene glycol or pressurized water is usually utilized. Direct steam generation in the PTC has also been a subject of study, proving its feasibility in future uses (Zarza, 2012). Development has been relevant in this area, where the performance research activities are focused on discovering more efficient fluids for heat transfer. A set of current and under development HTFs for tube-receiver technologies is listed below (Benoit, et al., 2016) followed by Table 3, which contains the operating temperatures of some of them:

- Liquid HTF:
  - Thermal oil: Therminol VP-1, Dowtherm, Therminol 66, etc.
  - Molten salts: Solar Salt, HITEC, HITEC XL, etc.
  - Liquid metals: liquid sodium, lead-bismuth eutectic, etc.
- Gas HTF:
  - Pressurized gases: air, CO_2, He, H_2.
  - Supercritical fluids: s-CO_2, s-H_2O.
- Water/Steam.

- Particle suspensions as a heat transfer media.

Table 3. Operating temperatures of liquid HTFs and particle suspensions (Benoit, et al., 2016).

Heat transfer fluid	Temperature range [°C]
Thermal Oil	
Therminol VP-1	12–400
Molten salts	
Solar salt	260–600
HITEC	140–530
HITEC XL	130–550
Liquid metals	
Na	98–883
LBE	125–1670
Particle suspension	
SiC	No lower limit-1800

Thermal energy storage

As known, solar energy suffers from the available solar radiation variability issue, which limits its development for certain processes. Thermal energy storage (TES) is crucial to address short and long term fluctuations, allowing dispatchable and stable energy supply from the solar system. In this matter, some CSP power plants have been designed to operate after daylight hours, reaching continuous 24-hour generation (The case of *Gemasolar* facility in Spain). Usually, the integration of the TES is complemented with the increase of the solar field size, to be able to produce an excess of thermal energy during the day, and use the stored fraction when required (Bianchini, 2013).

Thermal storage systems save the heat received by the HTF by using fluids of remarkable thermal properties and benefiting from sensible or latent heat and thermochemical storage (Pareja, 2012). Current electrical power generation applications usually dispose a molten salt system (sensible heat to avoid phase change), stored in a cold and a hot tank.

In general, TES system design depends on the type of CST technology and the HTF, though in general they could all present the following configurations (Bianchini, 2013):

- Direct or indirect systems: the first uses the HTF itself as a storage medium, while the second one uses different fluid that exchange its energy.
- Two tank or single tank disposition: the two tank approach stores the hot and cold fluid separately. On the other hand, in the single tank the fluid regions are separated by its density (considering the temperature gradient).

Note that the capital costs of the solar facility increase with the addition of the storage capability, since the oversize of the collector field (if applied) and the inclusion of heat exchange equipment and storage tanks represent substantial monetary values.

For the PTC case, specifically for power plant applications, molten salts have been used as the storage medium in the indirect two-tank configuration, being a reliable and efficient solution.

2.2.2.2 Design of a parabolic trough solar field

A few considerations to be taken into account during the design of a Parabolic Trough solar field are presented below, specifying for an industrial process integration:

- Three phases are relevant in a PTC solar field design: definition of the design point, calculation of the number of collectors to be connected in series on each row, and calculation of the number of parallel rows of the field (Zarza, 2012).
- The rated thermal output power from the solar field, as well as its inlet and outlet temperature are determined by the needs of the thermal industrial process.
- For industrial process heat applications, the solar field outlet temperature must be at least 15ºC higher than the steam temperature required, to compensate thermal losses that occur in the heat transport and exchange (if existing) processes. It also compensates the boiler pinch point and provides a temperature differential (Zarza, 2012).
- The selection of the HTF influences the design of the system and its integration to a certain process.

2.2.2.3 Parabolic trough system costs

CST systems, whether intended for process heat or electricity generation, involve high initial investments to later benefit of practically cost free energy. However, the much required maintenance also plays a role in the operation costs.

Among the components of a PTC power plant, the solar field is by far the costliest subsystem, representing between 35 and 49% of the total installed costs of the project (as seen in Fig. 14), where energy storage introduction is also responsible for a significant share of the investment costs (IRENA, 2012). Regarding the cost breakdown of the solar field components, the chart presented in the right side of Fig. 14 exposes that the structure of the PTC accounts for the greatest share of costs.

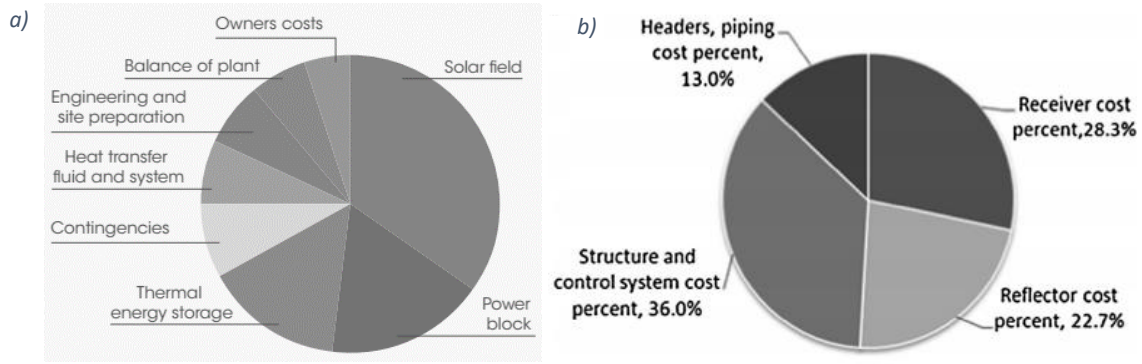

Fig. 14. Costs breakdown of a PTC power plant (a) (IRENA, 2012); Cost breakdown of the solar field of a PTC power plant (b) (Mokheimer, Dabwan, Habib, Said, & Al-Sulaiman, 2014)

Regarding the solar process heat at industrial applications, 50 to 70% of the total cost is related to the capital costs, while the rest covers the installation and integration. On a more specific approach, the solar field cost breakdown is said to be distributed as follows: over 50% for collector and its

installation, piping over 20%, buffer storage and heat exchange equipment around 11%, and control systems close to 5% (IEA-ETSAP & IRENA, 2015).

Economic performance reports have been published by specialized organizations like IRENA or IEA, based on the analysis of existing integrated facilities. The latest reports show a general energy average cost of 0.02-0.05 €/kWh for low temperature, while for medium temperature, the value is between 0.05-0.15 €/kWh. For parabolic trough systems specifically, the heating costs are in the range of 0.06-0.09 €/kWh while the capital costs are close to 600-2000 USD/kW, compared to the 3400-6000 USD/kW of parabolic trough power plants. It is important to state that the costs depend on the temperature level, demand continuity, size of the system and the radiation of the location (IEA-ETSAP & IRENA, 2015), therefore, the capital and heat costs obtained for a specific case scenario might not be within these range of values.

2.3 Integration of solar heat into industrial processes

As previously claimed, solar thermal has the potential to satisfy the heat demand of industrial processes. “Currently 120 operating solar thermal system for process heat are reported worldwide, with a total capacity of about 88 MW (125,000 m^2)” (Jebasingh & Herbert, 2016).

General information on integration of processes is described, followed by an approach focused on the solar heat integration, and its basic methodology. The possible system concepts are addressed to finally conclude with a set of examples of existing applications of solar energy into a manufacture process.

2.3.1 Process integration

Before addressing the solar integration subject, a brief definition of process integration is presented: “Systematic and general methods for designing integrated production systems, ranging from individual processes to total sites, with special emphasis on the efficient use of energy and reduction of environmental effects” (Gundersen, 2000).

In a procedure of this kind and according to Gundersen (2000), one of the first and fundamental stages is the establishment of objective performance targets before going to the design phase, for example; minimum total annual cost target, or minimum heat consumption from fossil fuel sources, etc. The same author states that three major features in methods are found for process integration: heuristic approach (about design and economy), thermodynamic, and optimization techniques. Combination of the features in current methods is used is a tendency used nowadays.

Concerning the industrial applications where said approaches can be utilized, the following ones are interesting for the proposed study: retrofit projects, improvement of efficiency (related to energy and material utilization), integration between processes and energy, and addressing of operability issues (flexibility, controllability, etc.). As the solar system is set to retrofit the existing ECA manufacture line, note that the “best retrofit projects are the ones that combine pure energy saving features with more general plant modifications” (Gundersen, 2000).

2.3.2 Solar heat integration

Many possibilities exist on the combination of an industrial process with a solar thermal plant, each one has advantages and disadvantages that need to be evaluated. The alternatives will determine the use of different equipment and components that have a direct impact on the final layout of the process, as well as on the investment costs, which should be reduced as much as possible (if the performance target is set that way). For the technical side, remember that the introduction of the solar energy supply should not interfere with the existing process operation, therefore the final design should be a trade-off between these considerations (Frein, Calderoni, & Motta, 2014).

According to Brunner (2015), when integrating solar heat into any industrial process the goal is to identify the most technically and economically adequate integration point and integration concept. These terms will be addressed frequently, hence brief definitions are included as follows:

- Integration point: “specifies a heating demand within an industrial or commercial plant that can be partly supplied by solar heat (Muster B. , 2015). For example, heating of an industrial process medium.
- Solar heat integration concept: refers by which point of the process (heat exchanger and hydraulic connection) solar heat can be transferred to it, considering the existing heat supply technology (Muster B. , 2015). For instance: Direct steam supply, hot water supply via an external heat exchanger, etc.

Introduction of solar heat is feasible at several stages of the heat supply and distribution network of a production facility, as represented on Fig. 15. The distribution network can be characterized as the process level of the plant regarding heat transfer to unit operations. Knowledge on the existing equipment in heat exchange, handling and control is crucial to understand how solar heat can be integrated into this level. On the other hand, supply level is associated with the operations of heat generation and distribution, also relevant for the integration methodology (Brunner, 2015).

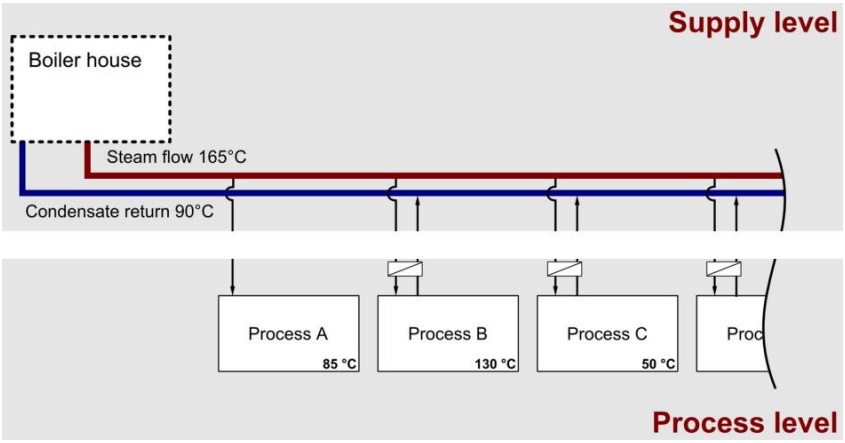

Fig. 15. Supply and process level representation of a system using steam as the medium (Lauterbach, n.d.)

Comprising the last paragraph in a sentence: a key aspect for solar potential in a process is its existing layout, regarding heat demand and required temperatures. Current drivers and barriers for the

deployment of solar system in industries are listed below, as summarized by the IEA-ETSAP and IRENA (2015):

- Drivers:
  - Risk reduction with increasingly volatile and rising prices of fossil fuels.
  - Fuel costs removal from the cash flow.
  - Reduction of emissions: following the current global trend.
- Barriers:
  - Still high investment costs and lack of finance alternatives.
  - Subsidies for fossil fuel in some countries.
  - Public awareness, regarding the current lack of sufficient information at disposal.
  - Lack of suitable design guidelines and tools. Though the results from Task 49/IV and Task 11.1 are aiming to overcome this issue.

2.3.2.1 Conventional heat supply of processes

Generation of energy as heat in industrial applications is characterized by the use of a group of HTFs and fuels. Usual heat transfer media comprises the thermal oil, saturated steam, superheated steam, pressurized hot water and air. Fuels burned include coal, gas, LPG, oil, biomass and biogas. Other sources like district heating or electrical driven heat process are also used (Muster, Schmitt, & Schnitzer, 2015). Storage is also relevant in this applications, acknowledging that its main target is to balance load demand and supply if required, whether at supply or process level. Common storage types involve: hot water, steam storage, latent and thermochemical heat storage.

In a general line, industrial and even commercial processes deliver the required heat in the next conventional forms:

- Heat exchangers: as known, they are devices used to efficiently transfer heat from two or more mediums that are at different temperatures (Stewart & Lewis, 2013). Two variants found: internal or external, though the last ones are used the most; whether the tubular, compact or extended surface heat exchanger.
- Direct heating system: through direct combustion or steam injection.
- Evaporators and dryers.
- Heat pumps.

2.3.2.2 Solar heat integration concepts

Based on the solar heat integration concept definition earlier exposed, the identification of possible integration concepts is performed. Concepts are classified according to its level of integration and type of consumer (for process level), and composed of the earlier described conventional industrial components. Table 4 summarizes the possible integration concepts for Solar Heating applications.

Since the production line of Expanded Cork Agglomerate is the focus, the integration concepts that seem to be suitable for it are detailed in the following subsections, in accordance to the Solar Heat Integration Guideline (Muster B. , 2015) and the general concepts from Table 4.

Table 4. Summary of possible integration concepts for solar heat process (Schmitt, Classification of integration concepts, 2015).

Level of integration	Heat transfer medium		Conventional way of heating		Solar heat integration concept	
Supply Level	S	Steam			PD/PI	parallel integration (direct or indirect)
					FW	heating of feedwater
					MW	heating of make-up water
	L	Liquid			PD/PI	parallel integration (direct or indirect)
					RF	return flow boost
					SC	heating of storages or cascades
Process level			E	external heat exchanger	PM	heating of process medium
					IC	heating of intermediate hot water circuit
					HB	heating of bath, machinery, or tank
					IS	heating of input streams
			I	internal HEX		
			S	steam supply	V	vacuum steam
					LP	low pressur steam

For high temperature steam requirements (above 150ºC), and where concentrating collectors are the chosen technology, the following concepts are suitable. Notice the selection of integration concepts that account for the process level.

Direct solar steam generation

As the name suggests, the steam is produced directly in the solar field, by using water as the HTF. Represented in Fig. 16, note the use of a steam drum to separate water-steam mixture, and the presence of a steam boiler apart from the solar field (hybridization approach). The condensate return is not an option for the ECA production line, since the steam has great dirt and resins content once it exits the autoclave.

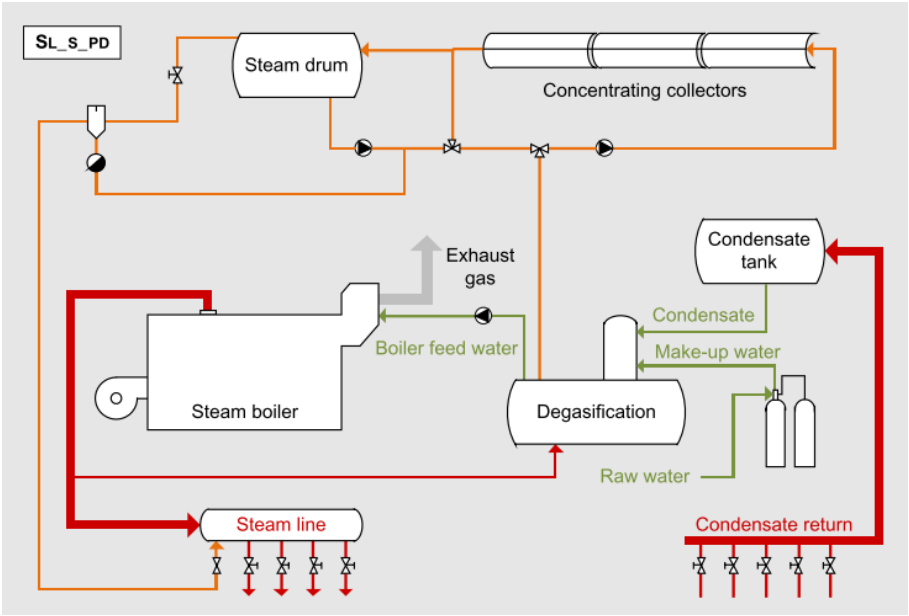

Fig. 16. Representation of the Direct Solar Steam Generation (Schmitt, Classification of integration concepts, 2015).

Indirect solar steam generation

Similar to the previous one, but with the particularity of an inclusion of a heat exchanger between the conventional steam line and the solar field. In this case, the collector can operate with a different HTF (Fig. 17).

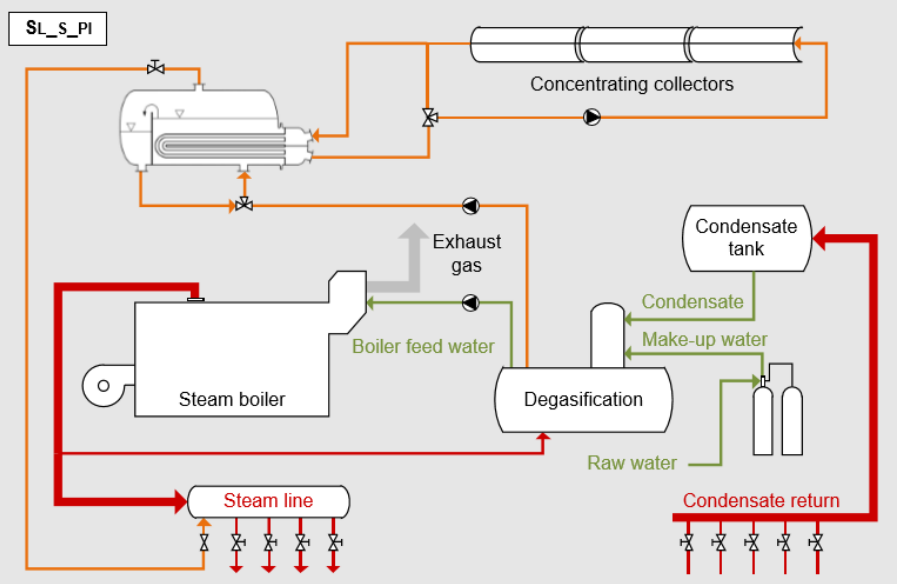

Fig. 17. Representation of the Indirect Solar Steam Generation (Schmitt, Classification of integration concepts, 2015).

Solar heating of boiler feedwater

This alternative could also be an interesting approach for the proposed integration, since a reduction in the biomass consumption in the boiler is attained. The concept is well explained in the diagram of Fig. 18.

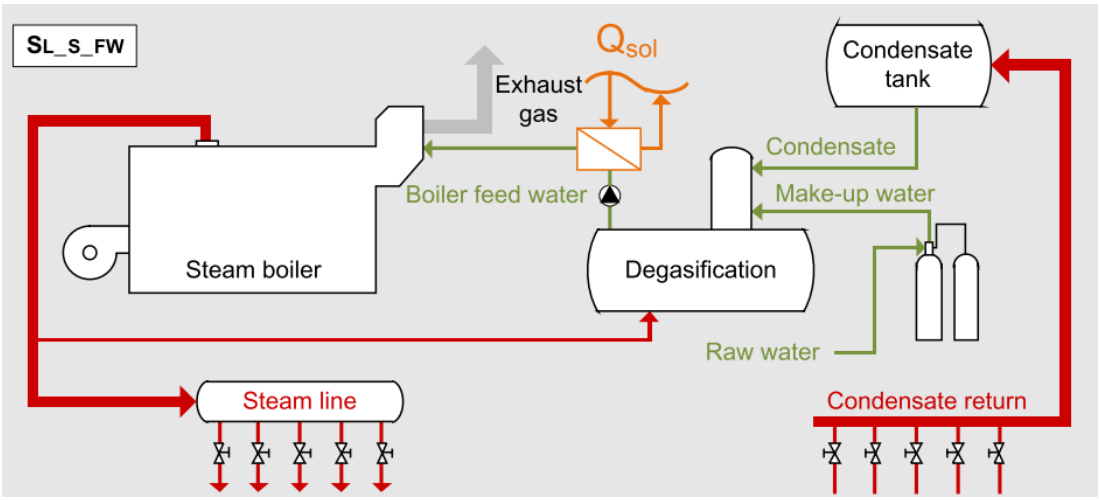

Fig. 18. Representation of the Solar Heating of boiler water (Schmitt, Classification of integration concepts, 2015).

Concerning the process level steam supply, none of the integration concept alternatives are suitable since their ranges of temperature are low (up to 135ºC), which is evidently far from the values

managed by the autoclaves. A process level concept like low temperature pre-heating could be analyzed but it is not, a priori, the scenario to address.

2.3.2.3 Solar process heat system concepts

Based on the integration concepts adequate for the planned integration, a set of specific systems that might be suitable can be designed. According to Helmke & Heß (2015), SHIP systems are subdivided into five different sections: collector loop, charge, storage, discharge, integration point and conventional process heat. Some systems might not include part of them, for instance without storage, the link between the integration point and the collector is direct. This information is easier to comprehend when looking at the subsection connection represented in Fig. 19. For detailed information on the components of each system, revision of the Integration Guideline section written by Helmke & Heß (2015) is recommended.

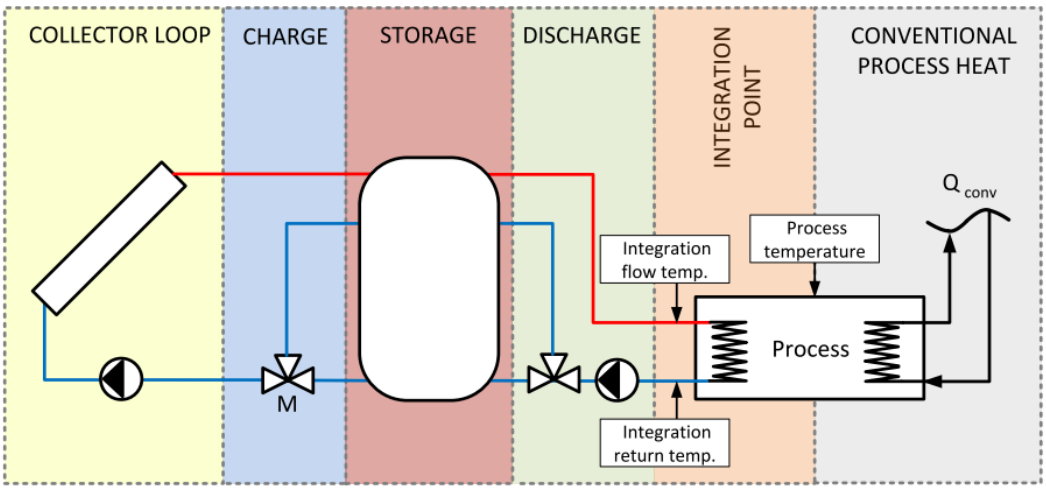

Fig. 19. General SHIP system for heating applications (Helmke & Heß, 2015).

2.3.2.4 Integration point identification

Several parts of the industrial process could be linked with the solar field, i.e., specific unit operation or heat sinks can be supplied with solar energy. However, it is not an easy task to select one of them as the final choice for the design, since each one might present different benefits. Note that this is one of the most important steps in a solar integration application, as mentioned by (Muster B. , 2015).

Many aspects should be taken into account to establish the point where the integration is most beneficial, both technically and economically. These aspects might always depend on the specific process configuration. For detailed integration point definition procedure and examples, consulting the guidelines written by Hassine (2015) is recommended.

2.3.3 Solar Heat Process Integration Assessment Methodology

Now that the solar integration basics were addressed, a step-by-step methodology to assess a process integration feasibility study is presented below (Table 5), along with some relevant comments on the stage. The phases can be divided into three major groups: pre-feasibility assessment, feasibility

study and decision/further activities (Schmitt, Assessment Methodology for Solar Heat Integration, 2015).

Table 5. Assessment methodology for SHIP. Constructed with data from (Schmitt, Assessment Methodology for Solar Heat Integration, 2015).

	STEP	COMMENTS
PRE-FEASIBILITY	Basic Data Acquisition	Preparation of questionnaire to obtain data from company.
	Preparation	Get an overview of process related information and review reports of performed projects of this kind.
FEASIBILITY STUDY	Company visit	Collect all the required information from the company (including production flow, heat supply system, etc.)
	Analysis of status quo	Estimation of energy consumption of single sections or processes Crosscheck data with available benchmarks
	Process optimization and energy efficiency	Highlight energy saving and energy recovery potential
	Identification of integration points	Apply a set of established criteria to the processes with heat demand, to define possible points of integration.
	Analysis of integration points	Identification of equipment and integrated plant parameters (technical and economic)
DECISION/FURTHER ACTIVITIES	Decision	Discussion of possibilities with the company
	Detailed Planning	Start detailed planning according to the decision, repeat some previous steps if required

2.3.4 Examples of existing SHIP facilities

The already mentioned SHIP database presents tens of examples of solar energy use in various industrial processes of different natures. A couple of PTC integrated installations and projects are described below. Special mention to the use of solar energy in a cork industrial process is made.

- Frito-Lay Inc.: for the Arizona located food plant, a considerably big project was developed with the aim to reduce the natural gas demand during peak summer days, by approximately 20%. With an installed power close to 3500 kW_{th}, the Direct Steam Generation concept produces at a temperature of 243ºC in its 384 PTCs. The integration point is the steam production for heating the oil to fry potato chips (AEE INTEC, 2015) (Ruby, 2010).

- Alanod factory: inserted in the metal product manufacture area, specifically in the high reflective surface-finished aluminium coil production. This German facility employs saturated steam at 4 bar and 143ºC in its process, coming from a 108 m^2 PTC solar field. The integration point is heating of a supply line and its integration concept is direct parallel integration in the existing steam line (AEE INTEC, 2015). Fig. 20 shows the collectors mounted on the roof of the plant.

Fig. 20. Alanod PTC facility (Lauterbach, n.d.).

- *Design and simulation of a solar field coupled to a cork boiling plant*: as seen in the cork industry overview, several process exist according to the type of product to manufacture. In this matter, Biencinto, González, Valenzuela, & Fernández (2014) performed a design and simulation of the inclusion of a solar thermal system into the production process of cork in an industry located in Spain; the specific process is the cork boiling, which consist of cork immersion for approximately one hour in boiling water (100ºC). The diagram of production is represented in Fig. 21.

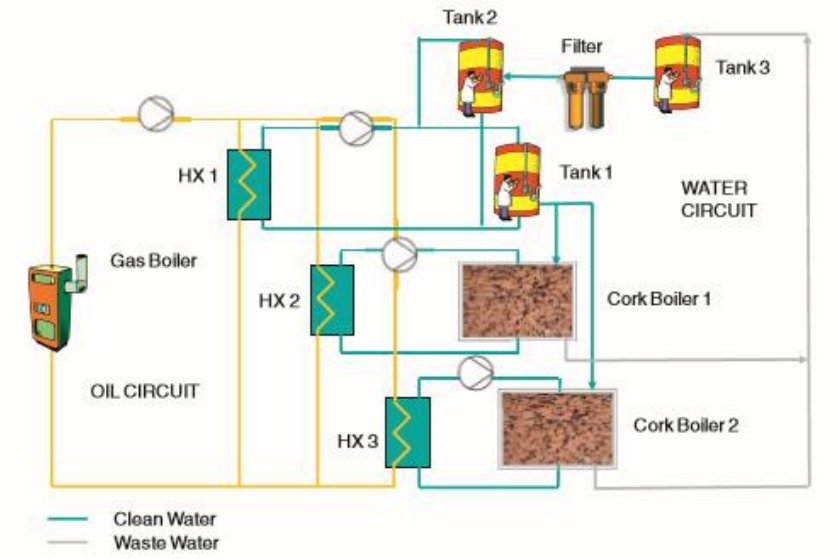

Fig. 21. Cork boiling process of ECOTRAFOR (Biencinto et al., 2014).

The collector used is not a parabolic trough system, but a fixed mirror solar concentrator with rotatory absorber. Even though this project does not involve ECA production or high temperature PTCs, it still is a good example of the potential of SHIP systems in the cork industry, while

resembling the general approach to be performed by the proposed subject. Notice the fact that a modeling of the solar field and process was performed in TRNSYS. The conclusions of the project showed that “this kind of solar installations would help the cork industry to reduce fossil fuel consumption, providing that the involved process is able to be adapted to the solar power conditions” (Biencinto et al., 2014).

Consulting the SHIP Database (AEE INTEC, 2015) is recommended if more information regarding the globally installed integrated systems is desired.

2.4 Software modeling and analysis of CST systems

This section addresses the available tools to simulate and analyze the behavior and performance of Concentrating Solar Thermal systems under a certain transient condition, whether in an electricity generation approach or in industrial process heat applications. Available alternatives for Parabolic Trough technology are included, with special emphasis on the TRNSYS software and its codes. The most commonly used tools between the currently available CST design and simulation options are listed by Mason (2011) as follows: SAM (System Advisor Module), Greenius, Thermoflex, IPSEpro, Ebsilon Professional and TRNSYS.

If an analysis on the concentrating solar thermal system components is contemplated, specific software is available, as categorized by Ho (2008):

- Solar collectors: ASAP, CIRCLE, FLUENT, SOLTRACE, TROUGH HELIOS.
- Heat transfer fluid and its handling: FLUENT, SAM, SOLERGY, TRNSYS.
- Total system performance: EXCELERGY, SAM, TRNSYS.

2.3.1 TRNSYS Software

It is defined as a software platform that allows the user to model different transient systems using modular components, each one of them represents a physical process or feature in the system, and they can be developed and added if required (Ho, 2008). The program is open source and uses the FORTRAN source code (Mason, 2011). “A component reads in a text-based input file and provides output through the solution of algebraic or differential equations” (Ho, 2008). Specific processes can be modeled as well as total-system performance analyses. Post-processing via graphing and reporting is also included in the platform (Ho, 2008).

The success of the program relies on its many features, which make it one of the most flexible energy simulation tools available. The most remarkable characteristics are listed below (Mason, 2011):

- The user can model almost any component or thermal cycle. If it is not included the user can develop the model and add it to the library.
- Includes control and operation strategies as part of the internal model.
- Validation study and quasi-dynamic analysis capability, as well as sensitivity analysis possibilities.
- Allows the input of meteorological data.
- Possibility of linking the results with an external software, like MS Excel or MATLAB.

Regarding the library, it includes a great amount of components from several areas of the engineering simulations. Relevant units for this case study are: solar thermal collectors, heat exchangers, thermal storage equipment, hydraulics, controllers, among others.

2.3.2 Parabolic trough system modeling in TRNSYS

The library of components of the program contains specific subsystems that constitutes parabolic trough or other CSP systems. Total-system routines are also inserted, specifically for power plant applications. According to Mason (2011), the parabolic trough power plant code included is based on the empirical model established by Frank Lippke in 1995, during the development of its study: *Simulation of the part-load behavior of a 30 MWe SEGS plant* (Type 396, solar field model, STEC). When looking at the embedded library, two subsections of the library are highlighted for the PTC case: the high temperature solar component library, and the solar component library. Other databases are also relevant if specific components are set to be introduced in a precise model (e.g. controller components, optimization components, utility components, etc.). From the two stated libraries, a couple of relevant codes are mentioned in Table 6.

Table 6. Relevant TRNSYS solar components (TESS, n.d.).

Library	***Component***	***Description***
High Temperature Solar Component	Type 1257	This subroutine models one or more concentrating parabolic trough solar collectors connected in series. The model accounts for the mass of the fluid in the absorber tube and the change in fluid properties with temperature.
Solar Library (TESS)	Type 536	Models linear parabolic concentrators used in high temperature applications. In the simplest form, fluid passes through a long evacuated tube that runs along an east-west axis and is horizontal to the plane of the ground or which runs on a north-south axis and is in a plane tilted with respect to the ground. Model based on theoretical equations developed in Solar Engineering of Thermal Processes (Duffie & Beckman, 2013).

Fig. 22 represents a scheme of the hybridization of a CSP plant with a biomass boiler; notice the use of the Type 1257 routine to model the solar field (highlighted in orange).

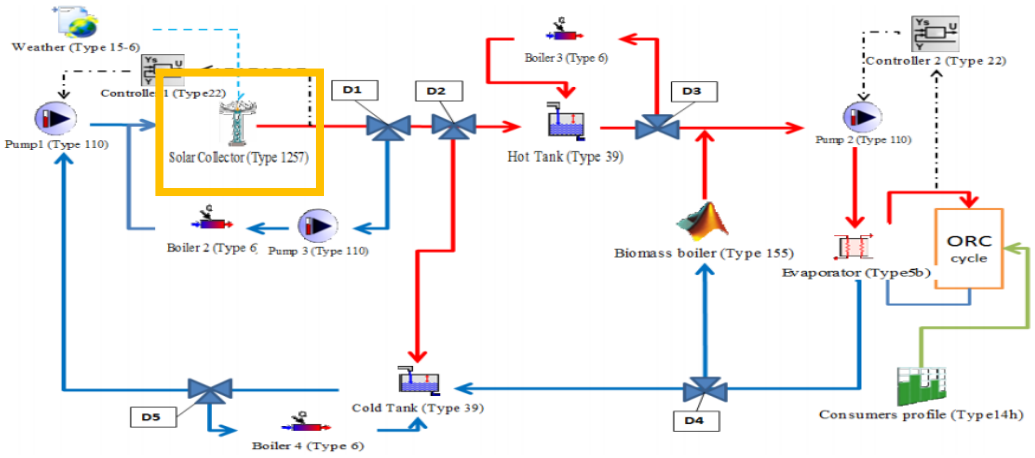

Fig. 22. Scheme of a hybrid CSP-Biomass plant (Flores, 2014).

A couple of published articles exemplifying the use of TRNSYS for Parabolic Trough transient analysis are described in Table 7, highlighting its flexibility concerning the designed model.

Table 7. Parabolic trough TRNSYS simulation examples.

Reference	*Title*	*Description*
(Jones, Blair, Cable, Pitz-Paal, & Schwarzboezl, 2001)	"TRNSYS Modeling of the SEGS VI Parabolic Trough Solar Electric Generating System"	Creation of a detailed performance model using the component library at disposal, allowing to model many different configurations. "Good agreement between model predictions and plant measurements was found, with errors usually less than 10%, and transient effects such were adequately modeled"
(Biencinto, González, & Valenzuela, 2016)	"A quasi-dynamic simulation model for direct steam generation in parabolic troughs using TRNSYS"	Describes and evaluates new simulation model for Direct Steam Generation in a Parabolic Trough plant. Steady-state approach is performed, though the model deals in a reasonable computing time with transient conditions such as start-up, shutdown and clouds. Performance was validated in the *Plataforma Solar de Almería*, Spain. New components were used, bringing long-term production analyses.

2.5 Economic performance assessments

Solar heat industrial integration projects involve the economic evaluation in its methodology. Moreover, the joint technical-economic feasibility studies are almost mandatory for any retrofit project, as the proposed case. Note that the results from the technical study have a direct influence on the inputs of this analysis.

Depending on the economic objectives of the project, performance assessment approaches vary, along with the type of indicators and the detail level of the analysis. At pre-feasibility stages, economic comparison relies on a specific cost of heat produced by the collector under the operation conditions defined (Giovannetti & Horta, 2016), considering the cost of the collector, the estimated annual energy, and the collector lifetime, obtaining what is called the SCOH (Simplified cost of heat). A deeper approach on performance includes known indicators: Internal Rate of Return (IRR), Net Present Value (NPV), Payback Period, and the Levelized Cost of Heat (LCOH) (Giovannetti & Horta, 2016), which is no more than the LCOE (Levelized Cost of Energy) applied for the process heat case.

The LCOE for a renewable system is, as explained by Castro (2012), the cost of production of each unit of useful energy, considering the capital costs, lifetime, annual expenses, and annual generation. The indicator takes into account the value of money during the estimated lifetime, using a factor called the discount rate. The LCOE consists of a suitable parameter for the comparison between studied alternatives, thus yielding the most economically favorable solutions. At advanced stages of the studies, the economic indicators mentioned previously might be necessary.

Additional information on the subject is addressed upon the performance evaluation of the modeled systems.

CHAPTER 3. SOLAR HEAT INTEGRATION ASSESSMENT

Acknowledging the potential of solar integration in the supply of energy of the ECA production line, the present chapter seeks to analyze and represent the thermal demands of the process by following the proposed evaluation methodology (See Table 5). The assessment stages covered in this chapter encompass the pre-feasibility steps, and part of the feasibility studies, concluding in the identification of possible integration points.

3.1 Case study

As it has been referred, the industrial process under study is the production line of Expanded Cork Agglomerate and its energy supply system, specifically the manufacture facility from *Sofalca, Lda*., and its steam generation system.

3.1.1 Pre-feasibility analysis

Prior to the data acquisition through technical visits and formal contacts with the company, a review on the thermal needs of the process and its outcomes is performed, thus obtaining the information presented in Chapter 2 of this document (specifically, section 2.1). Familiarization with the aspects involved in the heat generation and product manufacture is important to properly develop a solar integration that aims to enhance and not negatively influence the already existing processes.

3.1.2 Company visit

A total of two technical visits to the manufacture facility of the company were completed during the first stages of the project, with the main objective of acquiring data from the heat generation process itself. Likewise, it was useful to gather information concerning the requirements and interests of the company. Relevant questions regarding the following topics took part in the visit: current heat generation scheme, thermal energy production, daily and seasonal manufacture profiles, consumption of fuels, among others. The acquired information is structured in the following subsections.

3.1.2.1 Installed heat generation system

The requirement of high temperature steam by the process autoclaves (See section 2.1.2.1) is, by now, a known fact. Water vapor at around 350ºC and 40kPa gauge (0.4 bar) is necessary for the expansion of the cork resins. In order to obtain this steam parameters, the company utilizes a steam boiler unit with the *water-tube* variant, similar to the unit schematized on Fig. 23.

The basic operation consists of a biomass furnace working with cork powder as fuel, which is fed by a worm screw that controls the feedstock entering the system. The hot combustion gases flow inside the boiler case, heating the water that passes through the tubes. A water drum collects the incoming fluid, while the steam drum separates the mixture of saturated water and steam. Fig. 23 does not represent it, but the equipment installed possesses a superheating stage linked to the steam drum outlet. Summarizing, the unit is capable of vaporizing and superheating water at the required conditions.

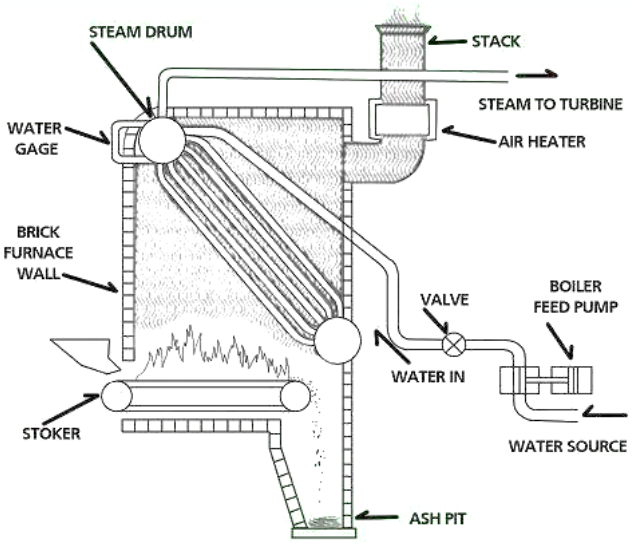

Fig. 23. Diagram of a water-tube boiler (Odesie, 2016).

The reported parameters of the boiler indicate that it is capable of achieving a pressure of 9.81 bar and a maximum temperature of 380ºC, by burning cork powder or firewood. In terms of power, the boiler tests show a 3000 kW vaporization capacity when working on a 4000 kg/h load.

The feedwater of the steam generator, which is the same fluid used in the autoclave operation, comes from underground natural deposits and is subject to previous treatment and filtering. Two tanks (10 and 6,5 m^3) assure the constant feeding of the boiler, as can be seen in the diagram of the water circuit of the facility (Fig. 24).

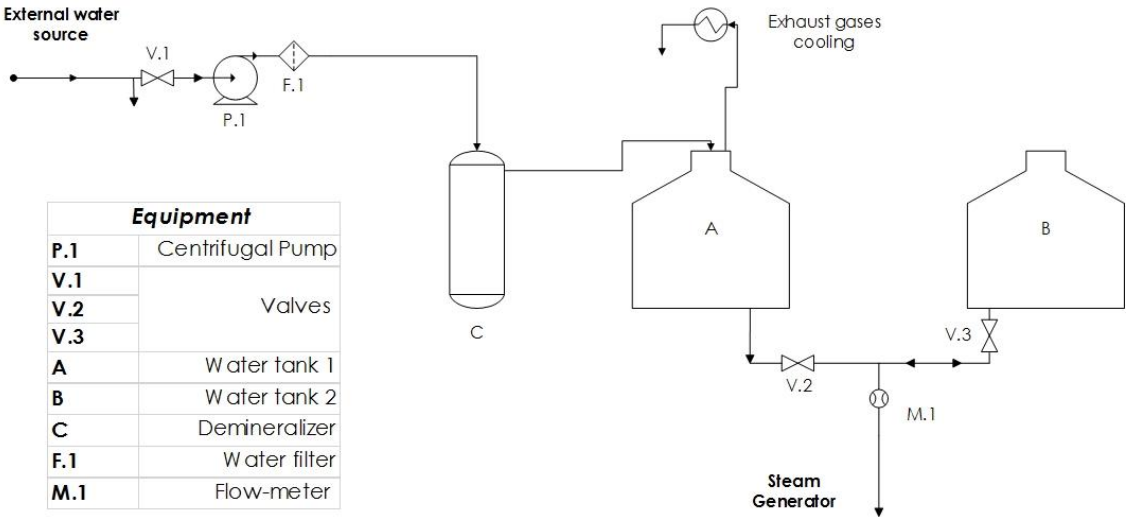

Equipment	
P.1	Centrifugal Pump
V.1	Valves
V.2	
V.3	
A	Water tank 1
B	Water tank 2
C	Demineralizer
F.1	Water filter
M.1	Flow-meter

Fig. 24. Layout of feedwater circuit of the facility.

Part of the incoming water from the external source is used for cooling of the exhaust gases of the furnace, considering that the steam generation room also includes equipment destined to treat combustion products before they are expelled to the environment.

3.1.2.2 Production information

On a not so technical aspect, the company provided relevant facts that must be taken into account in the analysis and integration processes:

- The manufacture operation follows the next schedule: weekdays from 8h to 19h, however, at Mondays, the start is delayed for a few hours due to general cleaning of the facility. Production stops during weekends and national holidays, as well as for three weeks of August and two weeks of December.
- There is not a significant seasonal variation in the production of the ECA blocks.
- Generated steam is almost totally consumed by the autoclaves; a quite small share is utilized in the spraying process once the cork expansion is finished.
- Boiler unit is reported to be operating at maximum capacity, hence the interest of the company on studying a new stream line installation or solutions that could liberate effort from the boiler.
- Space for a solar field is available.
- The cork powder excess is sold at a market price of 20€/ton.
- The energy content of the fluid leaving the autoclave is high, however, its recycling or use in preheaters is not a viable option, since its resin content is significantly high, causing it to leave solid residues in heat exchanging equipment.
- The worm screw that feeds the cork powder has a capacity of around 1300 kg/h.

3.1.2.3 Performed measurements

Specific parameters are required for the estimation of the thermal supply of the process, namely the temperature, pressure and flow rate of the water at the inlet and outlet of the steam generation unit. Since these values are usually variable during a certain time period, punctual measurements are not recommended, instead, multi-hour tests are performed, in which measurements are taken every certain period of time. This way, the behavior of a particular parameter is obtained, thus allowing more precise assumptions for the calculations.

Water consumption

Using the factory's installed flow-meter, two water volume values are registered with a two-hour difference between them, in order to estimate the water draw required by the boiler. Assuming continuous flow, the rate is estimated to be around 5.07 m^3/h, which corresponds to an approximate mass flow rate of 5070 kg/h, or 1.41 kg/s (Measurements indicated a consumption of 10.65 m^3 in 2h).

Since no mass is kept inside the boiler, the rate of steam leaving the unit is the same as the entrance, also being the process level flow rate.

Inlet water temperature

The temperature of the feedwater was monitored for five hours, with measurements taken each minute. The procedure was performed with the thermometer placed inside one of the storage tanks, obtaining the results represented in Fig. 25.

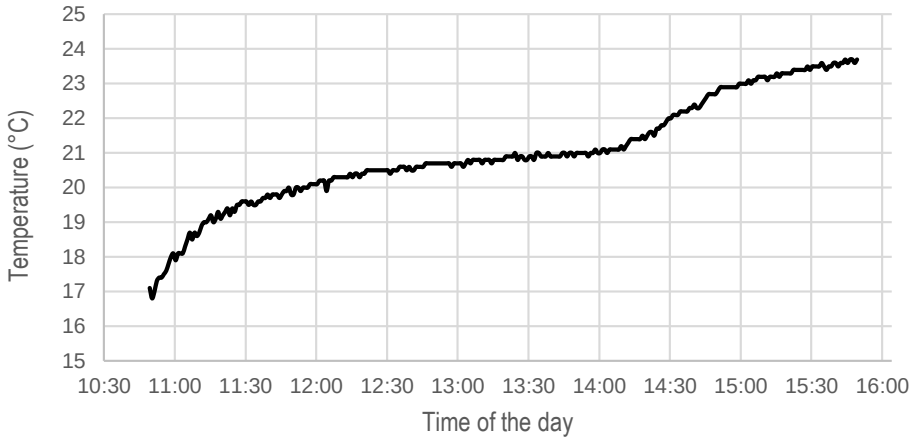

Fig. 25. Inlet water temperature variation.

Estimation of the daily temperature profile is not a feasible task, given the lack of information regarding its influencing factors and the fact that the measurements were taken for a short period of time of only one day of operation. However, for simplicity purposes, the average value is calculated and assumed as a good approximation for advanced calculations on thermal needs. Note that since the water source is a natural underground deposit, temperature during the year would not vary significantly, however the fact that the feedwater circuit is located inside the boiler room justifies the temperature increase along the day. The calculated average from the available data is 21ºC.

Steam parameters

The steam generator is equipped with instruments capable of showing on real time the temperature and pressure of the produced steam. A digital display presents, among other parameters, the temperature of the superheated steam and the pressure of the vaporization chamber (Fig. 26). Additionally, pressure gauges located in different stages of the boiler show the instantaneous gauge value.

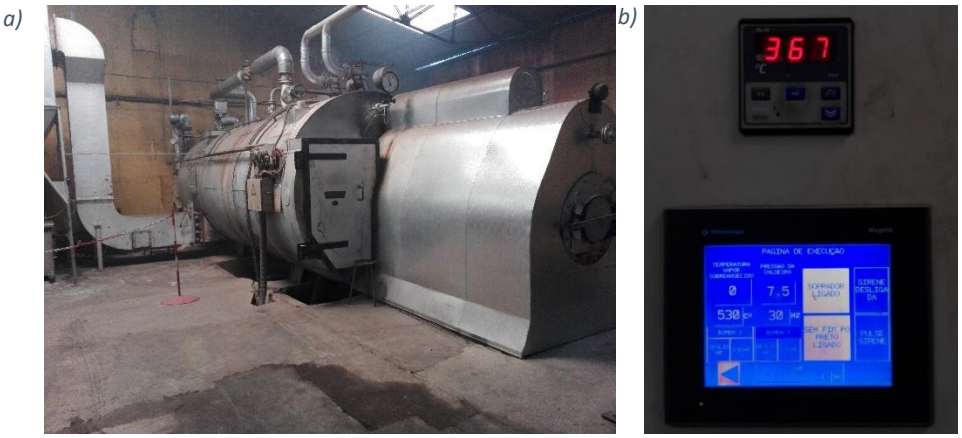

Fig. 26. SOFALCA Steam generator unit (a). Digital displays of the boiler control (b).

To understand the behavior of the steam generator, shown on Fig. 26, in terms of the variability of the outlet parameters, an approximate two-hour procedure was performed, in which the temperature

of the superheating and the gauge pressure of the vaporization stage were recorded. Measurements taken every thirty seconds (for 7200 seconds) facilitate the comprehension of the frequency of variation of the parameters. Fig. 27 represents the data, showing a relationship between the fluctuations observed in both parameters.

Concerning the pressure of the superheated steam, which is actually the outlet value of the supply level, the instrument located *downstream* exposes a pressure that is almost always 4 bar smaller than the one in the vaporization stage. Knowing this relation, no specific measurements were performed for this gauge, assuming that the difference is not variable.

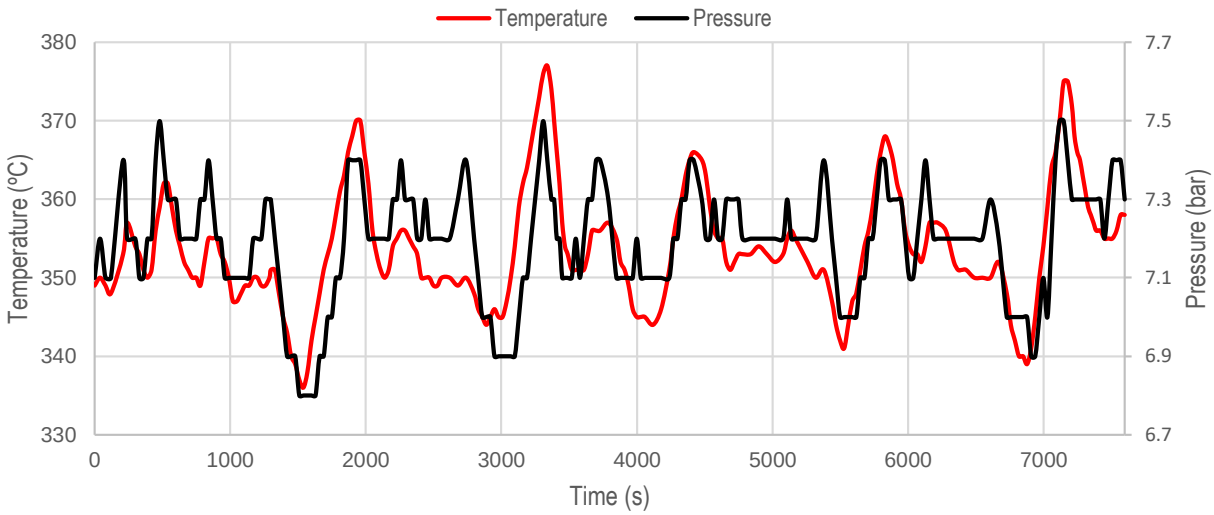

Fig. 27. Temperature and pressure variation of the boiler.

As seen from the curves represented above, pressure fluctuations seem to follow the variation of the temperature, obtaining most peak values for both parameters at the same time intervals. The observed behavior might probably be related to steam extractions to feed the autoclave at the start of the ECA expansion process. In this matter, one can refer the *cycles* seen in the curves, in which the time between maximum and minimum peaks is found every 1350 seconds, or 22 minutes (approximately). Still, average values of operation are interesting parameters to calculate, obtaining a saturated steam pressure of 7.19 bar (gauge), corresponding to 3.19 bar and 354ºC in the superheating stage.

Feedwater pump operation

Relevant data for the estimation of the energy demands of the process is now at disposal, nevertheless another parameter linked to the heat generation system are obtained, bringing information that could be relevant for advanced integration studies. Feedwater pump operation is represented graphically in terms of its consumed power during approximately 30 minutes of recording (Fig. 28). This aspect exposes the level of continuity of the operation, as a function of the requirements of the process level.

Notice that the feedwater pump presents start/stop behavior considering that it is a single-speed machine, in which the stops probably obey the water level inside the tanks; when the extraction of water

by the boiler drum decreases and the internal level of the storage is capable of handling the consumption, the pump does not operate. However, the time periods in which the pump is in stand-by are quite short.

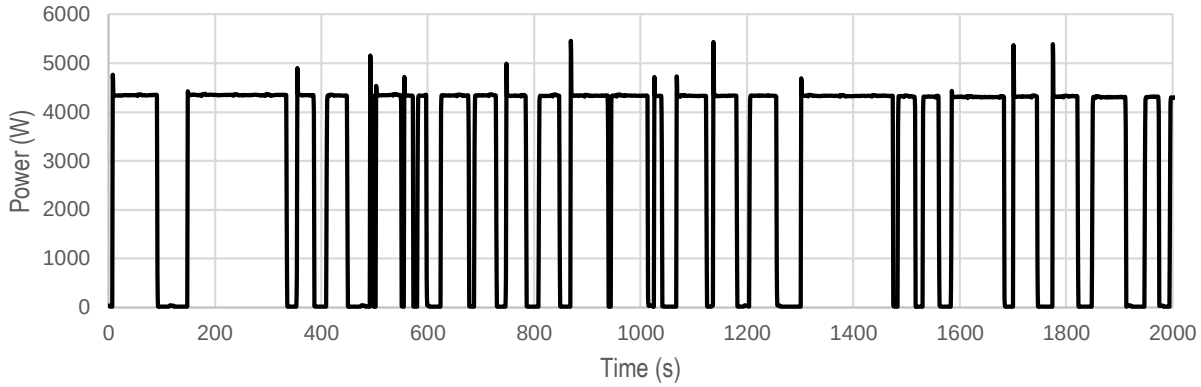

Fig. 28. Consumed power of the feedwater pump.

3.1.2.4 Data records

For long term analysis, data records are necessary, allowing the technical and economic evaluation of yearly performances as realistically as possible. In this matter, *Sofalca Lda* provided annual records of the water consumption of the process, in the form of volume measurements taken at the beginning and end of the daily operation (July 2015-August 2016). Fig. 29 presented below represents graphically the daily volume (in cubic meters) of water used by the company in the steam generation unit.

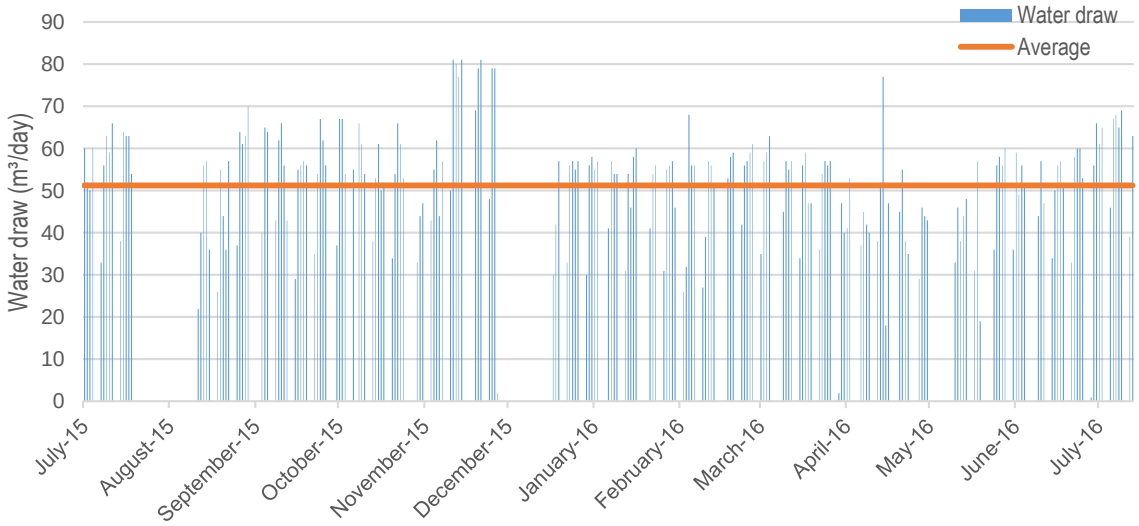

Fig. 29. Daily water consumption records.

With a simple look at the graph it is possible to confirm that there is in fact no significant seasonal variation in the production.

Now, by previously estimating the number of daily hours of operation (See section 3.1.2.2) as 7 and 11 hours for Mondays and the rest of the weekdays respectively, the hourly flow rate of feedwater is estimated for a day of operation (Fig. 30). The annual average is calculated neglecting weekends and holidays.

It is also interesting to compute the weekly and monthly averages since they represent profiles that can be easily integrated in the performance analysis. Fig. 31 shows these estimated mean flows, comparing it to the daily values.

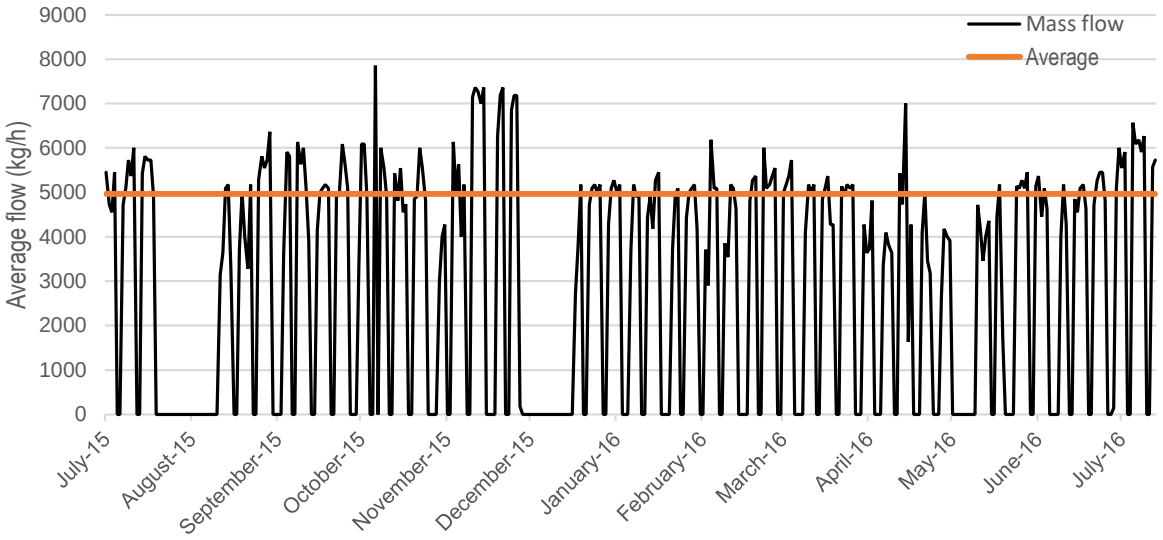

Fig. 30. Daily average mass flow in the boiler.

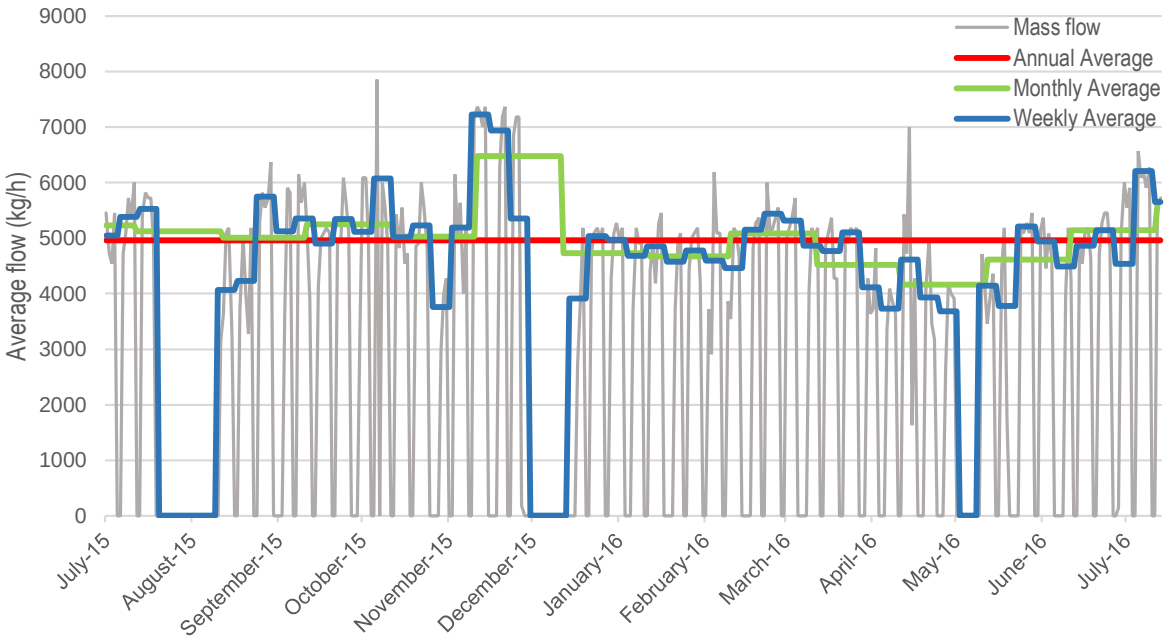

Fig. 31. Mass flow averages.

3.2 Thermal demand

With the gathered data, it is now possible to determine the energy supplied by the steam generation system, which also represents the thermal needs of the ECA production line. Boiler performance, data records assumptions and other considerations should be defined at this stage of the project, as described in the following sub-sections.

3.2.1 Performance of the steam generator

Knowing that the boiler is a water-tube type with a superheating stage, a brief thermodynamic performance characterization is done: water enters the boiler at the liquid state, where it reaches saturated steam conditions in the vaporization chamber; this process happens under constant pressure. Close to the steam drum exit, a throttling valve expands the vapor, reducing its pressure (reduction of approximately 4 bar) under constant enthalpy (Fluid Handling Inc, 2007), thus reaching a superheated state. At this point, the steam passes through the boiler once again to rise its temperature before finally entering the distribution network of the autoclaves.

To calculate the heat rate provided to the fluid, a simple thermodynamic equation is used:

$$\dot{Q} = \dot{m}(h_2 - h_1) \quad (1)$$

The heat rate can be calculated for the many stages of the steam generation process, namely the pre-heating, vaporization and superheating. The required enthalpies are calculated with the software *TermoGraf*, and using the assumptions presented in Table 8.

Table 8. Thermodynamic state parameters.

State	***Parameter***	***Absolute value***
Initial (Liquid water)	Temperature	21ºC
	Pressure	8.19 bar
Final (Superheated steam)	Temperature	354ºC
	Pressure	4.19 bar

The defined values correspond to the average of the collected and analyzed data. Mean values were chosen since it is necessary to establish a design point in order to obtain energy demand information. Notice the use of absolute pressure values, since the measured ones were in the relative scale. Therefore, with the previously described performance characteristics and values, the thermodynamic diagram of temperature-enthalpy is obtained (Fig. 32).

The thermodynamic processes represented are summarized below:

- 1→2 Preheating: Isobaric.
- 2→3 Vaporization: Isobaric
- 3→4 Expansion: Isenthalpic.
- 4→5 Superheating: Isobaric.

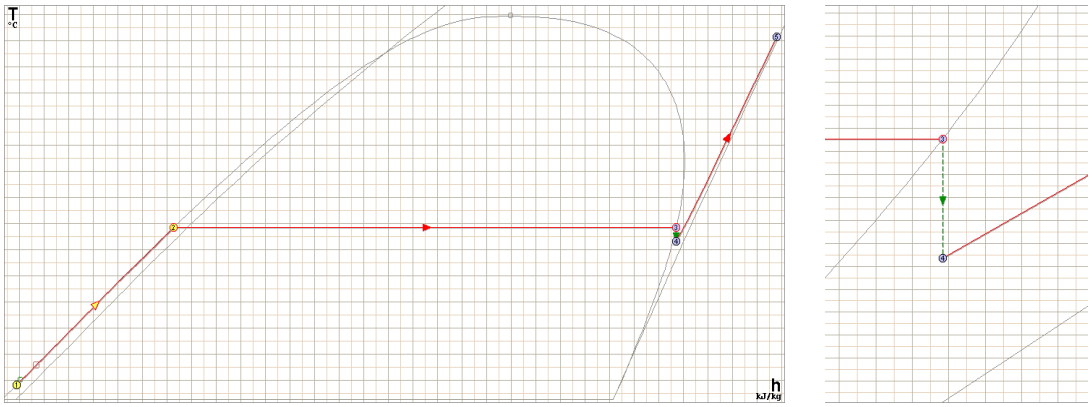

Fig. 32. T-h diagram (Left). Isenthalpic expansion detail (Right) (TermoGraf).

The software also presents the thermodynamic properties for each state, thus Table 9 summarizes the relevant ones for the present work:

Table 9. Thermodynamic states of the boiler process.

State	*Pressure (bar)*	*Temperature (ºC)*	*Enthalpy (kJ/kg)*	*Entropy (kJ/kgK)*
1	8.19	21.00	87.93	0.31
2	8.19	171.37	725.04	2.06
3	8.19	171.37	2769.14	6.65
4	4.19	158.41	2769.14	6.95
5	4.19	354.00	3176.67	7.73

For dimensioning purposes, the mass flow of the boiler is considered to be the one obtained in the technical visit, in order to be consistent with the assumptions, highlighting that the temperatures chosen were also measured that specific day. Therefore, the mass flow of the steam generator is 1.41 kg/s.

It is now possible to compute the power of the equipment at its different stages using Eq. 1. The results are presented in Table 10 shown below.

Table 10. Boiler power per process.

Process	*Description*	*Heat rate (kW)*
Process 1-2	Pre-heating	898.33
Process 2-3	Vaporization	2882.18
Process 3-4	Expansion	0
Process 4-5	Superheating	574.61

A total power of 4355.12 kW is estimated for the steam generator unit under the measured and assumed conditions.

3.2.2 Water consumption profile

The construction of a water consumption profile for a year of operation is performed to be later implemented in annual energy simulations, both for the already existing boiler unit and for the solar model under study. This stage is important since it allows the testing of the system under conditions that are not necessarily stable or constant throughout the periods of generation, or that are not what they were designed specifically for. It is expected to permit the computation of results that are closer to real operation and its variability.

The data records represented in Section 3.1.2.4 are reorganized to have a flow rate profile for a year starting on January. Weekly average flow rates are the values used to build said curves, due to the fact that they better represent the behavior of daily average flows. Summarizing, mass flow rate is assumed to be constant for each day of a certain week, based on the records provided by the company. Fig. 33 presents the constructed profile (mass flow in kg/h):

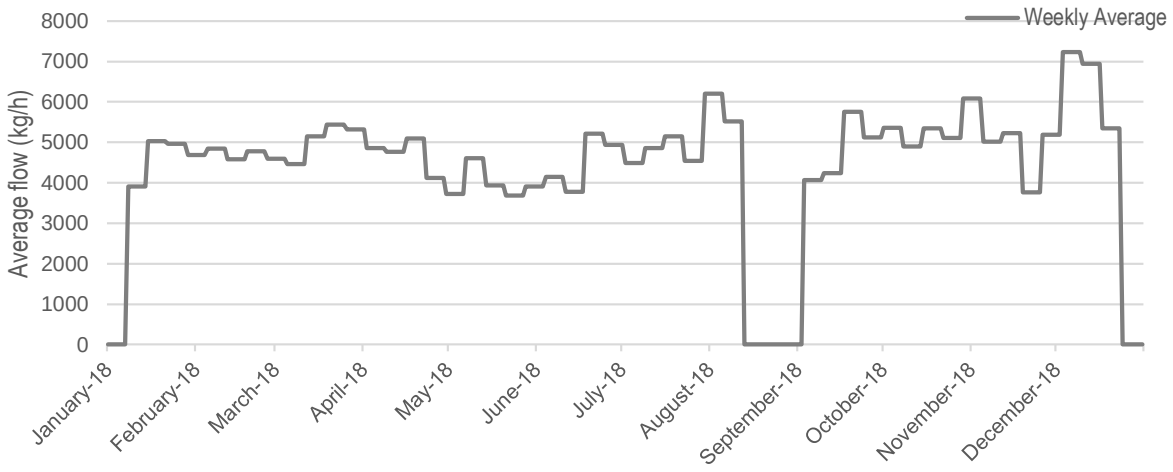

Fig. 33. Profile of flow rate of water.

3.3.3 Annual energy estimation

The final step in the thermal needs assessment is the estimation of the annual energy requirements of the ECA manufacture line, which is no more than the energy supplied by the boiler. To do so, and considering that the operation periods are irregular and have variable inputs (mass flow rate), a simple model is built on *TRNSYS*, using the *Simulation Studio* interface.

The model (Fig. 34) is programmed to compute the energy yield of the boiler for various stages, namely: preheating, preheating plus vaporization, and total yield. The basic principle is the following: an equation component calculates the instantaneous power for each time step of the simulation (Eq. 1), using the steam tables outcomes and the mass flow as inputs. The flow rate depends on the built profile and on the existence of generation at that precise instant; the shifts and schedule of the facility are simulated with specific functions, knowing the daily hours and annual periods of manufacture. Finally, energy is computed by integrating the power values for the desired period. A brief review on the used *types* (components of the software) and its goals is found at Table 11.

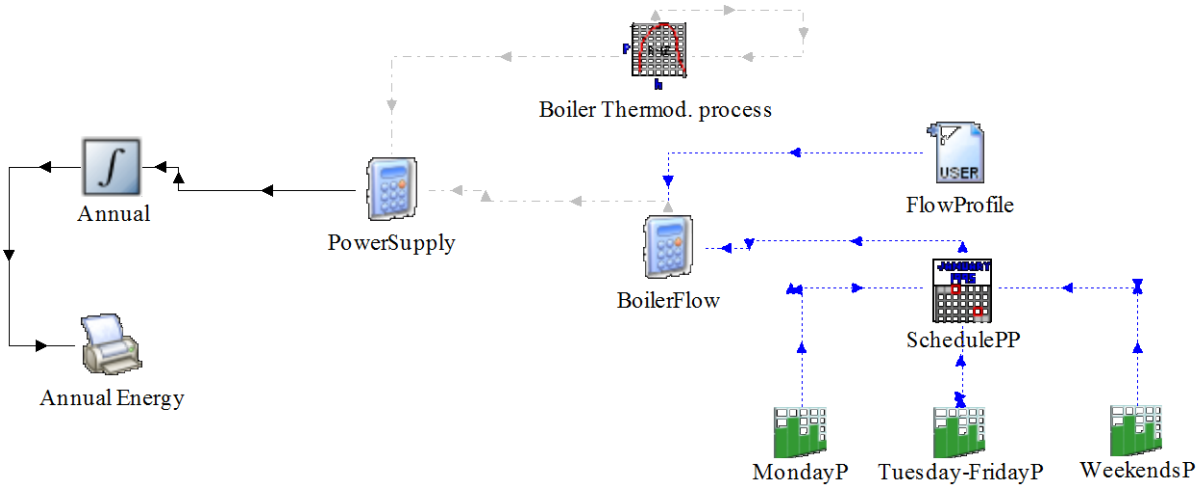

Fig. 34. Boiler annual generation model (Built with TRNSYS).

Table 11. Components of the boiler model (Built with information from TRNSYS).

Name	Type	Description	Function
PowerSupply	n.a.	Equation writer	Power calculations for the several stages of the boiler.
Boiler Thermod. Process	58	Refrigerant properties: calculates steam data using two state properties as inputs.	Calculation of the enthalpies for each state, using data from section 3.2.1 as inputs.
FlowProfile	9	Data reader	Reads an external .txt file containing the flow rate profile.
SchedulePP	41	Load profile sequencer	Organizes daily profiles and introduces holidays and occurrences.
MondayP	14	Time dependent forcing function	Simulates daily hours of operation.
Tuesday-FridayP			
WeekendsP			
BoilerFlow	n.a.	Equation writer	Designed to provide the instantaneous flow as a function of the profile and the schedule.
Annual	24	Quantity Integrator	Integrates the calculated power over the entire year of operation.
Annual Energy	25	Printer	Prints the results of the integration on an external file. The output is the energy yield.

Results of a simulation performed with a time period of 8760h and a time step of 1 minute are presented in Table 12, which summarizes the estimated thermal energy needs of the facility for each stage. Another integrator was also included to compute energy produced per month, in order to verify the seasonal behavior; results are represented on Fig. 35.

Table 12. Thermal energy production (annual).

	Boiler total energy	***Preheating + Vaporization***	***Preheating***
Annual energy (GJ)	35829.39	31102.89	7386.53
Annual energy (MWh)	9952.61	8639.69	2051.81

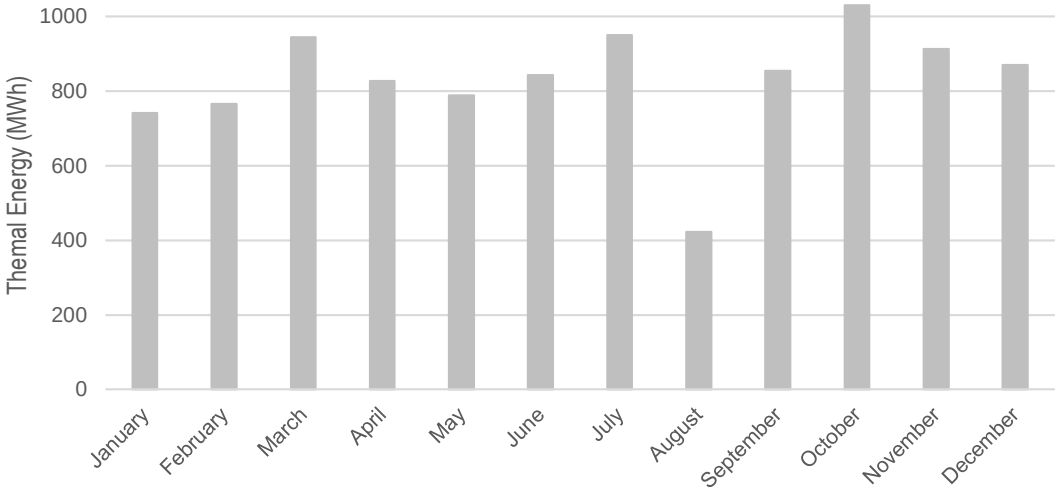

Fig. 35. Monthly thermal energy production.

Thermal energy demand presents a certain variation between months, though it does not seem to follow any trend. Differences are likely caused by quantity of hours of operation and flow values, in which August evidently suffers from the three holiday weeks.

3.3 Integration approach

One of the crucial steps of the assessment is the identification of integration points; in this particular case, and given the fact that not much information is known about the process level, the suitability of integration is defined for the supply level of steam. Analyzing the system, it seems feasible to consider the preheating of the boiler feedwater as the integration point of the study, since modifications on the already existing circuit would not be significantly deep and, most importantly, the power value is reachable (around 900 kW). A solar system designed to supply between 3000-4500 kW of thermal power would have dimensions and capital costs that might not be available or supported by the company. If desired, a steam generation by the solar system is a possible approach if just a fraction (in terms of mass flow) is generated by the solar field and the rest by the boiler.

Concerning the latter, the solar heat integration concept defined for this case study is: *Preheating of boiler feedwater via external heat exchanger*. Besides easier implementation, the selection of an external heat exchanger over an internal one obeys the possibility of addressing steam generation in future studies; leaving this option open. For preheating, the fact that water enters almost at saturated liquid might be advantageous in terms of work capacity relief of the system, and fuel consumption reduction.

CHAPTER 4. SOLAR SYSTEM DESIGN

To fulfill the objective of the integration based on the concept established above (Preheating of boiler feedwater via external heat exchanger), the present chapter describes the steps performed to design the solar system linked to the supply level; from its initial assumptions to the final scheme.

4.1 Solar system estimation

A simple solar thermal system is initially modeled on TRNSYS to design the solar field collectors and the heat exchanger required to supply the gained energy. This first approach delivers a first version of the solar field configuration, in terms of sizing.

4.1.1 Preliminary design

A three component system is built on TRNSYS in order to test, design and size the main equipment: pump, heat exchanger, and solar collectors. Using the *Simulation Studio*, the following model is constructed (Fig. 36):

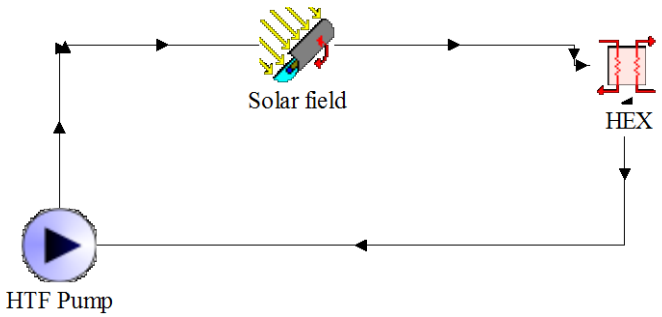

Fig. 36. Solar system preliminary design model (Built with TRNSYS).

The chosen components (referred as *types*) and its descriptions can be found on Table 13, while detailed information is obtained in the following subsections.

Table 13. Components of the preliminary solar model (Built with information from TRNSYS).

Name	*Type*	*Description*	*Function*
Solar field	536	Linear Parabolic Concentrator Solar Collector	Models the PTC collector array. Yields temperatures and energies.
HEX	5b	Counter flow heat exchanger.	External heat exchanger that supplies the solar gained energy to the feedwater.
HTF Pump	3d	Pump: single speed, no power coefficients.	Sets the flow rate of HTF in the circuit.

4.1.1.1 Parabolic trough collector

For the proposed ECA production line, and given its high temperature energy requirement, the concentrating collector type is the suitable system for the combination, thus it is selected for the study.

As known, many technologies are at disposal, though one of them stands out due to its maturity in the commercial operation: the parabolic trough. Within Task 49 reports, a compilation of the available market collectors appears, in which a remarkable product is found: the NEP PolyTrough 1800, a parabolic trough solar collector assembly (SCA) manufactured by *NEP Solar* (Horta, 2015), which is the one to be utilized in the model. A decisive factor on its selection is the online availability of performance data (efficiencies and testing) and complete dimension information, apart from its suitability in terms of temperature range.

As to the component modeling, Type 536 is chosen among the ones included in the TRNSYS 16 solar component libraries.

Type 536

General description of the Solar Library (TESS) component is found on Table 6, where it is stated that the type is based on theoretical equations from Duffie & Beckman (2013). The main expressions that rule the calculations performed by the component are presented below (variables defined in the *Nomenclature* section):

The useful energy gain equation is based on standard collector performance expressions plus a series of corrections applied to account for incidence angles, use of more than one collector in series, and flow rates other than used under test conditions. Equation 2 shown below is then the modified overall useful energy gains from the solar field. The terms between brackets indicate simple energy gains for a square meter of collector aperture, where $F_R(\tau\alpha)_n IAM\ I_{beam}$ is the quantity of energy in the receiver considering the optical losses and radiation incidence angle, while the negative term accounts for the thermal losses in the tubes. The factors R_1 and R_2 modify the energy yield computation according to test information and the number of collectors connected in series. Finally, the aperture area of each collector is included and the number of parallel rows of the solar field is taken into account.

$$Q_u = R_1 R_2 A_{aperture} N_{parallel} \left[F_R(\tau\alpha)_n IAM\ I_{beam} - \frac{F_R U_L}{ConcRat} (T_{in} - T_{amb}) \right] \quad (2)$$

Now, the temperature of the fluid leaving the collector is:

$$T_{out} = T_{in} + \frac{\dot{Q}_u}{\dot{m}_{fluid} Cp_{fluid}} \quad (3)$$

Note that the calculations consider the use of the collector inlet temperature minus the ambient temperature for the efficiency related aspects (Duffie & Beckman, 2013) in a linearized approach:

$$\eta = \eta_o - F_R U_L \frac{T_{i-} T_{amb}}{G} \quad (4)$$

Equations presented are taken from the documentation of Type 536 available in the software folder. For more information on the used variables, consulting the TRNSYS Documentation file is recommended.

The inputs required are: inlet temperature, inlet mass flow rate, ambient temperature, incident beam radiation, incidence angle and maximum outlet temperature. On the other hand, the necessary parameters are: number of collectors in series and parallel, aperture area and concentration ratio of the collector, intercept efficiency, efficiency slope, fluid specific heat and the tested flow rate (at which efficiency values were obtained). Additionally, the component requires an external file with the incidence angle modifiers.

NEP PolyTrough 1800

The chosen PTC has technical and performance data available online, placed at disposal by NEP Solar (n.d.) and SPF (2013) respectively; information summarized in Table 14.

Table 14. Technical and performance characteristics of the NEP PolyTrough 1800 (NEP Solar) and (SPF, 2013).

Dimensions	**Aperture area**	36.9 m^2
	Length	20.9 m
	Width (aperture)	1.845 m
	Height	1.75 m
	Concentration Ratio	54
	Specific weight of the assembly	30 kg/m^2
Performance	**Minimum flow rate**	900l/h
	Nominal flow rate	1800 l/h
	Maximum flow rate	3600 l/h
	Fluid content	19.6 l
	Maximum pressure	40 bar
	Thermal capacity (Empty)	7.2 kJ/K
	Tested flow rate	1400 l/h
	Tested fluid	Water
	η_o	0.689
	a_1	0.36 W/m^2K
	a_2	0.011 W/m^2K

At this point, all the data necessary for the type calculations is at disposal, nevertheless, some corrections need to be done to address differences between the input and parameter conditions and the values of the table, namely the efficiency and the tested flow rate.

The acquired efficiency parameters of the collector correspond to the quadratic expression of the overall efficiency and the mean temperature standard (Equation 5), while the type works with linear equations and collector inlet temperature (Equation 4), therefore a linearization and conversion process are performed.

$$\eta = \eta_o - a_1 \frac{T_m - T_a}{G} - a_2 \frac{(T_m - T_a)^2}{G} \quad (5)$$

The first step is the linearization of the quadratic curve represented on Fig. 37, it was built considering ambient temperature equal to 25ºC and a radiation of 800 W/m^2 (SPF, 2013).

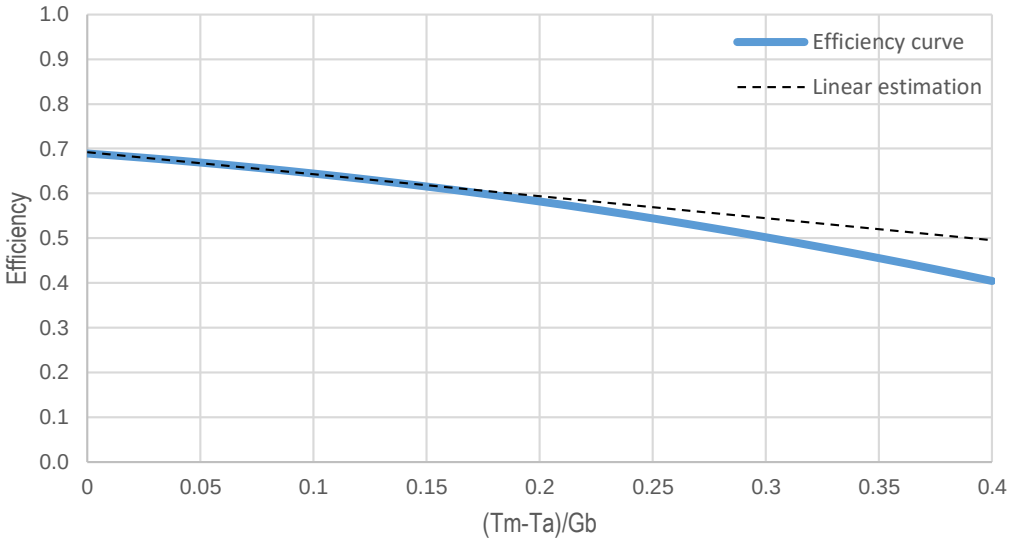

Fig. 37. Overall efficiency curve of the PTC.

Notice that this global efficiency accounts for optical and thermal losses, while the geometrical ones are considered in the energy equation of Type 536, with the introduction of the incidence angle modifiers.

Fig. 37 also represents the linearization of the curve for a range of temperatures in which the collector is expected to operate, yielding the following curve:

$$\eta = 0.6918 - 0.492 \frac{T_m - T_{amb}}{G} \quad (6)$$

For the thermal efficiency standard correction (mean temperature to inlet temperature curves), equations specifically designed for this purpose were developed by Duffie & Beckman (2013, p. 302). The method is shown in the equations below, in which both the η_o and the $F_R U_L$ from Eq. 6 are modified.

$$\eta' = \eta_{om} \left(1 + \frac{A_c (F_R U_L)_m}{2\dot{m} Cp}\right)^{-1} \quad (7)$$

$$F_R U_L{}' = (F_R U_L)_m \left(1 + \frac{A_c (F_R U_L)_m}{2\dot{m} Cp}\right)^{-1} \quad (8)$$

The mass flow rate and the specific heat correspond to the fluid used in the tests in which the efficiency was obtained. Computing the new values with equations 7 and 8, the modified curve is obtained (Eq. 9), where 0.6898 is the intercept efficiency and 0.4906 is the efficiency slope.

$$\eta = 0.6898 - 0.4906 \frac{T_{i-} T_{amb}}{G} \quad (9)$$

The tested flow rate adjustments are performed once the heat transfer fluid is defined, thus the subject is addressed later on.

4.1.1.2 Heat transfer fluid

Using an external heat exchanger allows the system to work with various fluids in the solar loop, however the HTF selected is thermal oil given its remarkable thermal properties and maturity in the parabolic trough operation. Notice that the PolyTrough 1800 can operate with water or thermal oil.

Even though the system is configured to preheat the feedwater, the thermal oil is also selected because it leaves the door open for an eventual study of retrofit with steam generation purposes, since the heat exchanger can be substituted by steam generation equipment.

In this matter, the model is dimensioned to work with Therminol® 66 by *Eastman*, considered to be one of the most popular high temperature thermal oils in the world (Eastman, 2016). Included in the CSP suitability portfolio of the company given its high thermal stability and wide range of temperatures. Relevant properties of the HTF are summarized in Table 15:

Table 15. Relevant properties of Therminol® 66 (Solutia, n.d.).

Composition		Hydrogenated terphenyl
Range of temperatures		-3 to 345ºC
@180ºC	***Density***	899.5 kg/m^3
	Specific heat capacity	2.122 kJ/kgK
	Dynamic viscosity	0.0106 poise
	Thermal conductivity	0.107 W/mK

The variable properties are defined for one value of temperature (close to expected operating conditions) since the used TRNSYS types do not allow parameter change during the simulations, even though it does not represent the actual behavior of fluids. Full list of properties as a function of the temperature is available at the Therminol® 66 data sheet (Solutia, n.d.).

4.1.1.3 Heat exchanger

To dimension the heat exchanger equipment, it is necessary to establish a few aspects related to parameters of operation, namely the fluids temperatures at the inlet and outlet, and the mass flow of each side (Cold side fluid: water, and hot side fluid: Therminol® 66). Knowing that the aim is to preheat water, the vaporization temperature represents the maximum that the feedwater can achieve.

A *design point* is defined, in which the inlet temperature and pressure of the heated fluid are the values from the measurements (See Table 8), i.e., 21ºC and 8.19 bar at the inlet of the cold side of the exchanger. For the outlet, the feedwater exits with a temperature of 165ºC and the same 8.19 bar. Notice that the vaporization temperature of water at said pressure is 171.37ºC, thus a 6-degree margin is left as a measure to avoid evaporation inside the equipment. Recalling what is referred on section 2.2.2.2: for industrial applications solar fluid temperature should be at least 15ºC higher than the required temperature, thus the outlet of the hot side of the exchanger is defined to exit at 180ºC. For the flow rate of the water, the 5070 kg/h value obtained in the technical visit is selected (similarly to what was performed for boiler energy calculations). The HTF mass flow is not yet known since it depends on the solar field sizing.

The counter flow equipment from TRNSYS requires the overall heat transfer coefficient (or UA), the inlet temperatures of both sides and the specific heat of both fluids. The last two are already defined, and to compute the transfer coefficient a specific method is applied: the effectiveness-NTU method.

The effectiveness-NTU method, or ε-NTU, is the process used for heat exchanger analysis when information on the outlet is unknown or incomplete (Incropera, DeWitt, Bergman, & Lavine, 2008). The overall heat transfer coefficient is found using the following equations (Incropera et al., 2008)

$$UA = C_{min} NTU \tag{10}$$

$$NTU = \frac{1}{C_t - 1} \ln\left(\frac{\varepsilon - 1}{\varepsilon C_t - 1}\right) \tag{11}$$

C_{min} is obtained by multiplying the Cp of the fluid by its flow rate. Previous calculations indicated that if the flow rate of the HTF is equal or smaller than the flow of feedwater, the temperature of the HTF outlet is negative for the evaluated parameters, thus the C_{min} is found in the cold side:

$$C_{min} = 4.19 \frac{kJ}{kgK} 5070 \frac{kg}{h} = 21243.3 \frac{kJ}{kgK} \tag{12}$$

The remaining variables are found with the following expressions:

$$C_t = \frac{C_{min}}{C_{max}} \tag{13}$$

$$\varepsilon = \frac{T_{co} - T_{ci}}{T_{hi} - T_{ci}} \tag{14}$$

Eq. 14 comes from simplifications performed due to the fact that the Cmin is in the cold side. Subscripts refer to hot and cold side (*h* and *c,* respectively), and inlet and outlet (*i* and *o*, respectively). Using Eq. 14, the effectiveness is 0.9056.

Since the mass flow rate of the HTF is unknown, several possible values are tested taking into account that it depends on the quantity of parallel rows of the solar field. One can say that the heat exchanger analysis is, in this case, also used for the estimation of the number of parallel PTCs. Assuming a nominal flow rate of 1619.1 kg/h of HTF per parallel row of collector assemblies (the nominal volume rate multiplied by the density of Therminol® 66) and using the previous set of equations, the following curve (Fig. 38) is obtained:

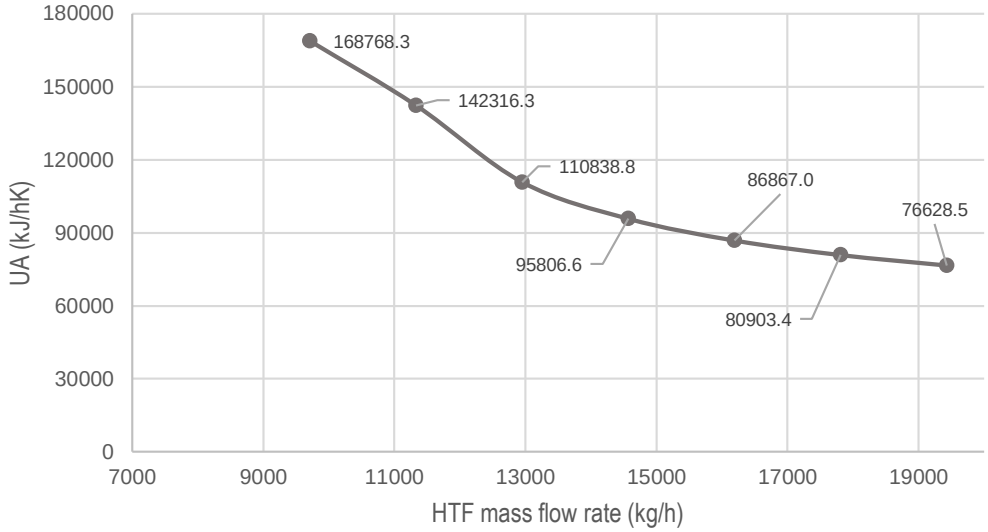

Fig. 38. UA estimation curve.

Analyzing the behavior of the curve, it is possible to see the relation between the size (note that the UA includes the area of exchange and not only the transfer coefficient) and the flow rate as: the greater the mass flow, the smaller the exchanger required. Since costs of the solar field are significantly higher, it is better to minimize the number of collectors in parallel by increasing the size of the heat exchanger. In this case, the selected UA is 142316.3 kJ/hK, which corresponds to a solar field with 7 parallel lines and a nominal HTF flow rate of 11333.7 kg/h.

4.1.2 Preliminary simulations

At this point, the size of the heat exchanger and the number of parallel rows of the solar field is defined, however the number of collectors per row (i.e. in series) is still an unknown. Simulations of the model of Fig. 36 with the computed parameters are performed, in which the number of collectors linked in series is increased for several values of direct beam radiation. This approach might give a general idea of the size of the field required to reach a certain temperature in the preheating, but not on the expected behavior of the system.

The calculations are performed according to the inputs and parameters established in Table 16, while the outputs of the simulation are represented in Fig. 39. The tested flow rate of the SCA is corrected to account for the use of a different HTF between the tests and the model, assuming that:

$$\dot{m}_{water_{test}} Cp_{water} = \dot{m}_{oil_{test}} Cp_{oil} \tag{15}$$

Other corrections are performed by the type, such as modifiers used to account for values of the collector flow rate other than the one used in the performance tests. Types are linked to provide outlet temperatures and flow rates to each other. In terms of simulation time, small values are sufficient, since the system is not dynamic and achieves stability considerably fast.

Table 16. Inputs and parameters of the preliminary simulation model.

	Parameters		***Inputs***	
Type 536 (Solar field)	**Collectors in series**	*Variable*	**Ambient temperature**	25ºC
	Collectors in parallel	7	**Incidence angle**	0
	Aperture area	36.9 m^2	**Incident beam radiation**	*Variable*
	Concentration ratio	54	**Maximum outlet temperature**	250ºC
	Intercept efficiency	0.6898		
	Efficiency slope	0.4906 W/m^2K		
	Fluid specific heat	2.122 kJ/kgK		
	Tested flow rate	152.42 kg/hm^2		
Type 5 (HEX)	**Specific heat of hot side fluid**	2.122 kJ/kgK	**Cold side inlet temperature**	21ºC
	Specific heat of cold side fluid	4.19 kJ/kgK	**Cold side flow rate**	5070 kg/h
			UA	142316.3 kJ/hK
Type 3 (HTF Pump)	**Maximum flow rate**	11333.7 kg/h	**Control signal**	0
	Conversion coefficient	0		

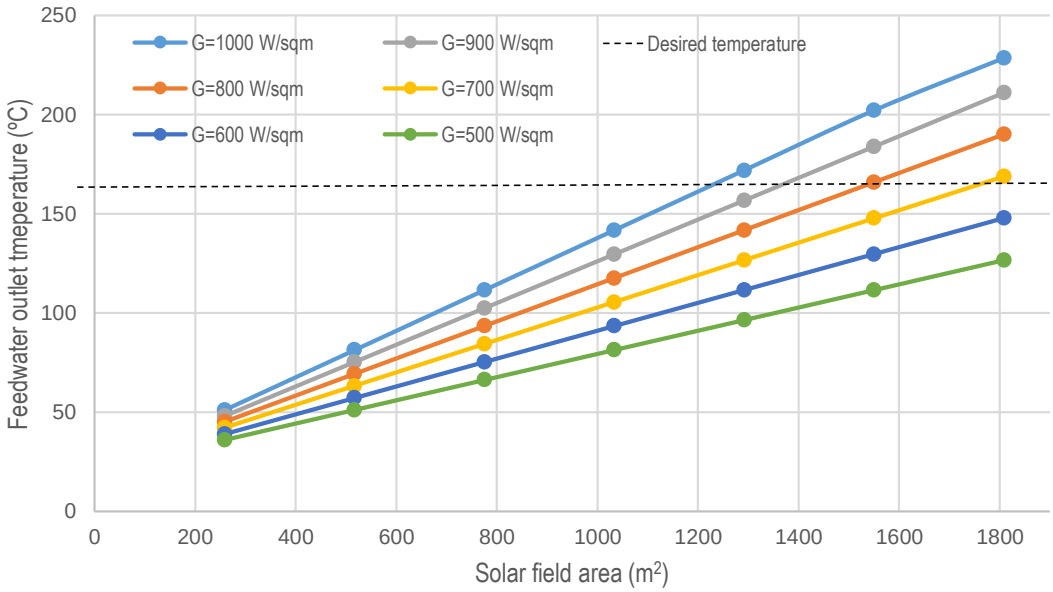

Fig. 39. Preliminary system simulation results.

As seen from the inputs, calculations are performed with direct normal irradiation, this is, no incidence angle influence. Analyzing the results, it is evident that the greater the size of the field (with the increase of the number of collectors per row), the higher the temperature of the feedwater leaving the heat exchanger. At this point, definition of the number of collectors in series is not yet possible, since it depends on the weather conditions of the studied location. However, one can say that for the design point, a solar field with a minimum of 4 collectors in series (configured in 7 rows, giving approximately 1000 m^2 of aperture) is required to reach the heat exchanger dimensioning temperatures.

4.2 Realistic model

Once the preliminary configuration and dimensions are selected, a realistic modeling and simulation of the solar preheating of the process fluid is done. The aim is to define an adequate system for later comparison between several possible configurations.

The main aspects introduced to the model in this stage of the study are:

- Piping system.
- Mass thermal capacities of the equipment.
- Real weather data.
- Energy storage.
- Control strategies.
- Process load profiles.

Initial assumptions and limitations of the software should be addressed prior to the construction of the model, as listed below:

- Since the objective of the solar system is to preheat the feedwater, the flow rate of the HTF in the solar loop is fixed, thus the temperature at the outlet does not have to reach a set value, as what would happen in a steam generation case.
- Dynamic situations are accounted for with the inclusion of the thermal capacities of the equipment.
- Most components used in the model do not allow variation in temperature/pressure dependent properties of fluids, therefore mean values at expected conditions of operation are considered.
- The assessments obey thermal behavior of the system, thus electrical energy used to operate it and maintain it is not among the subjects of study.

Other specific aspects appear in the description of the components involved in the system.

4.2.1 Solar integrated circuit

Based on the information obtained in Section 4.1 and the features mentioned above, a *Solar preheating model* is built with TRNSYS Simulation Studio, as represented in the diagram shown in Fig. 40.

This first version represents the HTF circuits of the energy source and the load, referred to as the solar circuit and the process circuit respectively, with connections to the weather data of the location

of the facility. Information regarding the design and characteristics of each component is organized throughout the next subsections, though a first description is made as introduction in Table 17.

If compared with the preliminary model, the major difference is the existence of two different circuits for the heat transfer fluid; measure that is necessary in order to introduce the energy storage system. Said modification induced the entrance of other complementary components, namely another pump and regulatory valves. Notice that both circuits operate with the same fluid.

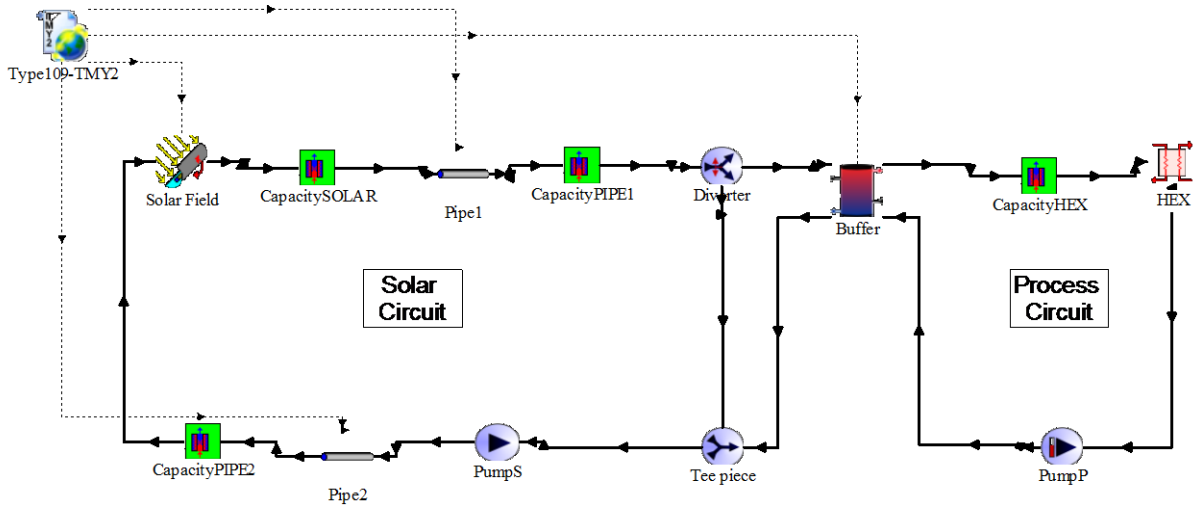

Fig. 40. HTF Solar and Process Circuits (Built on TRNSYS).

Table 17. Components of the solar integrated model (Built with information from TRNSYS).

Name	*Type*	*Description*	*Function*
Solar field	536	Linear Parabolic Concentrator Solar Collector	Models the PTC collector array. Yields temperatures and energies.
HEX	5b	Counter flow heat exchanger	External heat exchanger that supplies the solar gained energy to the feedwater.
PumpS	3d	Pump: single speed, no power coefficients.	Sets the flow rate of HTF in the solar circuit.
PumpP	110	Variable speed pump	Sets the flow rate of HTF in the process circuit, limiting if required.
Type109-TMY2	109	Data reader and radiation processor	Read and process the weather file of the location, providing radiation values, position of the sun, among others.
Capacity (SOLAR, PIPE1, PIPE2, HEX)	306	Lumped mass to simulate thermal capacity of components	Accounts for dynamic situations in terms of energy balance of the materials.
Buffer	4e	Storage tank: user-designated inlets, uniform losses.	Models a stratified tank working as the buffer of the system.
Diverter	11f	Controlled flow diverter	Controls whether the HTF enters the tank or not.
Tee piece	11h	Tee-piece	Joins the buffer return and diverted fluid in the solar circuit.

Pipe (1 and 2)	709	Circular fluid-filled pipe	Models the thermal behavior of fluid flow in a pipe.

4.2.1.1 Components from the preliminary design

Dimensioning of the solar field, heat exchanger and the solar loop pump components was already performed, nevertheless, small adjustments are required in the PTC to properly integrate the rest of the components. Since the position of the sun is variable, incidence angle modifiers (IAM) are included as an external file of type 536. These modifiers account for the geometrical efficiency of the collector and are obtained from the performance data sheet of the NEP PolyTrough 1800 (SPF, 2013), as seen on Fig. 41.

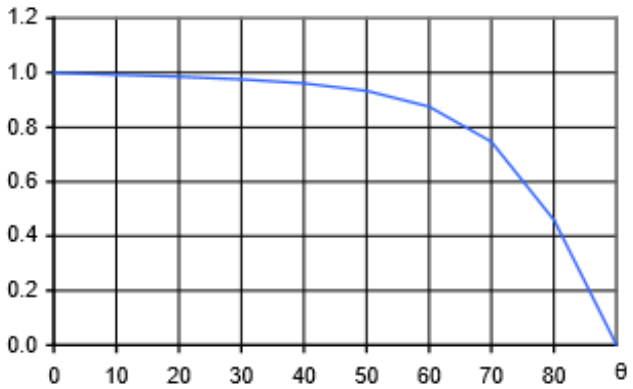

Fig. 41. IAM as a function of the angle of incidence (SPF, 2013).

4.2.1.2 Type 109 – Weather data

A component called Type 109 is used to introduce the weather conditions of the location into the model. Said type is designed to read and process TMY2 files, generating important data concerning solar radiation, solar position and other weather parameters. The meteorological data TMY2 format includes information about a typical meteorological year, based on data records taken from the software *Meteonorm*. Said file was obtained for the specific location of the factory.

Apart from the mentioned functions, the type is also capable of introducing collector surface orientation and solar position tracking for the solar field components. Considering that the study deals with a parabolic trough, tracking is performed in the single-axis variant, with axis orientations of North-South or East-West. The last aspect brings significant differences in the quantity and behavior of the energy yield of the solar field, as seen in Fig. 42:

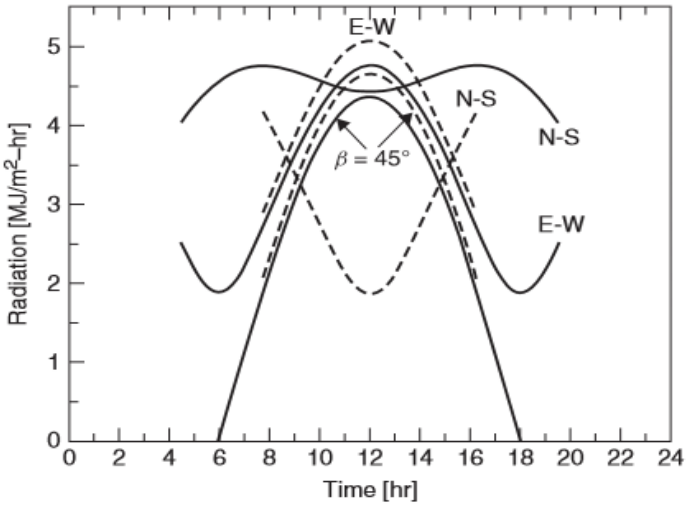

Fig. 42. Daily behavior of incident radiation for NS and EW solar collectors. Continuous line: summer. Dash line: winter (Duffie & Beckman, 2013).

To define single-axis tracking, Mode 3 of operation is selected, in which the surface orientation is defined as follows:

- North-South (NS): receiver tube parallel to the NS axis. Surface slope and azimuth angles are 0º.
- East-West (EW): receiver tube normal to the NS axis. Surface slope is 0º, but azimuth angle is 90º.

Relevant outputs for the model are: ambient temperature, incident beam radiation and incidence angle. Ambient temperature is used by types that account for the thermal losses to the environment.

4.2.1.3 Type 709 - Piping

Type 709 represents the piping system of the circuit, in which two sections are included, acknowledging that the solar field would be located at a considerable distance from the integration point. Assuming that the storage is located near the heat exchanger, the piping system links the solar loop to the tank using insulated steel pipes, that are modeled to account for thermal losses to the environment.

Estimation of the length of the pipes is not simple since it would depend on the final location of the solar field, nevertheless, a 130 m distance is defined considering the visual inspection performed within the technical visit. In terms of materials, Eastman recommends *Schedule 40 carbon steel* pipes for Therminol® 66. Concerning the insulation, Fiberglas™ by Owens Corning ® is selected since it is cheaper than most materials and presents properties that are suitable for the HTF and the application (Jenkins, 2016), however, for flanges and areas where leakage can occur, cellular glass is recommended since it deals better with possible combustion when there is contact with the fluid (Jenkins, 2016). For the TRNSYS model, the first solution is considered and its relevant characteristics are presented in Table 18, along with properties of the pipe material and its defined dimensions.

Piping diameters and conductivity are found from available Schedule 40 (Appendix A) and carbon steel tables, by previously defining that fluid velocity should be around 1-3 m/s (Sinnot, 2005) and knowing that the volumetric flow rate is the outlet flow from the solar loop (11333.7 kg/h, or around 12.6m^3/h). Insulation dimensions and properties obtained from the Fiberglas™ product data sheet

(Owens Corning, n.d.), though previous tests on the influence of its thickness indicated that for the expected temperature of operation greater values are not necessary.

Notice that both pipe models are designed with the same parameters.

Table 18. Main properties of the piping system.

Parameter	*Value*
Inside diameter	50 mm
Outside diameter	60.3 mm
Pipe length	130 m
Pipe thermal conductivity	54 W/mK
Insulation thickness	25 mm
Conductivity of insulation	0.051 W/mK

4.2.1.4 Type 306 – Thermal capacities

This type models the thermal capacity of the materials of the equipment, namely the solar collector assemblies, the pipes and the heat exchanger. The inclusion of this type obeys the necessity of considering transient simulations like start-ups and sudden drops in radiation for the *empty* equipment, since thermal capacity of fluids is already taken into account in equations where $\dot{m}Cp$ plays a role. The physical influence of the lumped mass component is well represented on Fig. 43:

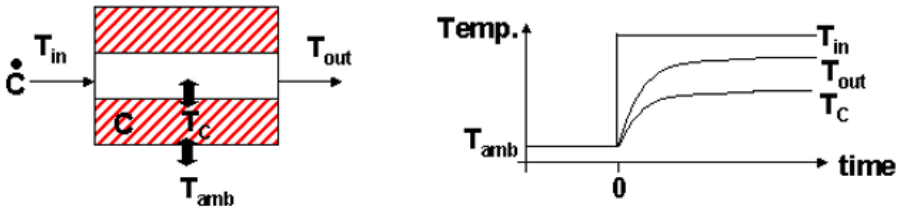

Fig. 43. Influence of the introduction of thermal capacities (Schwarzbözl, 2006).

Apart from incoming flow parameters, Type 306 requires the introduction of the mass and overall hear transfer factor (UA) of the equipment in order to calculate its gain of temperature and its capacity. Also, overall loss coefficient is requested but is not taken into account since the aspect is already approached by the equipment types. Determining these parameters is not trivial since technical information is not available at this point of the feasibility study, therefore, assumptions are made to estimate the values, as described in the following subsections.

Solar field thermal capacity

Performance data from SPF provides the $\dot{m}Cp$ directly, indicating a value of 7.2 kJ/K for a SCA with an aperture of 18.45 m^2, but since the SCA utilized has a size twice that value, the estimated capacity is then 14.4 kJ/K. The size of the field is not yet defined, so for the simulations, the total capacity is this previous value times the number of SCA modeled.

To estimate the UA of all the receiver tubes a supposition is made: the value is equal to the convective heat transfer factor of the fluid (*h*) times the internal area of the tubes of the entire field. Evidently, many aspects influence this coefficient, though for approximation purposes the *h* is considered to be enough. Notice that the conductivity of the receiver material is not used, assuming is not relevant in the calculations.

Knowing that the convective factor depends on velocities, temperatures and other factors, an evaluation is performed in an online simulator, designed by HTF manufacturers *Duratherm* (Duratherm, 2016). Using the known properties of Therminol® 66 (Table 15) and an estimated velocity of 0.5 m/s (calculated at nominal flow conditions and internal diameter of the receiver 34 mm); the estimated *h* is 567.3 W/m^{2}K. The internal area depends on the diameter of the receiver and the number of SCA simulated, thus a general value for the UA is not defined.

Pipes thermal capacity

The mass of the pipes is calculated using schedule 40 data (Appendix A), from which specific mass per length is provided. For the 130 meters of piping there are approximately 975 kg of carbon steel, which has a specific heat of 0.5 kJ/kgK.

The UA is obtained with the same assumption made for the receivers of the solar field, in this case the simulator yields a convective factor of 1325.8 W/m^{2}K; and once again Therminol® 66 data is used along with the calculated parameters of the pipe. The internal area is around 20.4 m^2, resulting in a UA of approximately 27000 W/K.

Heat exchanger thermal capacity

The overall heat transfer factor is obtained through an assumption that considers that the contributions are shared equally between the hot and the cold side of the exchanger, i.e. the convective factor times the area of contact is equal for both sides:

$$\frac{1}{UA} = \frac{1}{(hA)_{hot}} + \frac{1}{(hA)_{cold}} \tag{16}$$

Note that the conductivity of the pipes is once again neglected. Using the overall factor of the exchanger (defined in previous sections), the thermal mass UA is around 79000 W/K.

For the mass and specific heat, it is necessary to have approximate values of the dimensions and configuration of the equipment. Knowing that the exchanger should have a peak power greater than 800 kW, and operates with a fluid that presents combustible properties when leakage occurs, the shell and tube type is used as reference (Sinnot, 2005). For this design approach, Sinnot (2005, p.660) states that:

- Allocating fluids with the lowest flow rate in the shell-side will normally give the most economical design.
- The most toxic or dangerous fluid should be in the tube-side.

Therefore, the logical option is to pass the HTF through the tubes, and admitting that it is a light oil, the transfer coefficient has an average value of 625 W/m^{2}K; estimated for a shell and tube heat exchanger with thermal oil as the hot fluid and water as the cold fluid (Sinnot, 2005, p.637). With the U and the UA, the area is easily estimated as 63.25 m^2.

A commercially available exchanger with similar characteristics and ready to operate under this condition is the *Alfa Laval Aalborg MX* (Alfa Laval, n.d.). According to the manufacturer, the standard tubing has a diameter of 10 mm with a 1 mm thickness, on the other hand, shell and tube material could both be carbon steel (Cp of 0.5 kJ/kgK). Considering the area, volume of the pipes and the material; the estimated thermal mass is 546.1 kg.

It is relevant to state that detailed specifications or calculations of the heat exchanger are not approaches. These basic estimations are required for the capacitance computation only.

4.2.1.5 Type 4e – Storage system

The necessity of addressing short term fluctuations in the radiation, covering peak loads or damping fast transitions brings the use of storage tanks for the HTF. Since the aim is to maintain the temperature of the fluid and not to extend the production period significantly beyond the solar availability, smaller single tanks (stratified) are sufficient. Two-tank systems would be suitable for molten salt operation. As stated, TRNSYS Type 4 models a tank of this kind, where the stratification is modeled by choosing N volume segments, representing the degree of stratification. Type 4e variant allows variable inlets that can be chosen by the user.

In the model, the HTF leaves the tank through the top node, returning to the bottom one, where the connection to the heat source is also located. Entrance from the solar loop can be, as mentioned, variable, and will be defined in subsequent sections.

The modeled component has 8 nodes of thermal stratification, no auxiliary heaters and a tank loss coefficient of 3 kJ/hm^{2}K (pre-established in the component parameters). For sizing approximations, a market available tank is used as reference: *6000 liter Cordivari buffer tank* (water storage), that has the following height/diameter relation (Mibec, 2016):

$$H_{internal} = 1.31 D_{internal} \tag{17}$$

With cylinder volume expressions and the number of nodes, the node height is obtained (input of the TRNSYS type). A single volume is not chosen, since it depends on analysis performed ahead.

4.2.1.6 Type 110 – Process circuit pump

The use of a variable speed pump obeys control strategies and protection measures of the heat exchanger that are described in Section 4.2.2. However, the maximum flow rate is already defined and equal to the flow rate of the solar loop, i.e. 11333.7 kg/h of HTF. Heat conversion in the pump is not considered, similarly to what was defined for the solar pumping system.

The use of diverting and tee-piece valves (Type 11) is also related to control and operation strategies, but its main objective is to select the path of the HTF in the circuit.

4.2.2 Control and operation strategy

To complete the solar integration approach, control systems and specific load data must be introduced and modeled in the built circuit. Control strategies seek stability in daily operation and maximization of annual yield of energy. For this, specific operation conditions that take into account real thermal load data are required.

Considering all the defined parameters, assumptions and objectives, the *CST preheat of feedwater model* is finally built, as represented on Fig. 44.

Just like the HTF hydraulic circuit, the control scheme can be divided in two main areas: solar circuit control and process circuit control. Each one has different strategies and objectives but pursue the same end; stable and optimal operation. Before describing each part of the control method, a summary of the types used is shown in Table 19 presented below (excluding the components described in Tables 11, 13 and 17).

Table 19. Components of the solar heat integration model (Built with information from TRNSYS).

Name	***Type***	***Description***	***Function***
BoilerNeeds	n.a.	Equation writer	Defines the water mass flow rate flowing through the heat exchanger for every time step.
Radiation Controller	n.a.	Equation writer	Controls start-ups of the solar pump.
PumpSControl PumpPControl	n.a.	Equation writer	Joins several control signals into a single one.
ValveControl ProcessControl	2b	ON/OFF Differential controller	Generates a control signal (either 0 or 1) according to the set and compared temperatures.
FlowControl	22	Iterative Feedback Controller	Yields a control signal between 0 and 1 to maintain temperatures at a specific value.

As in boiler energy calculations, the final model introduces the feedwater flow rate annual profile (defined in section 3.2.2), using Type 9 and an equation linked to the manufacture schedules, yielding the instantaneous flow required to meet the load. This aspect influences the control method of the process circuit.

4.2.2.1 Solar circuit control

The function of this control section is to regulate the operation parameters of the solar loop, by controlling the hours of solar energy generation, the temperatures reached and the entrance to the storage system. Specific subsystems are discriminated below:

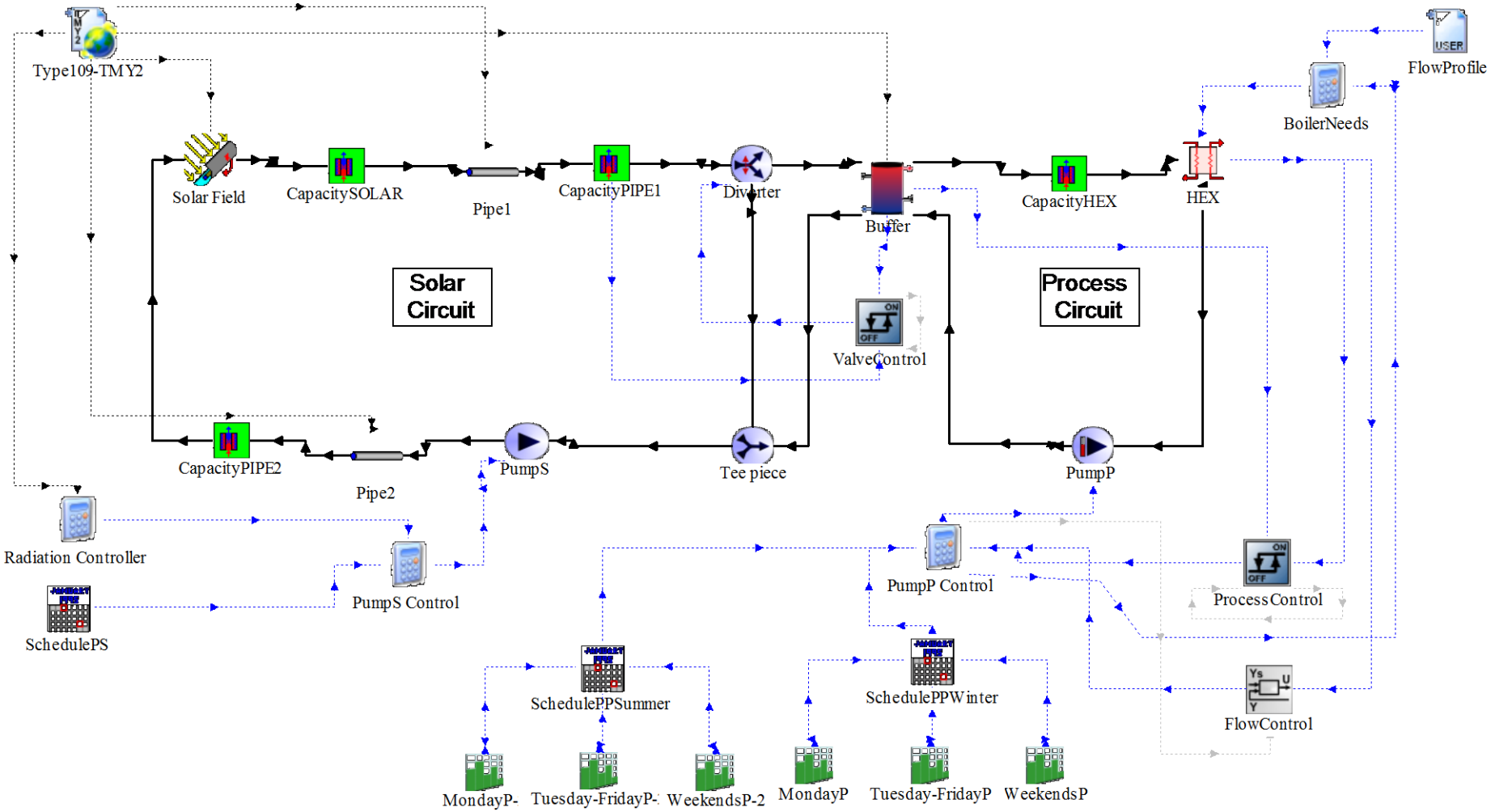

Fig. 44. Solar heat integration model (Built with TRNSYS).

- Solar circuit pump control (*PumpS Control*): using simple ON/OFF switch strategies, the pump is activated or deactivated according to the value of the incoming radiation and the defined schedule of operation:
    - Schedule: defines the annual days in which the pump should work, only stopping for summer and winter lengthy holidays, i.e. during approximately 5 weeks of the year.
    - Radiation sensor: as long as there is a value of incident beam radiation of around 30 W/m^2, the solar collectors ask for HTF flow.

  Essentially, the pump is designed to operate as long as there is incident energy, in order to supply the storage with high temperature HTF, seeking to maximize the annual yield of energy from the solar source.
- Solar collector temperature control (*Solar Field embedded function*): both the selected SCA and the Type 536 include mirror defocus as a control method to limit the temperature at the outlet of the array. Therefore, a defocus temperature of 185ºC is defined, since the designed solar temperature of the exchanger is 180ºC; the difference seeks to account for thermal losses that could occur in the hydraulic circuit, however, the NEP PolyTrough 1800 collector can operate at temperatures up to 250ºC if required.
- Storage entrance control (*ValveControl*): to avoid cooling of the HTF in the buffer tank, which might occur when the outlet of the solar field is at a lower temperature than the bottom node, the circuit is prepared to divert the incoming flow and return it to the solar loop. A combination of a ON/OFF differential controller and a set of valves aims to address this issue as follows: the controller compares the temperature of the HTF at the exit of the piping system with the temperature of the bottom node of the tank; if the HTF is just slightly hotter, type 2b sends a control signal to the valve, letting the fluid enter the storage, otherwise, the valve turns and sends the fluid to the tee-piece, that receives and directions the flow back to the solar circuit pump for another *round* of heating. The purpose of the diverter is purely diversion; no regulation of flow is considered.

A relevant operation aspect is found in the storage system, where bottom fluid only returns to the solar loop when hot HTF is entering the tank (at the same rate). Similarly, the return from the load occurs at the same rate as the fluid is being drawn to meet the load in the exchanger.

4.2.2.2 Process circuit control

In this case, control strategies are mainly focused on the regulation of the flow rate of HTF in the circuit, which is essentially the flow rate of the hot side of the heat exchanger. The component called *PumpP Control* has the function of generating a single signal and send it to the variable pump of the system. Said controller receives information as values between 0 and 1, from the following components:

- Schedules of operation (*SchedulePPSummer and SchedulePPWinter*): represent the daily hours of manufacture of the ECA blocks for a typical year of operation (As described in Chapter 3). Considers daily profiles by using the linked data from *Type 14* forcing functions. Distinction between summer and winter seasons is done to address the daylight saving time situations, since the weather data from Meteonorm was calculated for winter legal time (in this particular case, GMT). In this matter,

summer schedules are structured considering the start and end of manufacture one hour earlier. *PumpP Control* component selects the schedule to use according to the time of the year.

- Minimum temperature of operation (*ProcessControl*): a ON/OFF differential controller is introduced to analyze if the temperature in the top node of the tank is high enough to be able to preheat the feedwater at the designed conditions. To do so, the controller sets the minimum difference that should exist between the top node and the feedwater inlet; 15ºC of separation are established (which is the difference imposed in the heat exchanger design) for the start-up and 8ºC for the shut-down (lower dead band temperature). Additionally, the controller disposes of a high limit cut-out that shut-downs the pump if the water at the outlet of the exchanger reaches 171ºC, thus avoiding evaporation.
- Flow rate regulation (FlowControl): given the fact that in a preliminary state the system was designed for a 5070 kg/h feedwater flow, the introduction of process load profiles induces changes in the behavior of the outlet temperatures of the heat exchanger, namely vaporization issues. When design temperatures in the solar field are reached for water flow rates smaller than the design value, the fluid surpasses the 171ºC high limit cut-out, thus shutting the pump down continuously and compromising the stability of the system operation. To avoid said situation, flow regulation is defined for the process circuit by using *Type 22* controller and the variable pump component. The basic principle is the following: the controller compares the outlet temperature of the cold side of the exchanger with a set value (170ºC, as a safety measure) and generates a control signal (between 0.1 and 1) that is related to the maximum flow rate of the pump. When the exchanger does not need the nominal 11333.7 kg/h flow, the controller sends a value lower than 1 to the *PumpP Control* component, which associates the information from other strategies and regulates the variable pump.

Summarizing, stable generation is achieved by establishing proper conditions for the start-ups and interruptions of the global system, thus avoiding frequent fluctuations that might occur when the system is not prepared to work.

As seen, safety measures are a relevant aspect in the strategy, with flow regulation, high limit cut-outs and collector defocusing processes used to protect the heat exchanger equipment from vaporization of the feedwater.

4.2.3 Parameter optimization

At this point most components of the system are established, however some specific parameters can be optimized considering its influence in the global behavior of the integration approach: the solar field orientation and the entrance node of the tank.

The orientation of the solar collectors influences not only the annual energy yield, but also the seasonal and daily behaviors of the outlet temperatures (as seen in Fig. 42). To properly define the most adequate orientation, complete simulations for different configurations are required, that being said, this parameter is left as an open variable of the technical and economic performance assessments. Nevertheless, in a descriptive approach, seasonal variations in the generation are presented in Fig. 45.

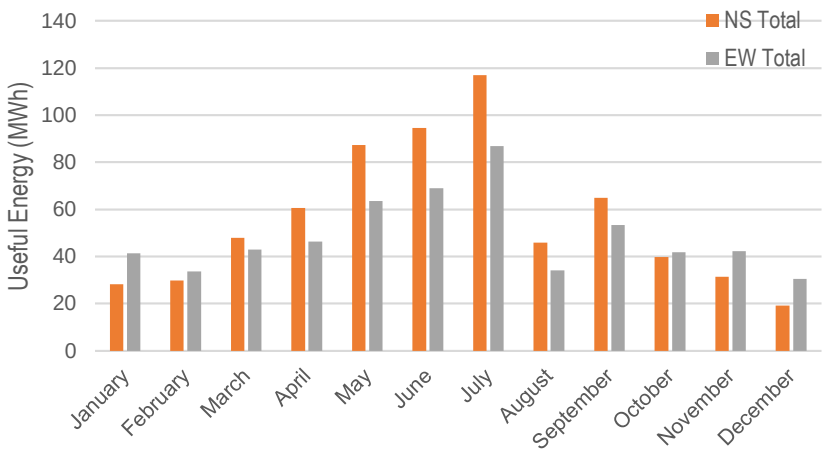

Fig. 45. Monthly results for NS and EW fields for a random model configuration.

As expected, EW solar fields present a more regular generation from month to month, though reaching lower values in great part of the year if compared with the NS alternative.

On the other hand, the entrance node can be optimized beforehand, considering that the node in which HTF from the solar loop enters the storage tank could be either one of the nodes, excluding the bottom one. Therefore, an annual simulation to estimate the solar fraction (Addressed on Chapter 5) is performed, in which systems configured with the seven possible entrances are tested. The stratified tank model is characterized as: node 1 corresponds to the top node, then, node 8 is the bottom one. The simulation is performed for a solar field with a NS orientation and with 4 collectors in series and 7 in parallel, along with a 6 m^3 storage is tested.

The greatest energy yield is found for the entrance at the top node, however the difference between this one and the rest is not significant. On the other hand, short term stability seems to be better for nodes closer to the middle. The following graph compares the annual energy yield of the tested entrance nodes as a function of the maximum value found (Fig. 46).

In a more qualitative analysis, the simulations showed that the problem of the entrance at the top node is that any sudden fluctuation coming from the solar loop is almost immediately felt in the heat exchanger. For entrance at node 3, for example, quick variations are smoother, especially in early morning and late afternoon operation.

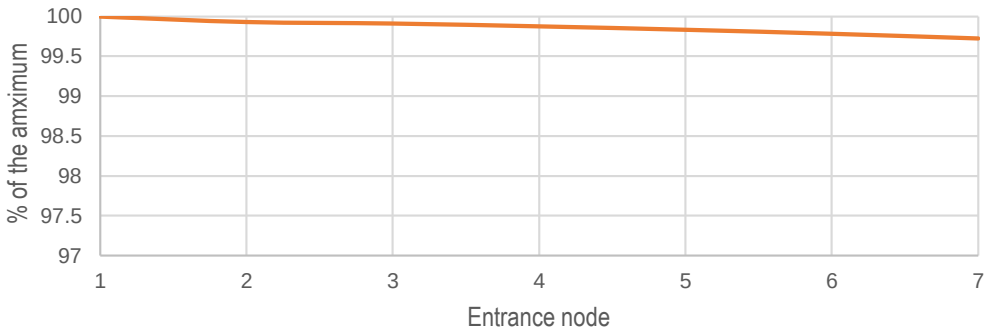

Fig. 46. Node entrance analysis as a function of the solar fraction.

Concerning the results, the selected entrance node is the third one from the top, highlighting its good short term stability and acknowledging that the solar fraction is extremely close to the maximum obtained value.

CHAPTER 5. OPTIMIZATION AND PERFORMANCE ASSESSMENT

The present chapter summarizes the performed simulations of the model, yielding relevant technical and economic data for the evaluation of the SHIP integration approach.

5.1 Performance Assessment

With the model assembled, it is now required to understand how it behaves for certain parameters, for this, simulations of the system are performed considering the next features:

- Solar field orientation: both NS and EW.
- Size of the tank: Variable.
- Number of collectors in series: Variable.

The combination of these features generates a set of solar integrated system configurations that are tested under the same load and weather conditions. To compare the alternatives, indicators like solar fraction or Levelized Cost of Energy (LCOE) are used for the technical and economic comparisons.

The aim is to select a solar system configuration that stands out from the rest in terms of solar energy utilization and favorable economic characteristics, which does not necessarily mean the one with the cheapest investment cost, but one that comprises both aspects. On the other hand, the seasonal behavior is not critical, this is, solar energy generation does not have to be regularly distributed along the year, since the saved cork powder can be stored for use during months in which the incident solar energy is lower. However, daily stability characteristics are important for the present analysis.

5.2 Model outputs and calculations

The technical performance assessment demands specific outputs from the simulations, namely energies and temperatures, which are obtained using output components (printers) and plotters from TRNSYS: Type 25 and Type 65, respectively.

However, results that summarize total annual values, as in energy gains or thermal losses, require the use of quantity integrators such as Type 24. The main indicator of performance is the useful energy of the heat exchanger, since it is the quantity of energy delivered for the preheating of the feedwater. To calculate it, links between the *Annual* integrator represented in Fig. 47 and the heat exchanger are made.

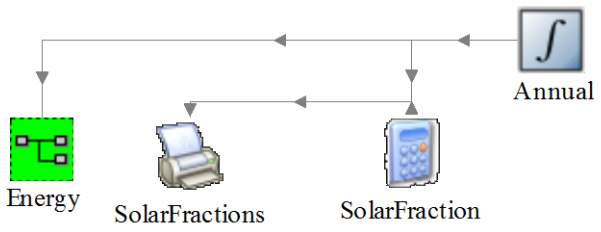

Fig. 47. Output system of the model (Built with TRNSYS).

This energy result is then used for other performance indicators calculations (technical and economic), and among them, the solar fraction. Said parameter describes the percentage of energy delivered by the entire system as a function of the supplied energy of the current heat generation system. In this particular case, the useful energy of the exchanger is compared to the quantity of heat used by the boiler in its preheat stage (as calculated in Chapter 3). Equation 18 shown below expresses the solar fraction used in the evaluation:

$$SolarFraction = \frac{Useful\ energy\ in\ the\ HEX}{Boiler's\ preheat\ energy} \tag{18}$$

5.3 Solar fraction analysis

Annual time periods are considered for the energetic evaluation of the model alternatives; thus the simulation obeys the next considerations:

- Simulation start time: 0h.
- Simulation stop time: 8760h.
- Simulation time step: 1 minute.

Knowing beforehand that the solar field is designed to have 7 collector rows in parallel, the number of collectors in series on each line is increased from 3 to 7 between simulations, even though the expected outlet temperatures for the first option do not reach the desired values (Fig. 39). Nevertheless, since the system now integrates other components and operation strategies, it is interesting to observe its behavior.

All the possible configurations for the solar fraction analysis are exposed in Table 20. Notice the introduction of the specific storage capacity (liters of storage per aperture area of the solar field), which facilitates the comparison of results and brings consistency to the selection of storage sizes.

These solar field and storage sizes are applied both for NS and EW simulations.

Table 20. Simulated configurations.

		Specific Storage Capacity				
		4 l/m²	**6 l/m²**	**8 l/m²**	**10 l/m²**	**12 l/m²**
Collectors in series	**Total Aperture Area (m²)**	**Vol. (m³)**	**Vol. (m³)**	**Vol. (m³)**	**Vol. (m³)**	**Vol. (m³)**
3	774.9	3.0996	4.6494	6.1992	7.7490	9.2988
4	1033.2	4.1328	6.1992	8.2656	10.3320	12.3984
5	1291.5	5.1660	7.7490	10.3320	12.9150	15.4980
6	1549.8	6.1992	9.2988	12.3984	15.4980	18.5976
7	1808.1	7.2324	10.8486	14.4648	18.0810	21.6972

Some model components are dependent on the solar field and tank sizes, namely the thermal mass capacity of the receiver tubes and the internal dimensions of the buffer. For each new simulation,

the variable parameters of those components (such as mass, UA, node height, etc.) have to be modified to fit the configuration. The alterations follow the equations described to compute them (Sections 4.2.1.4 and 4.2.1.5).

5.3.1 Simulation results

Performing the 50 simulations (25 for each solar field orientation) yields annual energy results that allow the estimation of the solar fractions exposed in Fig. 48 and Fig. 49, for NS and EW alternatives:

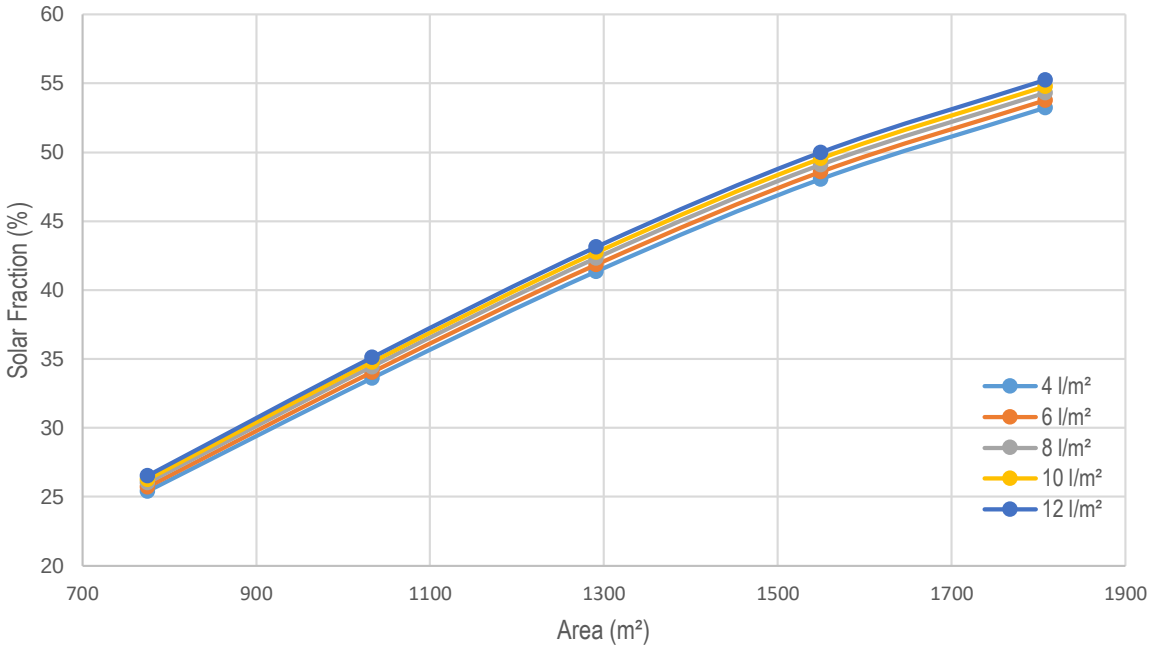

Fig. 48. Solar fraction results for the NS solar field.

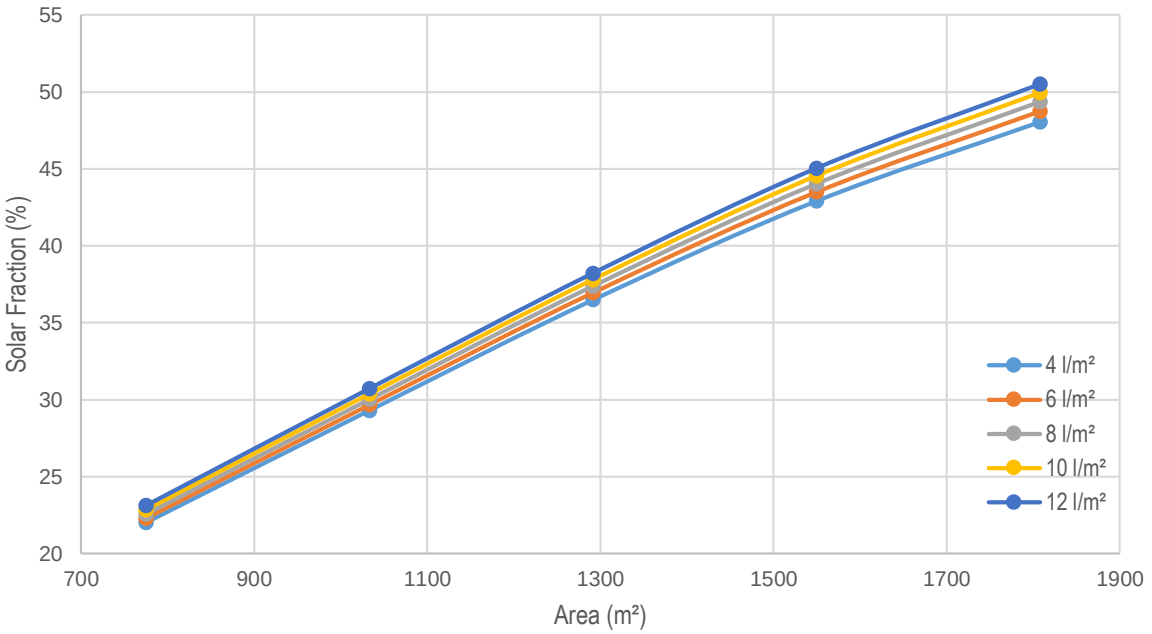

Fig. 49. Solar fraction results for the EW solar field.

The main conclusion from the graphical results is the evident greater solar fraction obtained when increasing the number of collectors in series and the storage capacity of the system, knowing beforehand that more collectors per line yield higher temperatures of the HTF. It also seems that storage capacity increase has a deeper influence in greater fields, probably related to the capacity of generation of such a big aperture area. Between collector orientations, the North-South approach presents overall higher values of solar fraction if compared to its East-West competitor; reaching a difference of 5 percentage points for the biggest configuration.

The maximization of solar energy criteria would define the system with the biggest dimensions as the most favorable, however the assessment considers other indicators to select the final system, thus leaving the decision for deeper approaches.

Even though the obtained values do not discriminate between suitable options, its annual energy results are useful for other aspects of the work, namely the LCOE analysis and the characterization of annual yields for each SCA orientation.

5.4 Hybrid solar field orientation scenario

The previous analysis exposed the fact that NS oriented collectors offer greater solar fractions, despite its seasonal variability. On the other hand, EW orientation is known to distribute the generation more uniformly during the year. In terms of daily yields, the shape of the outlet temperature curves follows the representation of Fig. 42.

Concerning the latter, the idea is to model a hybrid *NS+EW,* that would bring the best of both options to the daily and annual behavior of the system in terms of outlet solar loop temperatures. To do so, the 7 parallel rows are divided and part of them are oriented NS, while the rest is oriented EW.

Simple simulations for a random solar field and storage dimension are performed (6 collectors in series and 8 l/m^2 storage capacity), in which the configurations tested are:

- 4 parallel x 6 series in NS, and 3 parallel x 6 series in EW (4+3).
- 5 parallel x 6 series in NS, and 2 parallel x 6 series in EW (5+2).
- 6 parallel x 6 series in NS, and 1 parallel x 6 series in EW (6+1).
- 7 parallel x 6 series in NS.
- 7 parallel x 6 series in EW.

Regular NS and EW fields are also simulated for comparison purposes. Notice that each of the tested models have fields of 1549.8 m^2. To simulate this hybrid scenarios, modifications on the existing TRNSYS model are necessary, as represented in Fig. 50.

The only changes are done in the solar loop, in which an extra *Type 536* is introduced, along with diversion and tee-piece valves to handle the flow proportions in each SCA (1619.1 kg/h per parallel row).

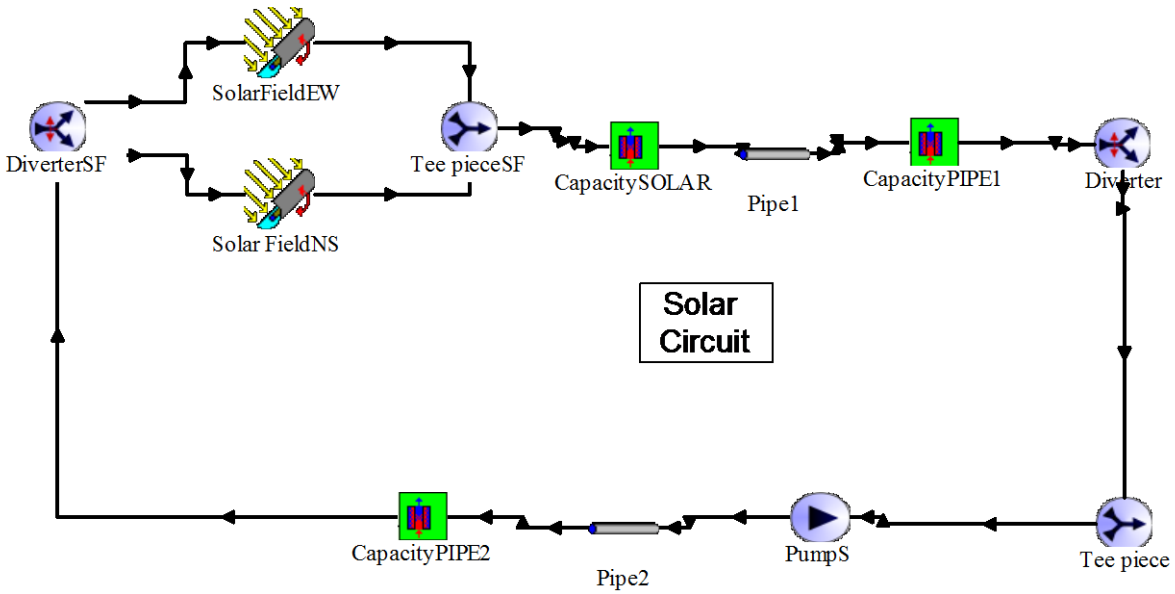

Fig. 50. Hybrid orientation solar circuit model (Built with TRNSYS).

Annual simulations produce the solar fractions presented in Table 21, which shows that the hybridization is not better than the single orientation NS option, at least in terms of annual useful energy.

Table 21. Solar fraction results of the hybrid scenario.

	Solar fraction (%)
NS	49.08
EW	44.03
4+3	47.41
5+2	48.09
6+1	48.65

In the daily stability aspect, which is a relevant criteria of assessment, temperature of the heat exchanger cold outlet is represented for winter and summer manufacture weeks, in order to analyze the influence of the hybridization when compared to regular NS or EW alternatives. Fig. 51 and Fig. 52 expose the latter for the 4+3 configuration.

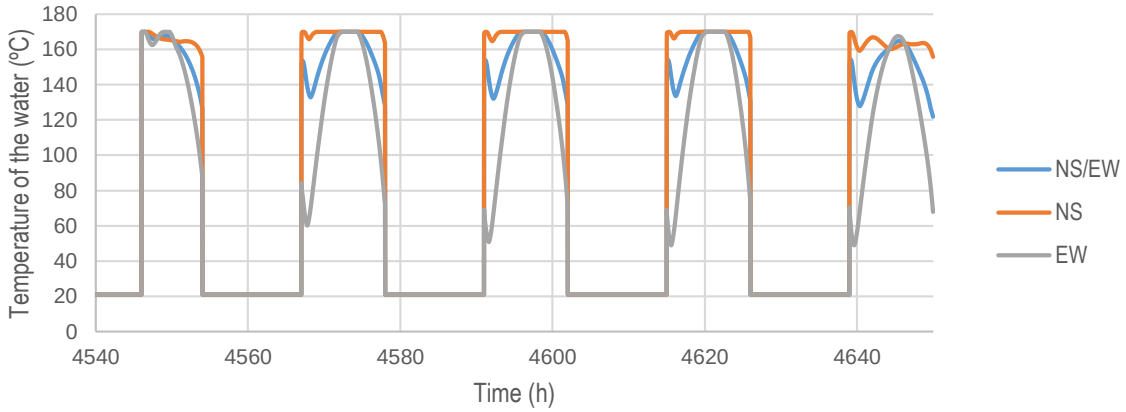

Fig. 51. Summer behavior of the outlet temperature of the heat exchanger.

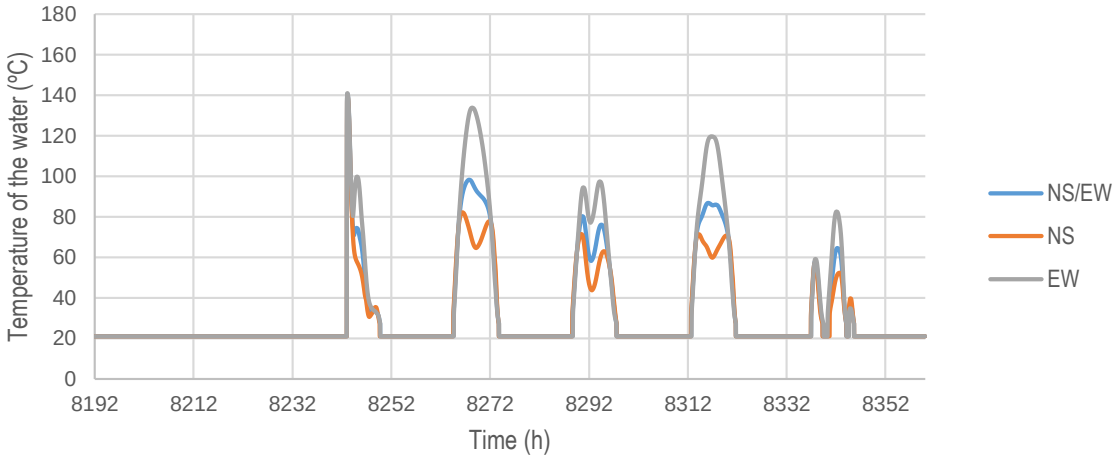

Fig. 52. Winter behavior of the outlet temperature of the heat exchanger.

Concerning the daily stability, there does not seem to be a clear advantage in the use of the layout hybridization when compared to the other alternatives, especially during summer operation. Given this fact and knowing that in terms of solar fraction the NS oriented field continues to possess the highest value, the use of a hybrid field does not compensate the modification and its consequences, at least for this case scenario.

5.5 LCOE Analysis

Economic analysis of the simulated configurations is now approached by estimating the Levelized Cost of the Energy produced (LCOE), which is no more than the total cost of installing and operating a project expressed in € per unit of generated energy over the lifetime of the system. Castro (2012, p.33) develops a simplified model of the indicator, as seen in the expressions below:

$$LCOE = \frac{I_t(i + d_{om})}{E_{annual}} \tag{19}$$

Where I_t is the total investment, i is the discount rate factor (or *Capital Recovery Factor*, Eq. 20), d_{om} are the operation and maintenance expenses (as a function of the total investment), and E_{annual} is the total useful energy yield in a year of operation.

$$i = \frac{a(1+a)^n}{(1+a)^n - 1} \tag{20}$$

$$a = [(1 + T_1)(1 + T_2)(1 + T_3)] - 1 \tag{21}$$

The discount rate (a) depends on the interest rate (T_1), the risk associated rates (T_2) and the inflation rates (T_3). Therefore, the required data for the LCOE is:

- Total investment (global system costs).
- Interest and inflation rates.
- Lifetime of the project.
- O&M specific costs.
- Annual yield of energy of the system.

Total investment costs and annual yield of energy depend on the configuration and size of the system, but the rest of the parameters can be established beforehand, as seen in Table 22:

Table 22. Economic assessment parameters.

Parameter		*Value*	*Source*
Lifetime of the project		25 years	(Silva, Berenguel, Pérez, & Fernández-Garcia, 2014)
O&M specific costs		2% of the Investment	(Kalogirou, 2003)
Rates	**T_1**	3.41%	(Banco de Portugal, 2016)
	T_2	0	*Not considered*
	T_3	1.80%	(Trading Economics, 2016)

From the latter, one can estimate the discount rate as 5.27%, considering no risks associated to the project (simplified approach, T_2 not considered), moreover, the capital recovery factor is 7.29%.

Since energy yields are already available from the solar fractions simulations, the next step is the estimation of the investment, which is defined to be on year 0 of the project. Considering the various configurations addressed, costs are divided in two: common costs and variable costs. The common costs are related to the equipment that does not change according to the configuration, include: pumps, piping, insulation and the heat exchanger. On the contrary, the variable costs change as a function of the size of the equipment, they cover: solar field, storage tank and its insulation, and the quantity of HTF.

Considering the characteristics and dimensions of the common equipment, investment expenses are obtained using chemical engineering design databases: *Matches* online database (Matches , 2016) and the *Cost Estimator Tool* (Peters, Timmerhaus, & West, 2016) from Plant Design and Economics for Chemical Engineers, 5th edition. Both tools are based on specialized industrial economics books. Table 23 summarizes the estimations:

Table 23. Common costs of the solar process heat system.

Equipment	*Description*	*Unit*	*Quantity*	*Unit cost ($)*	*Total cost ($)*	*Total cost (€)**
Pump	API 610 Compliance - Centrifugal pump	-	2	15100.00	30200.00	27362.51
HEX	Carbon steel shell and tube (A 63.25 m²)	-	1	36300.00	36300.00	32889.37
Piping	Carbon steel - Schedule 40	m	260	9.00	2340.00	2120.14
Insulation	Fiberglas™ - 25mm	m	260	16.00	4160.00	3769.14
***0.906043 €/$ (October, 2016)**				**Total**	**73000.00**	**66141.16**

For the variable costs, the listed aspects are taken into account:

- Solar collector assembly costs are estimated based on an existing industrial facility that coupled its production line with a 627m^2 NEP PolyTrough 1800 collector loop. The *Emmi Dairy Saignelégier*

factory from Switzerland invested around 315000 € on the solar field (including the SCAs, piping and support construction). Specific costs are 502.4 €/m^2 of aperture area (AEE INTEC, 2015). This value is used for the present work given the difficulty of finding approximate costs reported by the manufacturer.

- Storage tank: Shop fabricated carbon steel tank with 6.35mm. Costs individually obtained for each volume (Peters, Timmerhaus, & West, 2016), following the built curve represented in Fig. 53.

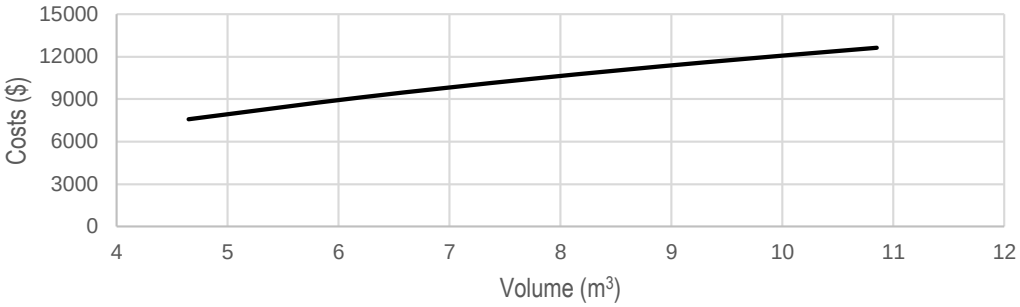

Fig. 53. Storage tank cost per volume.

- Storage tank insulation: Fiberglass with a 25.4 mm thickness, with a price of 81€/m^2 (Peters, Timmerhaus, & West, 2016).
- Therminol® 66 market price: 5.5-6 €/kg, as reported by the Eastman Chemical Company when directly contacted. The calculations are performed with a 5.75€/kg average value, and includes the HTF inside the tank, the piping system (0.5105m^3) and the receiver tubes of the collectors (0.0196 m^3/SCA).

By joining theses aspects and including the common costs, the global investment for each configuration is obtained. Finally, the LCOE (in eurocents per kWh) for the NS and EW fields can be estimated, yielding the following curves (Fig. 54 and Fig. 55), in which the solar fraction is once again represented for comparison purposes.

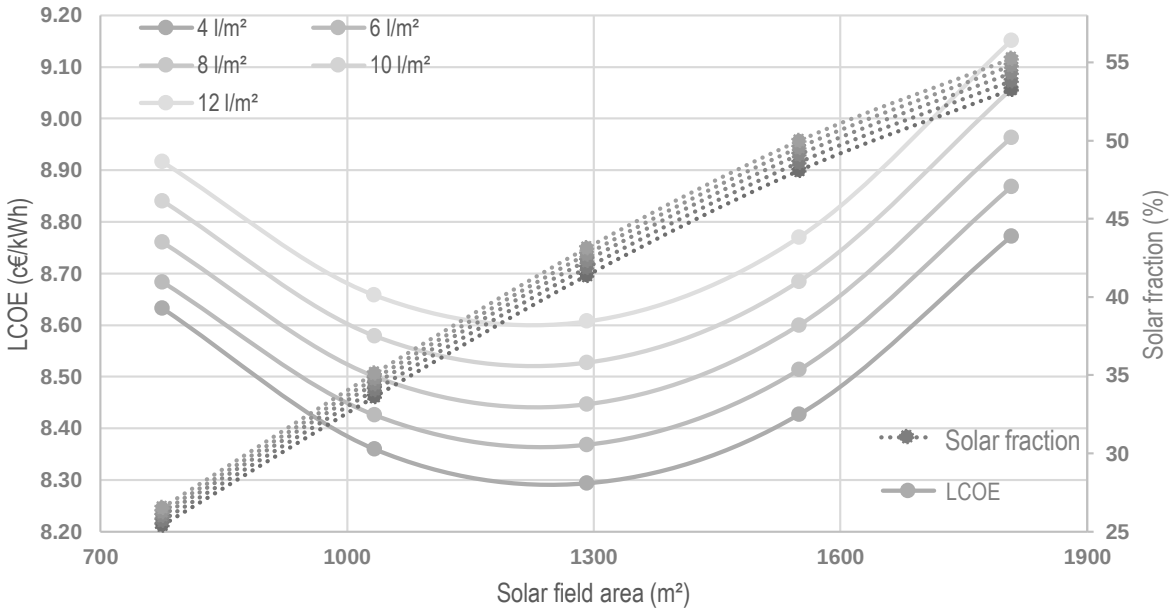

Fig. 54. LCOE for the NS configurations.

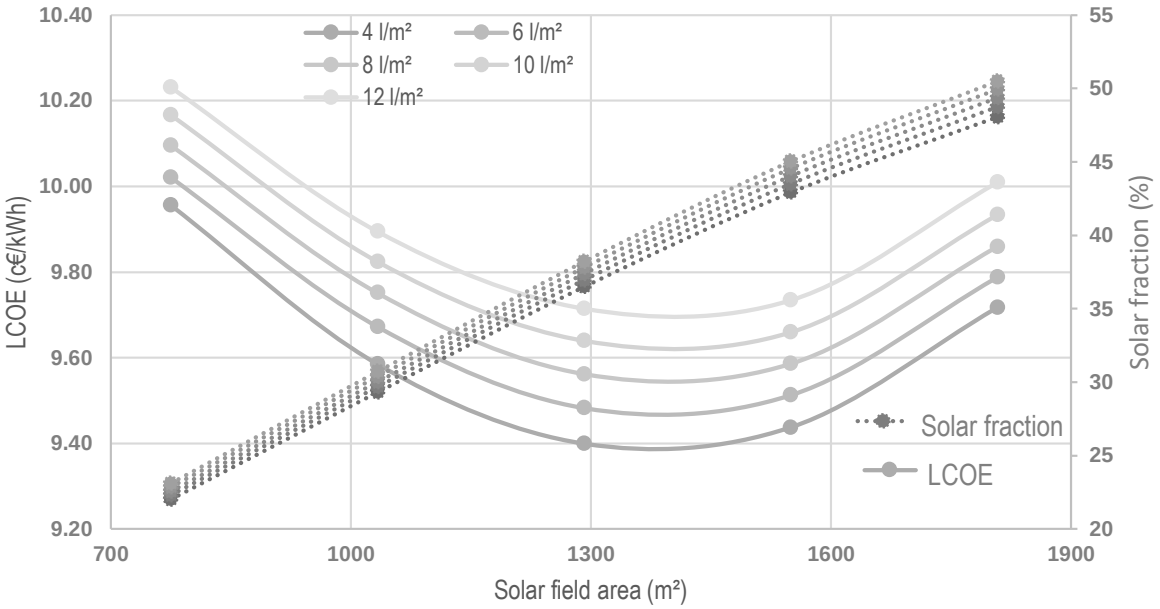

Fig. 55. LCOE for the EW configurations.

Comparing both LCOE results, the NS oriented fields present lower energy costs for the same dimensions of solar loop and storage, which is accompanied by greater solar fractions. Considering the latter, it is possible to state that the North-South orientation yields the most favorable technical and economic outputs.

Also, and looking at the behavior of the NS LCOE curve, the cheapest configurations are defined, corresponding to a solar field area of 1291.5 m^2, i.e. a solar array with 7 rows of 5 collectors in series. However, this might not yet be the most favorable option, since the difference between LCOE of diverse system configurations is small, but its difference in terms of produced energy is significant. This is, a system might produce slightly costlier energy but at quantities that the cheapest system is not capable of generating. To address this aspect, payback period analysis is performed.

Still, a considerable part of the systems can be neglected for the next assessment stage, since they produce less energy at a higher cost, therefore, solar fields with aperture areas smaller than the 1291.5 m^2 are discarded. Also, solar collector arrays with more than 1549.8 m^2 stay out of the next analysis since the produced energy starts to be considerably expensive.

5.6 Payback period analysis

The payback period economic indicator gives an idea of the number of years that would be necessary to recover the investment. It appears as a tool to assess the potential configurations obtained from the LCOE analysis. For this approach, solar integrated systems with aperture areas of 1291.5 m^2 and 1549.8 m^2 are evaluated at some of its specific storage capacities (Table 24).

To obtain said period, a cash flow analysis is performed, using data that was used for the LCOE analysis, namely the total investment, O&M costs, and the discount rate. The annual cash flows include the operation and maintenance expenses and the possible incomes. Since this system seeks to replace

part of the biomass consumption, the revenues are represented by the savings of cork powder, which has a potential market value. Little information is known regarding its prices, and the 2c€/kg at which the company sells it would not make the project economically feasible.

Table 24. Systems considered for the payback period analysis.

System	Area (m2)	Specific storage (l/m^2)	Investment (€)	Energy (MJ)
#1	1291.5	4	757625.941	3054951.67
#2	1291.5	6	773835.980	3092452.59
#3	1291.5	8	789537.082	3126096.26
#4	1549.8	4	894672.826	3550495.59
#5	1549.8	6	913789.480	3589521.71

Since no precise data is available, the calculations are performed for a range of mass values in order to obtain behavior curves and estimate the price at which the cork powder should be sold to make the project feasible. The quantity of biomass not consumed if the solar system is installed is computed using Eq. 22.

$$m_{corkpowder} = \frac{E_{annual}}{\eta_{boiler} HV} \tag{22}$$

The heating value (HV) of the feedstock is around 20 MJ/kg (Nunes, Matias, & Catalão, 2013), and the biomass boiler efficiency is approximately 70% (Cibo, n.d.).

Annual cash flows values correspond to the difference between revenues and expenses; its discounted value is then summed to the cumulative cash flow, which contains the initial investment. The process is repeated for each year until the investment is paid (The cumulative value is 0). The period in which this equilibrium is attained is called the payback period. A small section of the cash flow calculations is represented in Table 25.

Table 25. Cash flow operations for a 7x6 solar field.

Year	Cash flow (€)	Present value factor (€)	Discounted cash flow (€)	Cumulative discounted cash flow (€)
0	-913789.4802	1	-913789.4802	-913789.4802
1	58642.53271	0.9499258	55706.05487	-858083.4253
2	58642.53271	0.90235903	52916.61881	-805166.8065
3	58642.53271	0.85717412	50266.86153	-754899.9449
4	58642.53271	0.81425182	47749.78872	-707150.1562

By varying the prices of cork powder between 30c€/kg and 70c€/kg for the 5 systems, a series of values is found, thus yielding the curves plotted in Fig. 56.

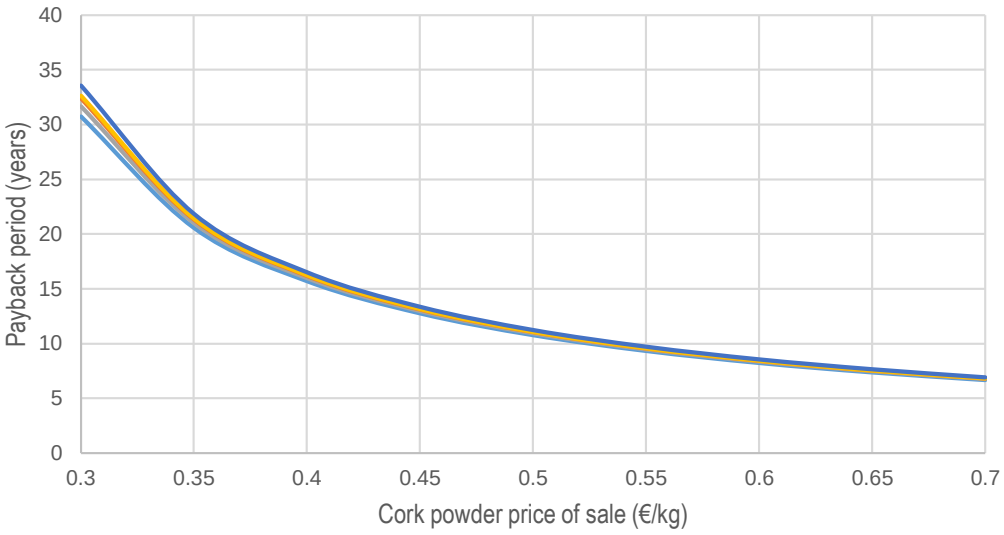

Fig. 56. Payback period variation with cork powder price increase.

Exemplifying, for a price of 0.5 €/kg the payback oscillates between 10.78-11.23 years. As expected, an increase of the price of sale yields smaller periods of investment return. Concerning the assessment of the five systems, the differences are not significant, but System #1 still presents the most favorable conditions. Though it is difficult to see in the plot, System #4 presents better economic results than System #3, even though the solar field is bigger. Also, notice that (from Fig. 54) it might be more economically attractive in some cases to increase the solar field size than the storage volume when seeking greater solar fractions. Given the many possible system configurations, the final selection of a single one depends on the criteria of the investors and the technical objectives of the facility.

Additionally, calculations of the payback period with a fixed cork powder price (2c€/kg) and a percentage of financial assistance on the initial investment are performed. These calculations indicated that the influence of the biomass sales is so low that the return of the investment in the first 10 years of the project only appears with subsidies close to 100% of the investment, confirming that the actual price of sale would not make the project financially viable. Therefore, the economic assessment approach should compare the LCOE of the various technologies available for industrial heat generation (Appendix B) in order to define the feasibility of the project.

5.7 Technical performance

In order to show the daily performance of the equipment that integrate the system, simulations for typical winter and summer days are executed. The simulated scheme is System #1, since it has the most economically attractive indicators. Its main parameters are exposed in Table 26.

Table 26. Parameters of System #1.

Number of parallel rows	7
Collectors per row	5
Aperture area	1291.5 m^2

Storage capacity	5.166 m^3
Axis orientation	North-South

5.7.1 Fluid temperatures

Temperatures of the HTF at the outlet of the solar array, at the outlet of the piping system (solar loop) and at the entrance of the hot side of the heat exchanger (tank top) are plotted for summer (Fig. 57) and winter days (Fig. 58). Additionally, temperature of the preheated feedwater is plotted.

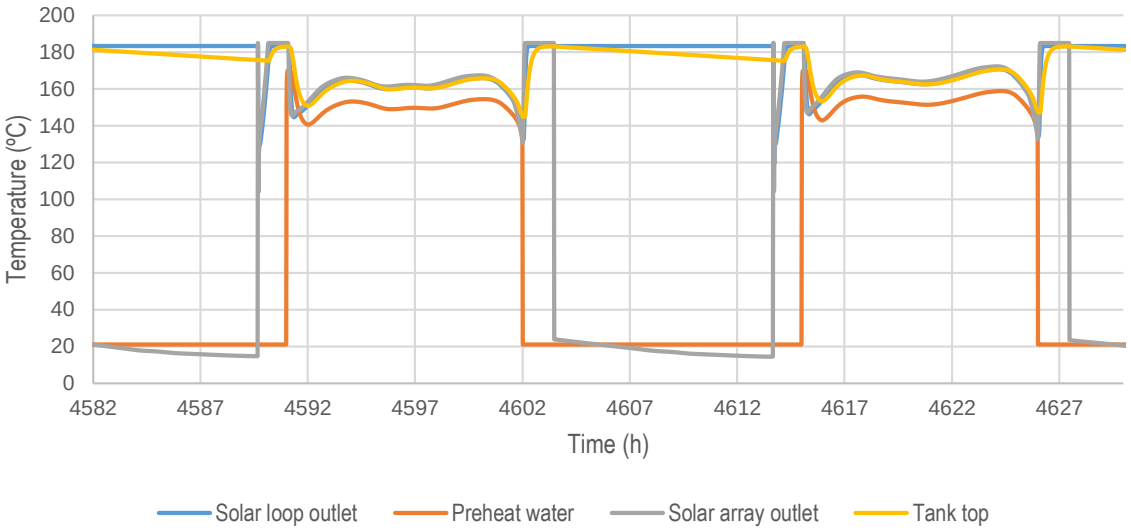

Fig. 57. Temperatures of the system for two consecutive summer days.

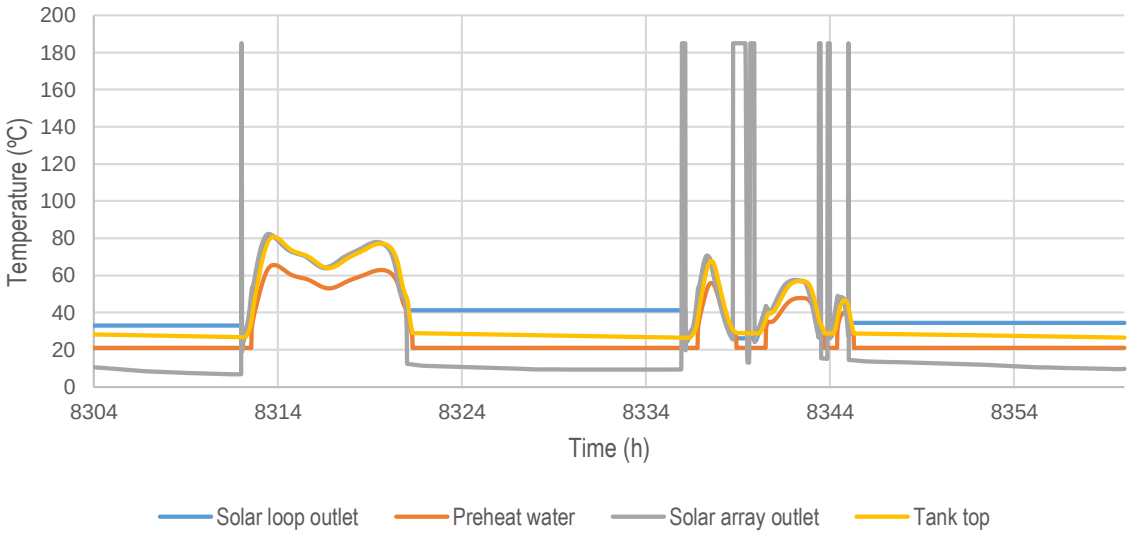

Fig. 58. Temperatures of the system for two consecutive winter days.

Comments on the results:

- The long hours of radiation during summer days originate charging of the tank before and after manufacture hours, since the control strategy was set that way.
- During clear summer days, preheating presents great daily stability.

- Winter days are influenced by the characteristics of the NS orientation.
- Charging of the storage allows a few minutes of high temperature operation when the system starts-up.
- The successive peaks in the last day of the winter are caused by the solar circuit diverter operation: the HTF passes through the field once again as is heated considerably.

5.7.2 Stratification in the tank

The level of stratification in terms of the HTF temperatures inside the buffer tank is represented for days of winter and days of summer (Fig. 59 and Fig. 60 respectively).

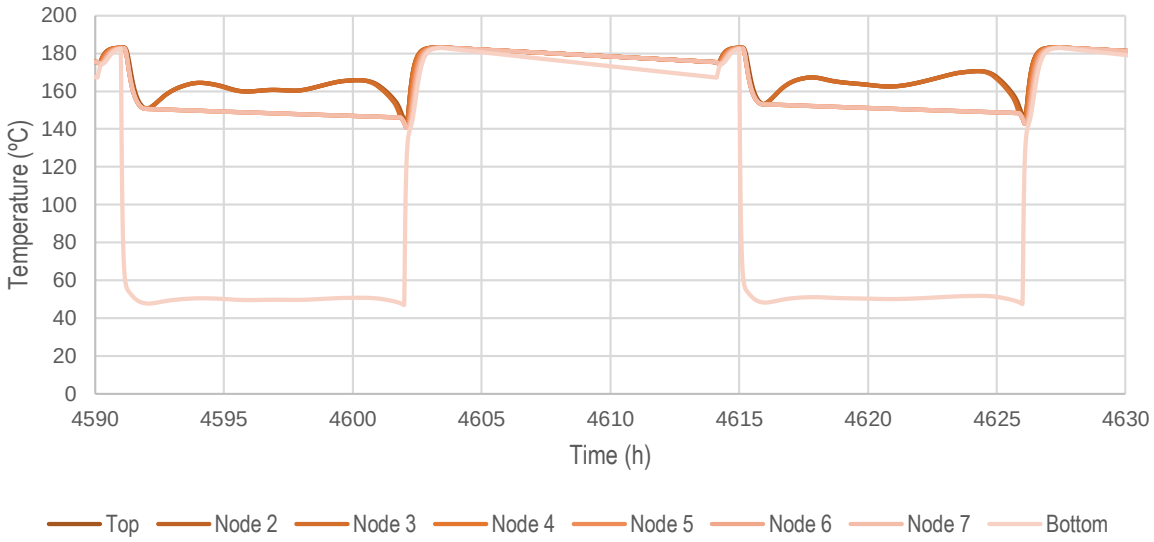

Fig. 59. Temperatures of the HTF inside the tank (Summer).

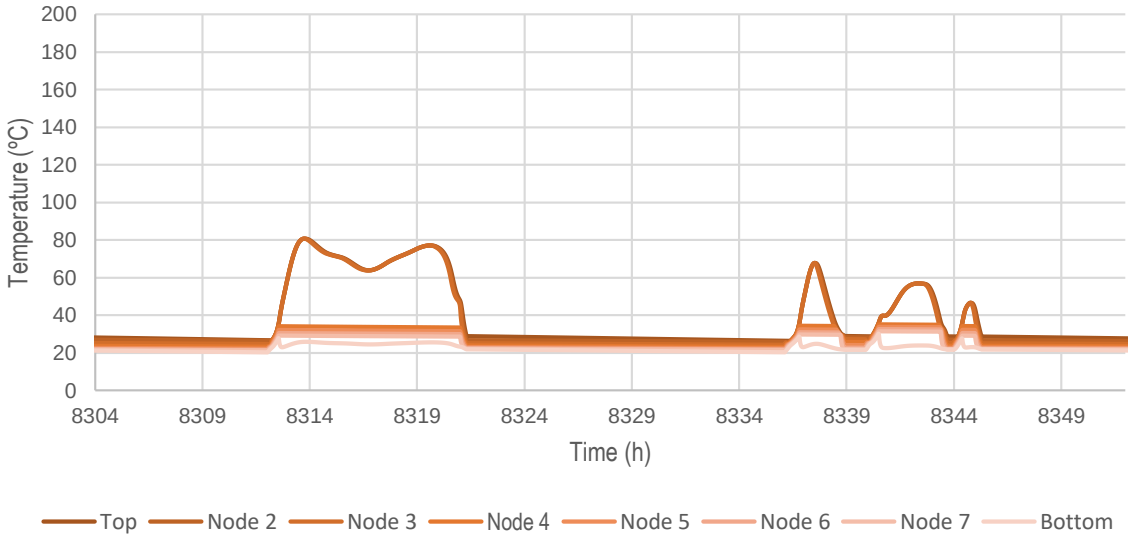

Fig. 60. Temperatures of the HTF inside the tank (Winter).

Since the storage tank does not have great dimensions, the solar loop is capable of maintaining it at a certain level of temperature in the summer, with very small differences between nodes. During winter operation most of the HTF is below the entrance temperature, given the fact that there is not

much energy available to charge the tank. Notice the behavior of the temperature of the top three nodes, corresponding to the entrance and top of the tank; where the values follow the solar field operation.

5.7.3 Thermal power

Incident radiation is compared with the instantaneous power delivered to the HTF in the receiver, as well as to the power of the heat exchanger equipment, in which the initial peak is due to the storage.

Summer (Fig. 61) and winter (Fig. 62) behaviors correspond to typical NS field performances.

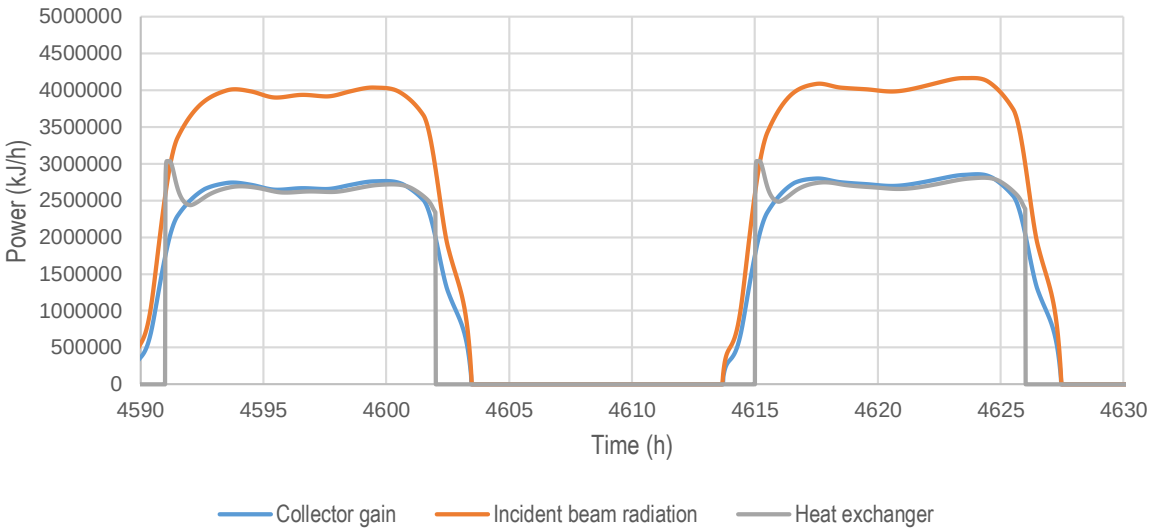

Fig. 61. Instantaneous power in the system (Summer).

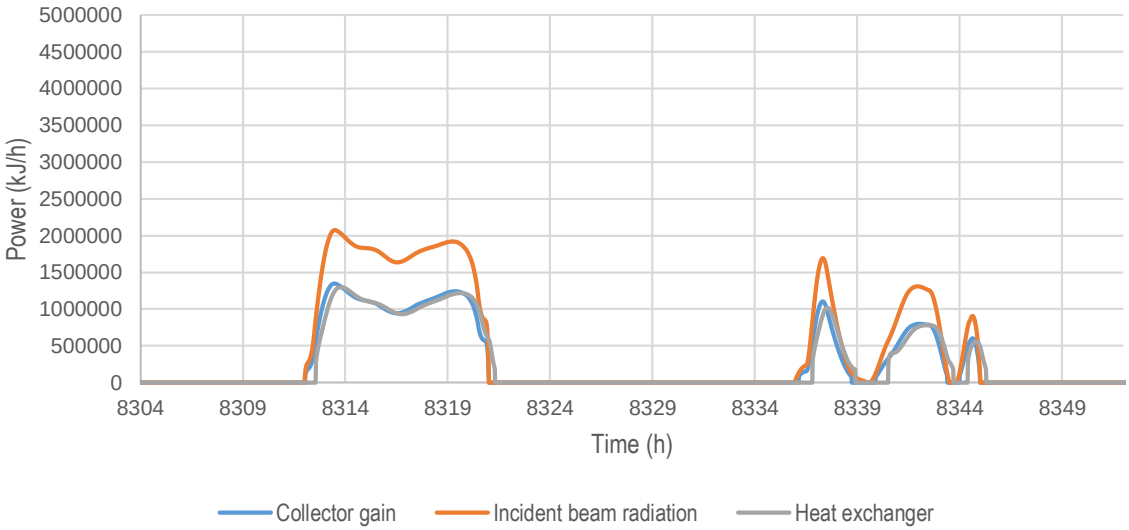

Fig. 62. Instantaneous power in the system (Winter).

5.7.4 Temperatures for reduced load cases

When the feedwater flow rate of the boiler is lower than usual and vaporization temperatures are likely to be achieved, the variable pump limits the flow rate as established. Fig. 63 shows this profile, in which significant daily stability is obtained for the design temperature of 170ºC.

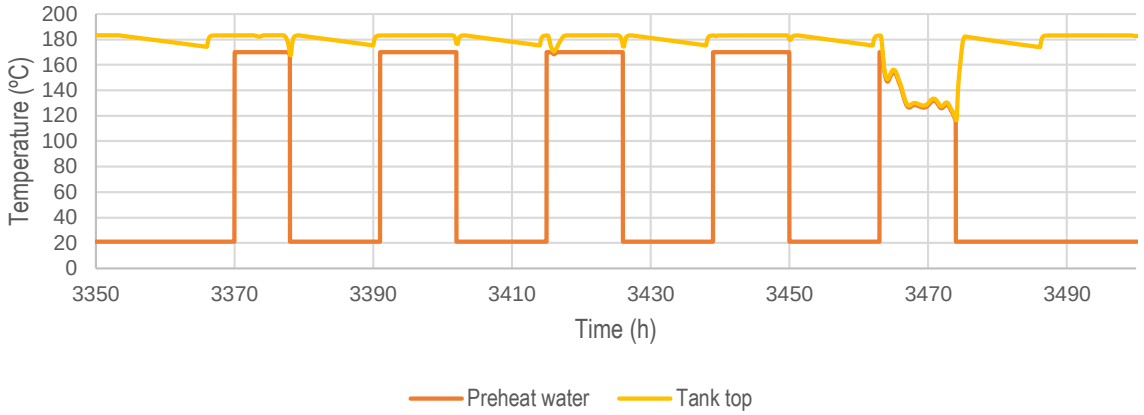

Fig. 63. Reduced load feedwater temperature behavior.

5.7.5 Total energy results

The summary of the annual results is presented in Table 27. The dumped energy is referred to the thermal energy lost during manufacture periods due to the defocus control of the collectors.

Table 27. Summary of the annual simulation results.

Useful energy	848.60 MWh
Energy gain in the field	1380.40 MWh
Incident beam energy (Surface)	2060.51 MWh
Dumped energy	8.35 MWh
Solar fraction	41.36 %
LCOE	8.30c€/kWh

Appendix B includes a table that shows typical LCOE values for other sources of thermal energy, in order to compare the obtained results with the other sources available. Notice that the comparison always depends on the conditions considered for the calculations of the economic indicator. In this particular case, the 83€/MWh are inside the range presented in the table.

CHAPTER 6. CONCLUSIONS AND RECOMMENDATIONS

The design of a parabolic trough solar collector system integrated into the feedwater preheating stage of the steam generation unit of *Sofalca, Lda.* was achieved, yielding performance indicators of its technical and economic behavior.

Remarks on the results and the overall development of the work are presented below:

- A brief bibliographic revision showed the solar integration potential of the Expanded Cork Agglomerate manufacture process thermal demands.
- Various integration points and integration concepts are possible for this particular industrial process.
- It is technically feasible to integrate solar process heat in the supply level of steam of the Expanded Cork Agglomerate manufacture process.
- The selection of a solar system configuration depends on the criteria of investors and/or facility owners.
- The LCOE of the analyzed systems is inside the range of typical values of heat generation in the European Union (EU28).
- The financial feasibility is only accomplished if adjustments on the cork powder price of sale are made.
- The most economically favorable configuration presents good temperature stability characteristics.
- The selection of a North-South axis orientation obeys both annual energy generation maximization and daily stability.
- The designed and modeled system is capable of generating thermal energy at a cost of 8.30c€/kWh, with a total annual yield of approximately 850 MWh.

Moreover, a set of recommendations are included, as obtained throughout the development and analysis of the system:

- Since the feedwater parameters are modified with the solar integration, specific studies on its influence on the boiler behavior are recommended.
- The analysis of the increase of the solar outlet HTF temperature is suggested, since the collector and the control system are capable of handling the modifications., and it might bring greater solar fractions.
- The use of water as the heat transfer fluid of the system could be a more economically attractive solution.
- Future studies might develop other system control strategies that maximize the solar obtained energy.

REFERENCES

ABENGOA SOLAR. (2013, April). A new generation of parabolic trough technology. *Sunshot CSP Program Review 2013*. Phoenix. Retrieved April 2016, from http://energy.gov/sites/prod/files/2014/01/f7/csp_review_meeting_042513_price.pdf

AEE INTEC. (2015). *Solar thermal plants database*. Retrieved December 28, 2015, from SHIP Plants: http://ship-plants.info/solar-thermal-plants

Alberici, S., & et al. (2014). Final report. *Subsidies and costs of EU energy*. Ecofys. Retrieved October 29, 2016, from https://ec.europa.eu/energy/sites/ener/files/documents/ECOFYS%202014%20Subsidies%20and%20costs%20of%20EU%20energy_11_Nov.pdf

Alfa Laval. (n.d.). Aalborg MX: Compact heat exchanger for oil and water heating or cooling. Retrieved August 2016, from http://www.alfalaval.com/globalassets/documents/industries/marine-and-transportation/marine/aalborg-mx..pdf

Alfa Laval. (n.d.). Product range heat exchangers. Retrieved September 2016, from http://www.alfalaval.com/globalassets/documents/industries/marine-and-transportation/marine/product-range-heat-exchangers.pdf

AREVA Inc. (2012). Solar Simplified. California, United States of America. Retrieved March 2016, from http://www.areva.com/mediatheque/liblocal/docs/activites/energ-renouvelables/ANP_U_336_V7_12_ENG.pdf

Banco de Portugal. (2016). A.10 Taxas de Juro bancárias - Empréstimos de Depósitos. Retrieved October 18, 2016, from https://www.bportugal.pt/pt-PT/Estatisticas/PublicacoesEstatisticas/BolEstatistico/Publicacoes/10-taxas%20juro%20bancarias.pdf

Barros, C. (2013). Produção de Pellets para valorização de resíduos provenientes da indústria corticeira. Portugal: Universidade do Minho. Retrieved October 3, 2016, from https://repositorium.sdum.uminho.pt/bitstream/1822/28198/1/tese_Carla%20Barros_2013.pdf

Benoit, H., Spreafico, L., Gauthier, D., & Flamant, G. (2016). Review of heat transfer fluids in tube-receivers used in concentrating solar thermal systems: Properties and heat transfer coefficients. *Renewable and sustainable energy reviews 55*, 298-315.

Bianchini, H. M. (2013). Avaliação comparativa de sistemas de energia solar térmica. Rio de Janeiro: UFRJ - Escola Politécnica .

Biencinto, M., González, L., & Valenzuela, L. (2016). A quasi-dynamic simulation model for direct steam generation in parabolic troughs using TRNSYS. *Applied Energy*, 133-142.

Biencinto, M., González, L., Valenzuela, L., & Fernández, A. (2014). Design and simulation of a solar field coupled to a cork boiling plant. *Energy Procedia, 48*, 1134-1143.

BrightSource Energy. (n.d.). Ivanpah Project facts. Oakland, California, USA. Retrieved January 8, 2016, from http://www.brightsourceenergy.com/stuff/contentmgr/files/0/8a69e55a233e0b7edfe14b9f77f5eb8d/folder/ivanpah_fact_sheet_3_26_14.pdf

Brunner, C. (2015, May). Task 49 - Solar Process Heat for Production and Advanced Applications. *2014 Annual Report*, 110-121. (P. Murphy, Ed.) SHS Secretariat. Retrieved April 2016, from http://www.iea-shc.org/data/sites/1/publications/IEA-SHC-Annual-Report-2014.pdf

Castro, R. (2012). *Uma Introdução às Energias Renováveis: Eólica, Fotovoltaica e Mini-hídrica.* Lisboa : IST Press.

Cibo. (n.d.). Energy efficiency and industrial boiler efficiency. Retrieved August 2016, from http://invenoinc.com/file/Energy-Efficieny-adn-Industrial-Boiler-Efficiency.pdf

CorkSpirit. (2016). *Arts and Crafts*. Retrieved September 17, 2016, from CorkSpirit: http://www.corkspirit.com/en/arts-and-crafts/natural-cork-grain-cork-powder-45/na00208-02-05mm-cork-grain-cork-powder-cork-dust-cork-granules-208

Duffie, J., & Beckman, W. (2013). *Solar Engineering of Thermal Processes* (4 ed.). Wisconsin, Madison: Wiley.

Duratherm. (2016). *Heat Transfer coefficient calculator*. Retrieved August 2016, from Duratherm: Heat Transfer Fluids: https://durathermfluids.com/calculators/heat-transfer-coefficient/

Eastman. (2016). *Concentrated Solar Power*. Retrieved October 22, 2016, from Therminol: https://www.therminol.com/applications/concentrated-solar-power

ESTELA. (2010). *Solar power from Europe's sun belt.* Brussels: ESTELA - European Solar Thermal Electricity Association.

Flores, F. M. (2014). *Analysis of a concentrating solar power generation system withh biomass boilers.* Caracas, Torino: UCV, Politecnico di Torino. Retrieved June 2016, from http://saber.ucv.ve/jspui/bitstream/123456789/9181/1/Tesis%20Franilena%20Flores%20C.I.%2020589842.pdf

Fluid Handling Inc. (2007). Session 1: Thermodynamics of steam. *Steam basics*. Retrieved September 20, 2016, from http://www.fluidh.com/cmsAdmin/uploads/thermodynamicproperties-websitewithnosteamtables.pdf

Frein, A., Calderoni, M., & Motta, M. (2014). Solar thermal plant integration into an industrial process. *Energy Procedia, 48*, 1152-1163.

Gil, L. (1996). *Cortiça: Produção, Tecnologia e Aplicação.* Instituto Nacional de Engenharia e Tecnologia Industrial.

Gil, L. (1997). Cork powder waste: An overview. *Biomass and bioenergy, 13*, 59-61.

Gil, L. (2013). Insulation Corkboard for Sustainable Energy and Environmental Protection. *Ciência e Tecnologia dos Materias, 25*, 38-41. Retrieved December 27, 2015, from https://www.researchgate.net/publication/259678121_Insulation_corkboard_for_sustainable_energy_and_environmental_protection_CT_Materiais_Vol_25_N1_jan_jul_2013_p_38-41

Giovannetti, F., & Horta, P. (2016, April). Comparison of process heat collectors with respect to technical and economic conditions - Technical report A.2.1. *Solar process heat for production and advanced applications*. SHC/SolarPaces.

Godinho, M. H., Martins, A. F., Belgacem, M. N., Gil, L., & Cordeiro, N. (2001). Properties and processing of Cork Powder filled cellulose derivatives Composites. *Macromolecular Symposia*, 223-228.

Grilo, T. (2014). Blackcork. Portugal. Retrieved December 27, 2015, from http://sofalca.pt/pdf/catalogo-blackcork.pdf

Gundersen, T. (2000). *A process integration primer - Implementing agreement on process integration .* SINTEF Energy Research. Trondheim, Norway: IEA.

Hassine, I. (2015). Identification of suitable integration points. *Solar Process Heat for Production and Advanced Applications - Integration Guideline*, 77-85. IEA - SolarPACES.

Helmke, A., & Heß, S. (2015). Classification of solar process heat system concepts. *Solar Process Heat for Production and Advanced Applications - Integration Guideline*, 61-76. IEA - SolarPACES.

Ho, C. K. (2008). *Software and codes for analysis of concentrating solar power technologies.* Albuquerque: Sandia National Laboratories.

Horta, P. (2015). Process Heat Collectors: State of the Art and available medium temperature collectors. *Technical report A.1.3*, 25. SHC/SolarPaces.

IEA-ETSAP & IRENA. (2015). *Solar Heat for Industrial Processes - Technology Brief.* Retrieved June 2016, from http://www.solarthermalworld.org/sites/gstec/files/news/file/2015-02-27/irena-solar-heat-for-industrial-processes_2015.pdf

Incropera, F., DeWitt, D., Bergman, T., & Lavine, A. (2008). *Fundamentals of Heat and Mass Transfer.* United States of America: John Wiley & Sons, Inc.

IRENA. (2012). Concentrating Solar Power. *Renewable energy technologies cost analysis series, 1(2/5)*. Retrieved June 2016, from http://www.irena.org/documentdownloads/publications/re_technologies_cost_analysis-csp.pdf

Jebasingh, V., & Herbert, J. (2016). A review of solar parabolic trough collector . *Renewable and sustainable energy reviews 54*, 1085-1091.

Jenkins, S. (2016). Insulating Heat-Transfer-Fluid Piping. *Chemical Engineering*, 38.

Joga, H. (2012). *Diseño de una planta termosolar de receptor central con sales fundidas como fluido de trabajo y sistema de almacenamiento.* Madrid: Universidad Carlos III de Madrid.

Jones, S. A., Blair, N., Cable, R., Pitz-Paal, R., & Schwarzboezl, P. (2001). *TRNSYS Modeling of the SEGS IV Parabolic Trough Solar Electric Generating System.* Washington, DC: ASME.

Kalogirou, S. (2003). The potential of solar industrial process heat applications. *Applied Energy*, 337-361.

Kearney, D. W. (2007). Parabolic Trough Collector Overview. Golden, Colorado, United States of America. Retrieved January 2, 2016, from http://www.nrel.gov/csp/troughnet/pdfs/2007/kearney_collector_technology.pdf

Lauterbach, C. (n.d.). Solar heat for industrial processes - technology and potential. Kassel University - Institute of thermal engineering. Retrieved May 2016, from http://solarthermalworld.org/sites/gstec/files/solar-heat-for-ind-processes-christoph-lauterbach.pdf

Lovegrove, K., & Stein, W. (2012). *Concentrating Solar Power Technology: Principles, Developments and Applications.* Cambridge: Elsevier.

Mason, S. (2011). World wide overview of concentrating solar thermal simulation tools. *Solar2011, the 49th AuSES Annual Conference*. Melbourne.

Matches. (2016). *Index of Process Equipment*. Retrieved October 2016, from Matches: http://www.matche.com/equipcost/EquipmentIndex.html

Mibec. (2016, August). *6000 L Buffer tank - Cordivari*. Retrieved from Mibec Thermal Solutions: http://www.buffertanks.co.uk/shop/6000l-buffer-tank-cordivari-2

ModernEnviro. (2014). *Expanded Cork Insulation coming to North America*. Retrieved December 30, 2015, from ModernEnviro: http://www.modernenviro.com/expanded-cork-insulation-coming-to-north-america/

Mokheimer, E., Dabwan, Y., Habib, M., Said, S., & Al-Sulaiman, F. (2014). Techno-economic performance analysis of parabolic trough collector in Dhahran, Saudi Arabia. *Energy conversion and management*, 622-633.

Muster, B. (2015). *Solar Process Heat for Production and Advanced Applications - Integration Guideline.* IEA - SolarPACES.

Muster, B., Schmitt, B., & Schnitzer, H. (2015). Thermal processes and heat distribution networks in industry. *Solar Process Heat for Production and Advanced Applications - Integration Guideline*, 11-30. IEA - SolarPACES.

NEP Solar. (n.d.). Technical data for the PolyTrough 1800. *PolyTrough 1800 Technical Specification v7* .

NREL. (2010). *TroughNet: Parabolic trough solar power network.* Retrieved January 2, 2016, from NREL: http://www.nrel.gov/csp/troughnet/solar_field.html

NREL. (2016). *Concentrating Solar Power Projects*. Retrieved January 7, 2016, from NREL/SolarPACES: http://www.nrel.gov/csp/solarpaces/parabolic_trough.cfm

Nunes, L., Matias, J., & Catalão, J. (2013). *Energy recovery from cork industrial waste: production and characterisation of cork pellets.* Elsevier. Retrieved December 30, 2015, from http://webx.ubi.pt/~catalao/jfue_Nunes_revised.pdf

Odesie. (2016). *Boiler types and classification*. Retrieved October 19, 2016, from MyOdesie: https://www.myodesie.com/wiki/index/returnEntry/id/3061

Owens Corning. (n.d.). Fiberglas Product Data Sheet. Retrieved August 11, 2016, from https://sweets.construction.com/swts_content_files/20865/706939.pdf

Pareja, I. (2012). Tecnologías de generación en plantas solares de receptor central: estudio comparativo. Madrid: Universidad Carlos III de Madrid. Retrieved from http://e-archivo.uc3m.es/bitstream/handle/10016/16627/PFC%20Israel%20Pareja.pdf?sequence=1

Pereira, H. (2007). *Cork: Biology, Production and Uses.* Amsterdam: Elsevier Science.

Peters, M., Timmerhaus, K., & West, R. (2016). *Equipment costs*. Retrieved October 2016, from McGrawHill Education: http://www.mhhe.com/engcs/chemical/peters/data/

Pintor, A., Ferreira, C., Pereira, J., Correia, P., Silva, S., Vilar, V., . . . Boaventura, R. (2012). Use of cork powder and granules for the adsorption of pollutants: A review. *Water research, 46*, 3152-3166.

Platzer, W. (2015). *Potential studies on solar process heat worldwide.* IEA SHC, SolarPaces. Retrieved January 6, 2016, from http://task49.iea-shc.org/data/sites/1/publications/151031_IEA_Task49_Deliverable_C5_Potential%20studies.pdf

Ruby, S. (2010). *Industrial process steam generation using parabolic trough solar collection.* Denver: American Ennergy Assets. Retrieved August 2016, from http://www.energy.ca.gov/2011publications/CEC-500-2011-040/CEC-500-2011-040.pdf

Schiel, K., & Keck, T. (2012). Parabolic dish concentrating solar power (CSP) system. In K. Lovegrove, & W. Stein, *Concentrating Solar Power technology: principles, development, and applications* (pp. 284-322). Cambridge: Elsevier.

Schmitt, B. (2015). Assessment Methodology for Solar Heat Integration. *Solar Process Heat for Production and Advanced Applications - Integration Guideline*, 31-33. IEA - SolarPACES.

Schmitt, B. (2015). Classification of integration concepts. *Solar Process Heat for Production and Advanced Applications - Integration Guideline*, 46-60. IEA - SolarPACES.

Schwarzbözl, P. (2006). *A TRNSYS Model Library for Solar Thermal Electric Components (STEC) 3.0.* Germany: SolarPaces/DLR.

Schweiger, H., Mendes, J., Schwenk, C., Hennecke, K., Barquero, C., Sarvisé, A., & al., e. (2001). POSHIP - The potential of solar heat for industrial processes. Barcelona, Lisbon, München, Köln, Madrid. Retrieved October 28, 2016, from http://www.solarpaces.org/images/pdfs/poship_final_report.pdf

SHC. (2015). 2014 Highlights. *SHC Task 49 - Solar Heat Integration in Industrial Processes*. Retrieved March 8, 2016, from http://task49.iea-shc.org/data/sites/1/publications/IEA_SHC-Task49-Highlights-2014.pdf

Silva, M. (2002). Estimación del recurso solar para sistemas termosolares de concentración. *(Tesis doctoral de Ingeniería Industrial)*. Sevilla, Espanha: Universidad de Sevilla.

Silva, R., Berenguel, M., Pérez, M., & Fernández-Garcia, A. (2014). Thermo-economic design optimization of parabolic trough solar plants for industrial process applications with memetic algorithms. *Applied Energy 113*, 603-614.

Silva, S., Sabino, M., Fernandes, E., Correlo, V., Boesel, L., & Reis, R. (2005). Cork: Properties, Capabilities and Applications. *International Materials Reviews, 50*, 345-365.

Sinnot, R. K. (2005). *Chemical Engineering Design* (4 ed., Vol. 6). Elsevier.

SOFALCA. (2015). *Cork Production*. Retrieved December 29, 2015, from SOFALCA: http://sofalca.pt/en/producao.html

Solitem. (2013). *Our products*. Retrieved January 4, 2016, from Solitem Group: http://solitem.de/

Solutia. (n.d.). Therminol 66. Retrieved from http://twt.mpei.ac.ru/TTHB/HEDH/HTF-66.PDF

SPF. (2013). Solar Collector Factsheet: NEP PolyTrough 1800. *C1549*. Switzerland.

STAGE-STE. (n.d.). STAGE-STE IRP: General Description & Objectives. Retrieved September 2016, from http://www.stage-ste.eu/docs/STAGE-STE%20General%20Description%20and%20Objectives.pdf

Stewart, M., & Lewis, O. (2013). *Heat exchanger equipment field manual .* Walthan, USA: Gulf Professional Publishing.

TermoGraf. (n.d.). TermoGraf v5.7 - Free licence. Universidad de Zaragoza.

TESS. (n.d.). General descriptions . *TESS Components Library*. Retrieved from http://www.trnsys.com/tess-libraries/TESSLibs17_General_Descriptions.pdf

Trading Economics. (2016). Portugal - Previsão - Indicadores Econômicos. Retrieved October 18, 2016, from http://pt.tradingeconomics.com/portugal/forecast

TRNSYS. (n.d.). TRNSYS 16. *Solar Energy Laboratory - University of Wisconsin, Madison*.

U.S. Department of Energy. (2013). *Power Tower System Concentrating Solar Power Basics*. Retrieved October 21, 2016, from Energy.gov: http://energy.gov/eere/energybasics/articles/power-tower-system-concentrating-solar-power-basics

U.S. Department of Energy. (2014, May). 2014: The Year of Concentrating Solar Power. United States of America. Retrieved May 2016, from http://energy.gov/sites/prod/files/2014/05/f15/2014_csp_report.pdf

Zarza, E. (2012). Parabolic-trough concentrating solar power (CSP) systems. In K. Lovegrove, & W. Stein, *Concentrating Solar Power Technology: Principles, Developments and Applications* (pp. 197-239). Cambridge: Elsevier.

Appendixes

A. Schedule 40 steel piping tables

Reference Data

Reference Data

Schedule 40 Steel Pipe Data

Nominal Pipe Size In.	mm	Pipe O.D. In.	mm	Wall Thickness In.	mm	Weight of Pipe Lbs./Ft.	kg/m	Weight of Pipe Filled With Water Lbs./Ft.	kg/m	Maximum Span* Ft.	Meter	Recommended Hanger Rod Sizes
3/8"	(10)	.675	(17.1)	.091	(2.3)	.6	(.9)	.7	(1.0)	7	(2.13)	3/8"-16
1/2"	(15)	.840	(21.3)	.109	(2.7)	.8	(1.2)	.9	(1.3)	7	(2.13)	3/8"-16
3/4"	(20)	1.050	(26.7)	.113	(2.9)	1.1	(1.7)	1.3	(2.0)	7	(2.13)	3/8"-16
1"	(25)	1.315	(33.4)	.133	(3.4)	1.7	(2.5)	2.1	(3.0)	7	(2.13)	3/8"-16
1 1/4"	(32)	1.660	(42.1)	.140	(3.5)	2.3	(3.4)	2.9	(4.3)	7	(2.13)	3/8"-16
1 1/2"	(40)	1.900	(48.2)	.145	(3.7)	2.7	(4.0)	3.6	(5.3)	9	(2.74)	3/8"-16
2"	(50)	2.375	(60.3)	.154	(3.9)	3.6	(5.4)	5.0	(7.5)	10	(3.05)	3/8"-16
2 1/2"	(65)	2.875	(73.0)	.203	(5.1)	5.8	(8.6)	7.9	(11.7)	11	(3.35)	1/2"-13
3"	(80)	3.500	(88.9)	.216	(5.5)	7.6	(11.2)	10.8	(15.9)	12	(3.66)	1/2"-13
3 1/2"	(90)	4.000	(101.6)	.226	(5.7)	9.1	(13.5)	13.4	(19.8)	13	(3.96)	1/2"-13
4"	(100)	4.500	(114.3)	.237	(6.0)	10.8	(16.0)	16.3	(24.2)	14	(4.27)	5/8"-11
5"	(125)	5.563	(141.3)	.258	(6.5)	14.6	(21.7)	23.2	(34.6)	16	(4.87)	5/8"-11
6"	(150)	6.625	(168.3)	.280	(7.1)	19.0	(28.2)	31.5	(46.8)	17	(5.18)	3/4"-10
8"	(200)	8.625	(219.1)	.322	(8.2)	28.5	(42.5)	50.1	(74.6)	19	(5.79)	3/4"-10
10"	(250)	10.750	(273.0)	.365	(9.3)	40.5	(60.2)	74.6	(110.9)	22	(6.69)	7/8"-9
12"	(300)	12.750	(323.8)	.406	(10.3)	51.1	(75.9)	102.1	(151.9)	23	(7.01)	7/8"-9
14"	(350)	14.000	(355.6)	.437	(11.1)	63.0	(93.7)	121.5	(180.7)	25	(7.62)	1"-8
16"	(400)	16.000	(406.4)	.500	(12.7)	83.0	(123.5)	159.5	(237.3)	27	(8.23)	1"-8
18"	(450)	18.000	(457.2)	.563	(14.3)	105.0	(156.2)	202.2	(300.8)	28	(8.53)	1"-8
20"	(500)	20.000	(508.0)	.593	(15.1)	123.0	(183.0)	243.4	(361.8)	30	(9.14)	1 1/4"-7
24"	(600)	24.000	(609.6)	.687	(17.4)	171.0	(254.5)	345.2	(513.7)	32	(9.75)	1 1/4"-7

Schedule 80 Steel Pipe Data

Nominal Pipe Size In.	mm	Pipe O.D. In.	mm	Wall Thickness In.	mm	Weight of Pipe Lbs./Ft.	kg/m	Weight of Pipe Filled With Water Lbs./Ft.	kg/m	Maximum Span* Ft.	Meter	Recommended Hanger Rod Sizes
3/8"	(10)	.675	(17.1)	.126	(3.2)	.7	(1.1)	.8	(1.2)	7	(2.13)	3/8"-16
1/2"	(15)	.840	(21.3)	.147	(3.7)	1.1	(1.6)	1.2	(1.7)	7	(2.13)	3/8"-16
3/4"	(20)	1.050	(26.7)	.154	(3.9)	1.5	(2.2)	1.7	(2.5)	7	(2.13)	3/8"-16
1"	(25)	1.315	(33.4)	.179	(4.5)	2.2	(3.2)	2.5	(3.6)	7	(2.13)	3/8"-16
1 1/4"	(32)	1.660	(42.1)	.191	(4.8)	3.0	(4.4)	3.5	(5.2)	7	(2.13)	3/8"-16
1 1/2"	(40)	1.900	(48.2)	.200	(5.1)	3.6	(5.4)	4.3	(6.5)	9	(2.74)	3/8"-16
2"	(50)	2.375	(60.3)	.218	(5.5)	5.0	(7.5)	6.3	(9.4)	10	(3.05)	3/8"-16
2 1/2"	(65)	2.875	(73.0)	.276	(7.0)	7.6	(11.4)	9.4	(14.1)	11	(3.35)	1/2"-13
3"	(80)	3.500	(88.9)	.300	(7.6)	10.2	(15.2)	13.0	(19.4)	12	(3.66)	1/2"-13
3 1/2"	(90)	4.000	(101.6)	.318	(8.1)	12.5	(18.6)	16.3	(24.3)	13	(3.96)	1/2"-13
4"	(100)	4.500	(114.3)	.337	(8.5)	15.0	(22.3)	20.0	(29.7)	14	(4.27)	5/8"-11
5"	(125)	5.563	(141.3)	.375	(9.5)	20.8	(30.9)	28.7	(42.6)	16	(4.87)	5/8"-11
6"	(150)	6.625	(168.3)	.432	(11.0)	28.6	(42.5)	39.9	(59.3)	17	(5.18)	3/4"-10
8"	(200)	8.625	(219.1)	.500	(12.7)	43.4	(64.5)	63.1	(93.9)	19	(5.79)	3/4"-10
10"	(250)	10.750	(273.0)	.593	(15.0)	64.4	(95.8)	95.5	(142.1)	22	(6.69)	7/8"-9
12"	(300)	12.750	(323.8)	.687	(17.4)	88.6	(131.8)	132.6	(197.3)	23	(7.01)	7/8"-9
14"	(350)	14.000	(355.6)	.750	(19.0)	107.0	(159.2)	158.2	(235.4)	25	(7.62)	1"-8
16"	(400)	16.000	(406.4)	.843	(21.4)	137.0	(203.9)	206.7	(306.6)	27	(8.23)	1"-8
18"	(450)	18.000	(457.2)	.937	(23.8)	171.0	(254.5)	259.5	(386.2)	28	(8.53)	1"-8
20"	(500)	20.000	(508.0)	1.031	(26.2)	209.0	(311.0)	318.4	(473.8)	30	(9.14)	1 1/4"-7
24"	(600)	24.000	(609.6)	1.218	(30.9)	297.0	(442.0)	455.2	(677.4)	32	(9.75)	1 1/4"-7

Based on ASTM A53-86.
1 cubic ft. of water weighs 62.41 lbs.
1 gallon (U.S.) weighs 8.335 lbs.
1 cubic meter of water weighs 999.97 kg.
1 liter weighs .999 kg.

Based on MSS SP-69 Table 3 & 4.
*Many codes require pipe hangers to be spaced every 10' (3.048 meters) regardless of size. Check local codes.
Spacing and capacities are based on water filled pipe. Closer hanger spacing may be required where additional valves and fittings increase the load.

B. Levelized cost of heat in the EU28 for various technologies.

Different European Union regions are distinguished for many of the technologies. “The large cost gap between industrial boiler and domestic heating technologies is almost entirely caused by much lower natural gas prices for industry. In general, the cost of the natural-gas based technology is largely driven by the cost of fuel, while for technologies running on other fuels (heat pumps, biomass boilers), capital expenditures cost plays a larger role” (Alberici, et al., 2014).

Source: (Alberici, et al., 2014).